ESTIMATING PARTICULATE EMISSION RATES FROM LARGE BEEF CATTLE FEEDLOTS

by

HENRY F. BONIFACIO

B.S., University of the Philippines - Diliman, 2001
M.S., Kansas State University, 2009

AN ABSTRACT OF A DISSERTATION

submitted in partial fulfillment of the requirements for the degree

DOCTOR OF PHILOSOPHY

Department of Biological and Agricultural Engineering
College of Engineering

KANSAS STATE UNIVERSITY
Manhattan, Kansas

2013

Abstract

Emission of particulate matter (PM) and various gases from open-lot beef cattle feedlots is becoming a concern because of the adverse effects on human health and the environment; however, scientific information on feedlot emissions is limited. This research was conducted to estimate emission rates of PM_{10} from large cattle feedlots. Specific objectives were to: (1) determine feedlot PM_{10} emission rates by reverse dispersion modeling using AERMOD; (2) compare AERMOD and WindTrax in terms of their predicted concentrations and back-calculated PM_{10} emission rates; (3) examine the sensitivity of both AERMOD and WindTrax to changes in meteorological parameters, source location, and receptor location; (4) determine feedlot PM_{10} emission rates using the flux-gradient technique; and (5) compare AERMOD and computational fluid dynamics (CFD) in simulating particulate dispersion from an area source.

PM_{10} emission rates from two cattle feedlots in Kansas were determined by reverse dispersion modeling with AERMOD using PM_{10} concentration and meteorological measurements over a 2-yr period. PM_{10} emission rates for these feedlots varied seasonally, with overall medians of 1.60 and 1.10 g /m^2-day. Warm and prolonged dry periods had significantly higher PM emissions compared to cold periods. Results also showed that the PM_{10} emissions had a diurnal trend; highest PM_{10} emission rates were observed during the afternoon and early evening periods.

Using particulate concentration and meteorological measurements from a third cattle feedlot, PM_{10} emission rates were back-calculated with AERMOD and WindTrax. Higher PM_{10} emission rates were calculated by AERMOD, but their resulting PM_{10} emission rates were highly linear ($R^2 \geq 0.88$). As such, development of conversion factors between these two models is feasible. AERMOD and WindTrax were also compared based on their sensitivity to changes in meteorological parameters and source locations. In general, AERMOD calculated lower concentrations than WindTrax; however, the two models responded similarly to changes in wind speed, surface roughness, atmospheric stability, and source and receptor locations.

The flux-gradient technique also estimated PM_{10} emission rates at the third cattle feedlot. Analyses of PM_{10} emission rates and meteorological parameters indicated that PM_{10} emissions at the feedlot were influenced by friction velocity, sensible heat flux, temperature, and surface

roughness. Based on pen surface water content measurements, a water content of at least 20% (wet basis) significantly lowered PM_{10} emissions at the feedlot.

The dispersion of particulate from a simulated feedlot pen was predicted using CFD turbulence model (k-ε model) and AERMOD. Compared to CFD, AERMOD responded differently to wind speed setting, and was not able to provide detailed vertical concentration profiles such that the vertical concentration gradients at the first few meters from the ground were negligible. This demonstrates some limitations of AERMOD in simulating dispersion for area sources such as cattle feedlots and suggests the need to further evaluate its performance for area source modeling.

ESTIMATING PARTICULATE EMISSION RATES FROM LARGE BEEF CATTLE FEEDLOTS

by

HENRY F. BONIFACIO

B.S., University of the Philippines - Diliman, 2001
M.S., Kansas State University, 2009

A DISSERTATION

submitted in partial fulfillment of the requirements for the degree

DOCTOR OF PHILOSOPHY

Department of Biological and Agricultural Engineering
College of Engineering

KANSAS STATE UNIVERSITY
Manhattan, Kansas

2013

Approved by:

Major Professor
Ronaldo G. Maghirang

Copyright

Abstract

Emission of particulate matter (PM) and various gases from open-lot beef cattle feedlots is becoming a concern because of the adverse effects on human health and the environment; however, scientific information on feedlot emissions is limited. This research was conducted to estimate emission rates of PM_{10} from large cattle feedlots. Specific objectives were to: (1) determine feedlot PM_{10} emission rates by reverse dispersion modeling using AERMOD; (2) compare AERMOD and WindTrax in terms of their predicted concentrations and back-calculated PM_{10} emission rates; (3) examine the sensitivity of both AERMOD and WindTrax to changes in meteorological parameters, source location, and receptor location; (4) determine feedlot PM_{10} emission rates using the flux-gradient technique; and (5) compare AERMOD and computational fluid dynamics (CFD) in simulating particulate dispersion from an area source.

PM_{10} emission rates from two cattle feedlots in Kansas were determined by reverse dispersion modeling with AERMOD using PM_{10} concentration and meteorological measurements over a 2-yr period. PM_{10} emission rates for these feedlots varied seasonally, with overall medians of 1.60 and 1.10 g /m^2-day. Warm and prolonged dry periods had significantly higher PM emissions compared to cold periods. Results also showed that the PM_{10} emissions had a diurnal trend; highest PM_{10} emission rates were observed during the afternoon and early evening periods.

Using particulate concentration and meteorological measurements from a third cattle feedlot, PM_{10} emission rates were back-calculated with AERMOD and WindTrax. Higher PM_{10} emission rates were calculated by AERMOD, but their resulting PM_{10} emission rates were highly linear ($R^2 \geq 0.88$). As such, development of conversion factors between these two models is feasible. AERMOD and WindTrax were also compared based on their sensitivity to changes in meteorological parameters and source locations. In general, AERMOD calculated lower concentrations than WindTrax; however, the two models responded similarly to changes in wind speed, surface roughness, atmospheric stability, and source and receptor locations.

The flux-gradient technique also estimated PM_{10} emission rates at the third cattle feedlot. Analyses of PM_{10} emission rates and meteorological parameters indicated that PM_{10} emissions at the feedlot were influenced by friction velocity, sensible heat flux, temperature, and surface

roughness. Based on pen surface water content measurements, a water content of at least 20% (wet basis) significantly lowered PM_{10} emissions at the feedlot.

The dispersion of particulate from a simulated feedlot pen was predicted using CFD turbulence model (k-ε model) and AERMOD. Compared to CFD, AERMOD responded differently to wind speed setting, and was not able to provide detailed vertical concentration profiles such that the vertical concentration gradients at the first few meters from the ground were negligible. This demonstrates some limitations of AERMOD in simulating dispersion for area sources such as cattle feedlots and suggests the need to further evaluate its performance for area source modeling.

Table of Contents

List of Figures

List of Tables

List of Nomenclature

Acronyms

AERMOD	American Meteorological Society/Environmental Protection Agency Regulatory Model
AERMOD-EC	AERMOD using eddy covariance-based parameters
AERMOD-PD	AERMOD using AERMET-generated meteorological files
AFOs	Animal feeding operations
ARM	Atmospheric Radiation Measurement
bLS	Backward Lagrangian stochastic technique
CFD	Computational Fluid Dynamics
CAFOs	Concentrated animal feeding operations
EC	Eddy covariance
EDP	Evening dust peak
FB	Fractional bias
IQR	Interquartile range
ISCST3	Industrial Source Complex – Short Term Model
NAAQS	National Ambient Air Quality Standards
NAEMS	National Air Emissions Monitoring Study
NOAA	National Oceanic and Atmospheric Administration
NRC	National Research Council
PFL	Profile data file
PM	Particulate matter
$PM_{2.5}$	Particulate matter with equivalent aerodynamic diameter of 2.5 µm or less
PM_{10}	Particulate matter with equivalent aerodynamic diameter of 10 µm or less
RANS	Reynolds-averaged Navier-Stokes
SD	Standard deviation
SFC	Surface data file
SJVAPCD	San Joaquin Valley Air Pollution Control District
TEOM^{TM}	Tapered element oscillating microbalance
USDA	U.S. Department of Agriculture
U.S. EPA	U.S. Environmental Protection Agency
WindTrax-SD	WindTrax using sonic anemometer data
WindTrax-3V	WindTrax using wind speed, surface roughness and Monin-Obukhov length data

Notations

A	Total feedlot pen area (m^2)
a_i	Function in the Lagrangian stochastic technique
$b_{i,j}$	Function in the Lagrangian stochastic technique
C, c	Concentration, particle concentration ($\mu g/m^3$)
C_A	Predicted concentration in the reverse dispersion modeling using an assumed emission rate (e.g., $\mu g/m^3$)

C_o	Measured concentration downwind of the source (e.g., µg/m^3)
C_{CFD}	Concentration calculated by CFD (e.g., µg/m^3)
dc/dz	Vertical concentration gradient for flux-gradient technique (µg/m^3-m)
$d\xi_j$	Random parameter in the Lagrangian stochastic technique
D_x	Effective diffusion (i.e., molecular and eddy) coefficient in x-direction (m^2/sec)
D_y	Effective diffusion (i.e., molecular and eddy) coefficient in y-direction (m^2/sec)
D_z	Effective diffusion (i.e., molecular and eddy) coefficient in z-direction (m^2/sec)
EF	Emission factor (kg/1,000 hd-day)
F_{dw}	Downwind factor for the Gaussian plume model, equivalent to inverse of wind speed
F_{cw}, P_y	Crosswind factor for the Gaussian plume model; probability density function for describing the lateral concentration distribution
F_v, P_z	Vertical factor for the Gaussian plume model; probability density function for describing the vertical concentration distribution
$F_q(x)$	Source depletion factor
F/S_o	Normalized flux
g	Gravitational acceleration (m/sec^2)
H, h_{abl}	Atmospheric boundary layer height (m)
i	Subscript denoting the three directions (downwind, crosswind, and vertical)
j	Subscript for the direction evaluated
k	Turbulent kinetic energy
k_v	von Karman constant (0.4), expressed as k in Chapter 6
K_c	Eddy diffusivity for PM_{10} (m^2/sec)
K_m	Eddy diffusivity for momentum (m^2/sec)
L	Monin-Obukhov length (m)
N	Number of cattle in thousand (e.g., 30 for 30,000 head)
P	Pressure force
psd	Particle size distribution
Q, Q_p	Emission rate (e.g., µg/m^2-sec)
Q_A	Assumed emission rate in reverse modeling (e.g., µg/m^2-sec)
Q_o	Back-calculated emission rate in reverse modeling (e.g., µg/m^2-sec)
Q_{yr}	Mean emission rate (g/m^2-day)
R_a	Aerodynamic resistance (sec/m)
R_p	Quasi-laminar sublayer resistance (sec/m)
R^2	Coefficient of determination
S	Generation term
S_c	Schmidt number
S_{CF}	Slip correction factor
TSP	Total suspended particulate
x	Downwind direction; particle position in the Lagrangian stochastic technique for Chapter 2; fetch (m) for Chapter 5
u	Particle velocity in the Lagrangian stochastic technique for Chapter 2
u_x, u	Downwind component of velocity/wind speed (m/sec), wind anemometer-based wind speed (m/sec)
u_y, v	Crosswind component of velocity/wind speed (m/sec)
u_z, w	Vertical component of velocity/wind speed (m/sec)

u_*	Friction velocity (m/sec)
v_i	Sonic anemometer parameter (i.e., wind speed components, temperature)
V_d	Deposition velocity of particles (m/sec)
V_g	Settling velocity of particles (m/sec)
w_o	Vertical touchdown velocity in the backward Lagrangian stochastic technique
w_*	Convective velocity scale (m/sec)
y	Crosswind direction
z	Vertical direction
z_m	Sampler measurement height, expressed as z in Chapter 7 (m)
z_o	Surface roughness (cm, m)
z_u	Length scale
ε	Turbulent dissipation rate
ϕ	Fluid property transported for the general transport equation
$\overline{\phi}$	Average component for the fluid property
ϕ'	Fluctuation component for the fluid property
ϕ_m	Nondimensional correction parameter
ρ	Particle density (g/cm^3) for Chapter 3; air density for Chapter 7
μ	Air viscosity (g/cm-sec)
μ_t	Turbulent viscosity (g/cm-sec)
σ	Standard deviation for a wind velocity component (i.e., downwind, crosswind, vertical)
σ_k	Turbulent Prandtl number for turbulent kinetic energy
σ_ε	Turbulent Prandtl number for turbulent dissipation rate
τ_{ij}	Viscous stress component for the Navier-Stokes equation
Γ, Γ_D	Diffusion coefficient
Γ_L	Laminar component of diffusion coefficient
Γ_T	Turbulent component of diffusion coefficient
ψ	Stability terms in vertical profiling of velocity
$< v_i \times v_j >$	Mean product between two sonic anemometer-based parameters
$< v'_i v'_j >$	Covariance between two sonic anemometer-based parameters
$< v_i >$	Average of a sonic anemometer-based parameter (v_i)

Acknowledgements

I would like to express my gratitude to the following who contributed to my research and graduate program:

- My major professor, Dr. Ronaldo Maghirang, for the opportunity given to me to pursue both M.S. and Ph.D. graduate studies at Kansas State University. Thank you for sharing your knowledge and insights, and for guiding me as I pursued my graduate degrees for the last five and a half years.
- My graduate committee, Dr. Larry Glasgow (Department of Chemical Engineering, KSU), Prof. Pat Murphy (Department of Biological and Agricultural Engineering, KSU) and Dr. John Prueger (USDA Agricultural Research Service, Ames, Iowa), for their willingness and time spent to be members of my committee, and for the insights shared on my research. I also would like to thank Dr. Duane Davis (Department of Animal Sciences and Industry, KSU) for serving as my graduate committee outside chair.
- The USDA NIFA Special Research Grant "Air Quality: Reducing Air Emissions from Cattle Feedlots and Dairies (TX and KS)" through the Texas AgriLife Research and Extension Center of the Texas A&M University System, USDA NIFA Research Project No. 2009-35112-3544, "Characterization and Measurement of Air Emissions from Large Cattle Feedlot," Kansas Agricultural Experiment Station, and USDA Agricultural Research Service for supporting this research. The cooperation of the feedlot managers/operators and KLA Environmental Services is also acknowledged.
- For those I worked with, those who served as co-authors in my manuscripts, and those who gave me opportunities to learn more outside my research: the K-State BAE Air Quality group, namely Edna Razote, Dr. Li Guo, Dr. Orlando Aguilar, Howell Gonzales, Curtis Leiker, Jeremy Meeks, Youjie Xu, and Darrell Oard; our project collaborators, Dr. Steven Trabue (USDA-ARS, Iowa), Dr. Kenwood Scoggin (USDA-ARS, Iowa), Dr. Laura McConnell (USDA-ARS, Maryland), Dr. Brent Auvermann (Texas A&M University), Dr. Joseph Harner (BAE Department, KSU), and Dr. Bernardo Predicala (Prairie Swine Centre, Saskatchewan, Canada).

I also would like to acknowledge the BAE faculty, staff, and graduate students; the Filipino community in Manhattan, and the K-State Philippine Student Association (PhilSA) for making my stay here at K-State and Manhattan remarkable.

I would like to thank my family, my parents and siblings. Mama and Papa, thank you for the love and encouragement, and for the sacrifices both of you had to endure all these years.

And lastly, to Lord, our God, for giving me wisdom and strength, thank You.

CHAPTER 1 - **Introduction**

1.1 Background

The beef cattle feeding industry in the U.S. is projected to grow in the coming years. Although U.S. Department of Agriculture (USDA) reported a slight decrease (6%) in the total number of beef cattle feedlots in the past three years, the number of large capacity-cattle feedlots has increased steadily. For example, the number of feedlots with more than 16,000 head-capacity increased by 6% in 2010 and was maintained in 2011; the number of 50,000+ head-capacity feedlots increased by 8 and 3% in 2010 and 2011, respectively (National Agricultural Statistics Service, 2010, 2011, 2012). Considering all feedlots, cattle inventory for the month of February increased by 3 and 1% for years 2010 and 2011, respectively; for 16,000+ head capacity feedlots, cattle inventory increased by 7% in 2010 and 5% in 2011 (National Agricultural Statistics Service, 2010, 2011, and 2012). Almost 78% of all cattle fed in 1,000+ head-capacity feedlots, approximately 9 million cattle, are located in the High Plains states of TX, KS, OK, NE, and CO (National Agricultural Statistics Service, 2010, 2011, and 2012).

With the steady growth of the beef cattle feeding industry, air quality issues related to cattle feeding operations are also expected to rise (Midwest Plan Service, 2002). Pollutant emissions associated with open-lot beef cattle feedlots that can affect air quality include particulate matter (PM), gases such as ammonia (NH_3), methane (CH_4) and other greenhouse gases (GHGs), and odorous volatile organic compounds. Based on latest steps taken by U.S. Environmental Protection Agency (EPA) concerning concentrated animal feeding operations (CAFOs) (CFR, 2011), cattle feedlots may eventually be subjected to air pollutant emissions regulations. As stated by U.S. EPA, more research data on gaseous and PM emissions from CAFOs are needed (CFR, 2011; Purdue Applied Meteorology Laboratory, 2009). In 2005, U.S. EPA established the National Air Emissions Monitoring Study (NAEMS) and worked with several owners/stakeholders of various CAFOs to measure data on gaseous and PM emissions on several participating CAFOs units that would be used to collect science-based pollutant emission rates, and to develop and evaluate air pollutant emission estimation methodologies for CAFOs (U.S. Environmental Protection Agency, 2005; CFR, 2011). Having accurate pollutant emissions data and appropriate emission estimation techniques would benefit CAFOs as they can estimate

their emissions and evaluate their air pollutant abatement measures. None of the CAFO units monitored in NAEMS represented the beef cattle feeding operations.

Clearly, data on gaseous and PM emissions are still limited for large open-lot cattle feedlots. More research is needed to quantify and characterize air emissions from cattle feedlots. Quantifying air emission rates from open feedlots is difficult, largely because of their unique characteristics, including surface heterogeneity, wide variation in source geometry, and temporal and spatial variability of emission rates. National Research Council (NRC) (2003) summarized various techniques appropriate for estimating air pollutant emission rates from area sources like cattle feedlots. Techniques suggested are (1) micrometeorological techniques (e.g., eddy covariance, flux-gradient, etc.), (2) mass balance technique, (3) atmospheric tracers, and (4) atmospheric dispersion models. Based on emission studies on open sources such as agricultural lands and feedlots, commonly used techniques in determining emission rates from open area sources include micrometeorological techniques and atmospheric dispersion models. For atmospheric dispersion model, the current U.S. EPA preferred model is the American Meteorological Society/Environmental Protection Agency Regulatory Model (AERMOD), a Gaussian-based model capable of modeling area sources (CFR, 2005; Cimorelli et al., 2004; Turner and Schulze, 2007). Despite being the U.S. EPA regulatory model, AERMOD's use in emission studies on open area sources, like CAFOs, is limited compared to other techniques. Techniques that had been in used in most recent emission studies involving area sources are micrometeorological techniques (Myles et al., 2011; Muller et al., 2009; Prueger et al. 2005) and WindTrax dispersion model (Flesch et al., 2009; Galvin et al., 2006; Leytem et al., 2011).

For PM emissions from cattle feedlots, several estimates of emission rates are available from previous studies. These estimates were determined either by mass balance techniques (Countess Environmental, 2006; San Joaquin Valley Unified Air Pollution Control District, 2010) or atmospheric dispersion models (Wanjura et al., 2004; McGinn et al., 2010), which included ISCST3 (i.e., Gaussian model, the previous U.S. EPA preferred model) and WindTrax (i.e., Lagrangian model); the published U.S. EPA PM_{10} emission factor was derived using a simple Gaussian model (Midwest Research Institute, 1988). Comparison of these estimates, however, might not be meaningful due to their differences in derivation, which included differences in length of measurement periods (i.e., most were based on several measurement days only), feedlot characteristics (e.g., number of cattle, pen surface conditions), concentration

and meteorological measurements (e.g., equipment used, measurement design), and emission estimation technique. From these same reasons, use of these PM emission estimates on evaluating PM concentrations downwind might not always be appropriate for all feedlots. More important, limitations of these emission estimation and/or emission simulation techniques must be addressed. One limitation is that air pollutant emission rates maybe model-specific, which means that the emission rate derived with one model may not be suitable for another (Hall et al., 2002; Faulkner et al., 2007). Another limitation is that studies on performances of these techniques in estimating emission and/or modeling dispersion from area sources are still limited, mainly to the fact that quantifying accurate emissions rates from open area sources is challenging. As a result, the identification of the technique that gives the most accurate estimate remains a challenge.

This dissertation addresses several research issues concerning air pollutant emission estimation for open area sources, specifically for cattle feedlots. Using PM_{10} concentrations and micrometeorological/meteorological parameters measured at several commercial cattle feedlots in Kansas, PM_{10} emission rates were determined by various techniques that included two atmospheric dispersion models and a micrometeorological technique. As the current U.S. EPA regulatory model, AERMOD's performance on area source modeling was assessed by comparing it to other derived PM_{10} emission rates, and its response to several meteorological parameters, and by evaluating its dispersion simulation.

1.2 Research Objectives

The overall goal of this dissertation was the development of science-based PM_{10} emission rates for large commercial beef cattle feedlots. The objectives were to:

1. Determine PM_{10} emission rates from beef cattle feedlots by reverse dispersion modeling with AERMOD.
2. Compare AERMOD (i.e., Gaussian model) and WindTrax (i.e., Lagrangian model) in terms of their predicted PM_{10} concentrations and emission rates.
3. Investigate the sensitivity of AERMOD and WindTrax to changes in meteorological parameters and area source-receptor locations.
4. Determine PM_{10} emission rates using the flux-gradient method.
5. Simulate the dispersion of particulates from an area source using computational fluid dynamics (CFD) and compare predicted results from AERMOD.

1.3 Rationale

Along with the growth of the beef cattle feeding industry in the U.S. is the expected rise in air quality concerns related to cattle feeding operations. To date, U.S. EPA has undertaken several actions to learn more about air emissions from CAFOs, which include cattle feedlots. Based on these developments, air pollutant emissions from CAFOs may eventually be regulated. As expressed by U.S. EPA, more science-based data are needed to gain more knowledge on CAFOs air pollutants, particularly from large beef cattle feedlots, and to serve as guidelines on establishing air regulations applicable for CAFOs. Several studies had been conducted to determine air pollutants from cattle feedlots; however, most of these focused on gaseous emissions and only a few dealt with PM. Starting December 2005, the U.S. EPA identified AERMOD as its current regulatory model for dispersion. With AERMOD capable of modeling almost all types of sources (i.e., point, area, and volume), standardization of atmospheric dispersion simulation and air emission rate determination is feasible. However, use of AERMOD in modeling area sources is limited. More study is needed on the use of AERMOD on area sources, such as cattle feedlots; performance of AERMOD should also be evaluated by comparing it to techniques commonly used in area source modeling.

Work performed in this dissertation provides technical information on estimation of PM_{10} emissions from cattle feedlots that will be useful to scientists, engineers, policy makers on air quality regulations, and CAFOs producers/operators. PM_{10} emission rates derived were based on measurement periods significantly longer than those in previous studies. Different approaches of estimating emission rates and/or simulating particle dispersion were presented and compared; results of comparison may be used in development of conversion factors between models and/or improvement of modeling performance of techniques used. Findings presented in this dissertation will also be useful on research on air pollutant emissions other than PM_{10}.

1.4 Organization of the Dissertation

This dissertation has eight chapters. Chapter 1 states the objectives and significance of the research. Chapter 2 is a review of literature on PM emissions from cattle feedlots and on different techniques on estimating emissions. Chapter 3 is a study that determined PM_{10} emission rates from two cattle feedlots in Kansas by reverse dispersion modeling with AERMOD. Chapters 4 and 5 compare AERMOD and WindTrax dispersion models in terms of their

estimated PM_{10} emission rates for a Kansas cattle feedlot and of their response to different modeling inputs, respectively. Chapter 6 estimates PM_{10} emission rates from cattle feedlots using the flux-gradient technique. Additional analyses on the flux-gradient technique are summarized in Appendices A, which is a verification of turbulent fluctuations of PM_{10} emissions at the studied feedlot, and B, which is a partial comparison of the flux-gradient technique to both AERMOD and WindTrax. Chapter 7 is a study that evaluated the performance of AERMOD and CFD turbulence model in simulating particle transport/dispersion. Additional graphs for AERMOD and CFD dispersion simulations are included in Appendix C. And last, Chapter 8 provides the conclusions and recommendations.

1.5 References

Cimorelli, A.J., S.G. Perry, A. Venkatram, J.C. Weil, R.J. Paine, R.B. Wilson, R.F. Lee, W.D. Peters, R.W. Brode, and J.O. Paumier. 2004. *AERMOD: Description of Model Formulation*, EPA-454/R-03-004. NC: U.S. Environmental Protection Agency.

CFR. 2005. Code of Federal Regulations, 40 CFR, Part 51: Revision to the guideline of air quality models: Adoption of a preferred general purpose (flat and complex terrain) dispersion model and other revisions.

CFR., 2011. Code of Federal Regulations, 40 CFR, Part 60: Call for Information: Information related to the development of emission-estimating methodologies for animal feeding operations.

Countess Environmental. 2006. *Western Regional Air Partnership (WRAP) Fugitive Dust Handbook,* Contract No. 30204-111. Denver, CO: Western Governors' Association.

Faulkner, W. B., J.J. Powell, J.M. Lange, B.W. Shaw, R.E. Lacey, and C.B. Parnell. 2007. Comparison of dispersion models for ammonia emissions from a ground-level area source. *Trans. ASABE* 50:2189-2197.

Flesch, T.K., L.A. Harper, J.M. Powell, and J.D. Wilson. 2009. Inverse-dispersion calculation of ammonia emissions from Wisconsin dairy farms. *Trans. ASABE* 52:253-265.

Galvin, G., C. Henry, D. Parker, R. Ormerod, P. D'Abreton, and M. Rhoades. 2006. Efficacy of Lagrangian and a Gaussian model for back calculating emission rates from feedyard area sources. Paper presented at the Workshop on Agricultural Air Quality, Potomac, MD, June 5-8, 2006.

Hall, D.J., A.M. Spanton, M. Bennett, F. Dunkerley, R.F. Griffiths, B.E.A. Fisher, and R.J. Timmis. 2002. Evaluation of new generation atmospheric dispersion models. *Int. J. Environmental and Pollution* 18:22–32.

Leytem, A.B., R.S. Dungan, D.L. Bjorneberg, and A.C. Koehn. 2011. Emission of ammonia, methane, carbon dioxide, and nitrous oxide from dairy cattle housing and manure management systems. *J. Environ. Qual.* 40:1383-1394. doi:10.2134/jeq2009.0515.

McGinn, S.M., T.K. Flesch, D. Chen, B. Crenna, O.T. Denmead, T. Naylor, and D. Rowell. 2010. Course particulate matter emissions from cattle feedlots in Australia. *J. Environ. Qual.* 39:791-798. doi:10.2134/jeq2009.0240.

Midwest Plan Service. 2002. Outdoor air quality – Midwest Plan Service-18 Manure Management System Series 18. Section 18. Ames, IA: Midwest Plan Service.

Midwest Research Institute. 1988. *Gap Filling PM_{10} Emission Factors for Selected Open Area Dust Sources,* EPA-450/4-88-003. NC: U.S. Environmental Protection Agency.

Muller, J.B.A., M. Coyle, D. Fowler, M.W. Gallagher, E.G. Nemitz, and C.J. Percival. 2009. Comparison of ozone fluxes over grassland by gradient and eddy covariance technique. *Atmos. Sci. Let.* 10:164-169. doi:10.1002.asl.226.

Myles, L., J. Kochendorfer, M.W. Heuer, and T.P. Meyers. 2011. Measurement of trace gas fluxes over an unfertilized agricultural field using the flux-gradient technique. *J. Environ. Qual.* 40:1359-1369. doi:10.2134/jeq2009.0386.

National Agricultural Statistics Service. 2010. Cattle on Feed February 2010. Washington, DC: National Agricultural Statistics Service, U.S. Department of Agriculture. Available at www.nass.usda.gov.

National Agricultural Statistics Service. 2011. Cattle on Feed February 2011. Washington, DC: National Agricultural Statistics Service, U.S. Department of Agriculture. Available at www.nass.usda.gov.

National Agricultural Statistics Service. 2012. Cattle on Feed February 2012. Washington, DC: National Agricultural Statistics Service, U.S. Department of Agriculture. Available at www.nass.usda.gov.

National Research Council. 2003. *Air Emissions from Animal Feeding Operations: Current Knowledge, Future Needs*. Washington, D.C.: National Academy of Sciences.

Prueger, J.H., T.J. Gish, L.L. McConnell, L.G. McKee, J.L. Hatfield, and W.P. Kustas. 2005. Solar radiation, relative humidity, and soil water effects on Metolachlor volatilization. *Environ. Sci. Technol.* 39:5219-5226.

Purdue Applied Meteorology Laboratory. 2009. *Qualtity Assurance Project Plan for the National Air Emissions Monitoring Study,* Revision No. 3. West Lafayette, IN: Purdue University.

Turner, D.B., and R.H. Schulze. 2007. *Practical Guide to Atmospheric Dispersion Modeling*. Dallas, TX: Trinity Consultants, Inc. and Air & Waste Management Association.

U.S. Environmental Protection Agency. 2005. *Consent Agreement and Final Order*. Available at www.epa.gov/compliance/resources/agreements/caa/cafo-agr-050121.pdf. Accessed March 6, 2012.

Wanjura, J.D., C.B. Parnell, B.W. Shaw, and R.E. Lacey. 2004. A protocol for determining a fugitive dust emission factor from a ground level area source. Paper presented at American Society of Agricultural Engineers (ASAE) Proceedings, Ontario, Canada. August 1-4, 2004. ASAE Paper Number 044018.

CHAPTER 2 - **Literature Review**

2.1 Particulate Matter (PM) Emissions from Cattle Feedlots

2.1.1 Sources and Control in Cattle Feedlots

Commercial beef cattle feedlots are large open lots exposed to the outside environment, making particulate and gaseous emissions difficult to control and impossible to confine within the feedlot vicinity. The primary PM source in feedlots are the pen surfaces composed mainly of soil and manure, with the amount of manure depending on feedlot practices (e.g., cattle stocking density, pen cleaning, and manure harvesting frequency). Frequent removal of this soil/manure layer by pen cleaning and manure harvesting will greatly reduce the PM emissions. PM generation from the pen surface is triggered by cattle activity through hoof action on the dry, loose soil/manure layer on the pen surface, and is influenced by the hoof's speed, force and resulting penetration depth (Guo et al., 2011; Razote et al., 2006). Within a given day, cattle tend to be more active during the early evening period (Auvermann et al., 2006; Mitloehner, 2000); the increased cattle activity is likely one of the main factors contributing to high PM concentrations during this period (Bonifacio et al., 2011; Sweeten et al., 1988). Several studies suggested that limiting the cattle activity may lead to significant reduction in PM emissions; methods that can control cattle activity include increasing the stocking density (Romanillos and Auvermann, 1999) and manipulating the feeding schedule/practices (Mitloehner, 2000).

The water content of the pen surface also influences the PM emissions; the higher the water content, the lower the PM emission potential (Miller and Woodbury, 2003). Water is added to the pen surface through cattle excretion of urine, precipitation and any water application system, and is removed through evaporation. Watering pen surfaces is one of the common practices of managing dusty conditions at open-lot feedlots and surrounding areas (Alberta Cattle Feeders' Association, 2002; National Resources Conservation Service, 2003). Water can be applied using either solid-set sprinkler system or traveling gun sprinkler system/water trucks (Amosson et al., 2006; Amosson et al., 2007). Previous studies have quantified efficiencies of water application in suppressing dust emissions at cattle feedlots. Laboratory experiments on a simulated pen surface showed that application of 3.2 mm water had PM_{10} control efficiencies of at least 42% (Razote et al., 2006; Guo et al., 2011). Field measurements done at a Kansas feedlot

equipped with a solid-set sprinkler system, which had an application rate of 5 mm/day (L/m^2-day), revealed PM_{10} control efficiencies ranging from 32 to 80% (Bonifacio et al., 2011).

Other sources of PM in cattle feedlots include unpaved roads, truck/equipment engine emissions, and feed mill operations. PM emissions from unpaved roads are generated during daytime because of road traffic; during this period, trucks travel around pens for cattle feeding and, trucks/tractors are used for manure harvesting operations. Manure harvesting operations can be year-long operations, depending on management practice, number of pens, and labor and equipment availability. Factors affecting unpaved road PM emissions are vehicle weight, miles travelled, traffic volume and unpaved road material properties (Midwest Research Institute, 1988; U.S. Environmental Protection Agency, 2001). Another PM source is wind erosion. Based on a U.S. EPA document (1995), wind speeds greater than 19 km/hr (5.28 m/sec) can lead to significant dust generation from open sources; a feedlot study indicated that wind speeds of 3 to 3.3 m/sec can already trigger significant dust generation from unpaved roads (McGinn et al., 2010).

2.1.2 Factors Affecting Particulate Matter Concentrations

Three main variables influencing concentrations downwind of a pollutant source are: (1) pollutant emission rate at the source – the higher the emission rate, the higher the downwind concentration because more pollutant is released to the atmosphere; (2) wind speed – the higher the wind speed, the lower the concentration because of dilution effects; and (3) atmospheric conditions – the more stable the atmosphere, the higher the concentration because of less vertical mixing/dispersion (Cimorelli et al., 2004; Flesch et al., 1995). Effects of these three variables on concentrations can be observed at cattle feedlots by examining PM concentration trends within the day. Early evening period has the highest PM concentrations because of higher PM emissions from the pens brought about increased cattle activity during this period and stable atmospheric conditions (Auvermann et al. 2006). Because of unstable atmospheric conditions (i.e., stronger vertical mixing), afternoon period has relatively lower PM concentrations in spite of dust-generating activities (e.g., cattle activity, cattle transfer, feeding, pen cleaning, feed milling) taking place. Lowest PM concentrations, on the other hand, can be observed during early morning hours, likely because of the absence of activities capable of dust generation.

To lower the PM concentration downwind of feedlots, variables affecting PM emission and dispersion must be controlled. As discussed, several measures can be implemented to reduce the amount of PM generated from different sources within the feedlot, such as pens and unpaved roads; these include control of the pen's soil/manure layer depth, manipulation of cattle activity, and water application on both pen surfaces and unpaved roads. Installation of shelterbelts/windbreaks upwind and downwind of the feedlot can lessen effects of wind by reducing wind-generated PM and limiting the PM transport downwind of the source, respectively (Wang et al., 2001; Midwest Plan Service, 2002).

2.1.3 Health and Environmental Concerns on Particulate Matter from Animal Feeding Operations

PM is a criteria air pollutant primarily due to its adverse effects on human health (CFR, 2010; Cooper and Alley, 2002). PM pollution can be grouped as coarse ($PM_{2.5}$ to PM_{10}) and fine particulates ($PM_{2.5}$) (U.S. Environmental Protection Agency, 2011). PM can also be classified based on its impact on human health, specifically on how far it penetrates the human respiratory system: particulates that cannot penetrate beyond the nose region are considered inhalable; coarse particles that can reach bronchiolar regions are called thoracic particles; and fine particles, referred to as respirable particles, can reach the alveolar regions of the lungs (Mitloehner and Calvo, 2008). Several health studies suggested that both PM_{10} and $PM_{2.5}$ can cause cardiopulmonary problems to human population; some of the lung- and heart-related problems include difficulty in breathing, increased asthma attacks, chronic bronchitis, irregular heartbeat and nonfatal heart attacks (U.S. Environmental Protection Agency, 2011). Development of these cardiopulmonary problems is also noted to be affected by other factors such as age, pre-existing health conditions, and length of exposure (Duzgoren-Aydin, 2008).

PM has been an integral part of health studies done on CAFOs. Although most of these studies focused on CAFO workers' health, potential risks presented are also applicable to public as PM in the air can be transported over long distances (Duzgoren-Aydin, 2008). PM from cattle feedlots are mainly soil and manure emitted from pen surfaces and silt materials generated from unpaved roads. And like in other CAFOs, feedlot PM emissions may contain microorganisms, endotoxins/toxins, animal dander and allergens that can trigger allergic reactions and endotoxin-

related illnesses to high-risk population (Kirkhorn and Schenker, 2002; Mitloehner and Calvo, 2008).

PM also has negative impacts on the environment. In large concentrations, PM, especially the fine particulates, reduces visibility as it can produce haze due to particle's light scattering and absorption properties, and lead to fog/smog formation (Cooper and Alley, 2002). Atmospheric PM can affect the ecosystem as it settles on either ground or water, altering the physical and nutritional conditions of soil and water formations, and thus hindering plant growth (Cooper and Alley, 2002; U.S. Environmental Protection Agency, 2011). PM can also cause corrosion and erosion of structures and properties as it can adsorb and carry toxic chemicals amidst transport (Cooper and Alley, 2002).

2.1.4 U.S. EPA National Air Emissions Monitoring Study on Concentrated Animal Feeding Operations

Air pollutant emissions from cattle feedlots and other CAFOs are not regulated; as agricultural operations, CAFOs have been exempted from regulations concerning air quality (National Research Council, 2003; Lester, 2006). Recent developments, however, demonstrate the increasing concern on air quality issues associated with CAFOs. On January 21, 2005, U.S. EPA (2005) finalized the *Consent Agreement and Final Order* to address air pollutant emissions from CAFOs that included ammonia (NH_3), hydrogen sulfide (H_2S), particulate matter (TSP, PM_{10}, $PM_{2.5}$), and volatile organic compounds (VOCs) . With this agreement, U.S. EPA worked with owners/stakeholders in measuring air emissions from various CAFO facilities. Consequently, a two-year National Air Emissions Monitoring Study (NAEMS) was established to gather air pollutant emissions data that would be used in developing and improving emission estimation techniques, which can then be utilized by CAFOs to determine and control their air emissions (U.S. Environmental Protection Agency, 2005). A total of 25 CAFOs facilities participated in NAEMS, yet none of them represented the beef cattle feeding industry (Lester, 2006; Purdue Applied Meteorology Laboratory, 2009). One facility monitored in NAEMS was a dairy facility with an open-lot setting similar to cattle feedlots; still, use of air emission measurements from this facility for cattle feedlots would be inappropriate as its animal capacity was very low (3,400 head) compared to typical commercial beef cattle feedlots (e.g., tens of

thousands) (Grant and Boehm, 2010). In addition, air emission data collected from this dairy facility were only on NH_3 and H_2S (Grant and Boehm, 2010).

To obtain more data on CAFOs air pollutant emissions, on January 19, 2011, U.S. EPA released a *Call for Information* requesting for quality-assured emission data on NH_3, H_2S, TSP, PM_{10}, $PM_{2.5}$, and VOCs for swine, dairy, beef, egg-layer, broiler and turkey operations that can be added to the emission data collected through NAEMS (CFR, 2011).

2.2 Emission Estimating Techniques

The foundation of air pollutant transport simulation is the mass transfer equation written as:

$$\frac{\partial C}{\partial t}+\frac{\partial (Cu_x)}{\partial x}+\frac{\partial (Cu_y)}{\partial y}+\frac{\partial (Cu_z)}{\partial z}=\frac{\partial^2 (D_x C\ )}{\partial x^2}+\frac{\partial^2 (D_y C\ )}{\partial y^2}+\frac{\partial^2 (D_z C\ )}{\partial z^2}+S \quad (2\text{-}1)$$

where C is concentration, u_x, u_y and u_z are components of wind speed in downwind (x-), crosswind (y-) and vertical (z-) directions, respectively, D_x, D_y, and D_z are effective diffusion coefficients in x-, y-, z-directions, respectively, and S is generation/source term (Heinsohn and Kabel, 1999). The left-hand side of the equation is composed of the accumulation term ($\partial c/\partial t$) and the three convective mass transport terms, whereas the right-hand side has the generation term (S) and the three diffusion (i.e., molecular and eddy) transport terms.

Air emission estimation techniques appropriate for sources with surface areas of 10^2 to 10^6 m^2 include reverse atmospheric dispersion modeling and micrometeorological methods (National Research Council, 2003), and these techniques are developed using reduced forms of eq 2-1 (Flesch and Wilson, 2005; Heinsohn and Kabel, 1999; Meyers and Baldocchi, 2005). Common requirement for these emission estimation techniques are concentration measurements, meteorological measurements, and area source dimensions. Shortcomings shared by these techniques include assumption of surface homogeneity, which implies constant and uniform emission rate throughout the area source, and limitations in concentration and meteorological sensors (National Research Council, 2003).

2.2.1 AERMOD

AERMOD is the latest dispersion model preferred by U.S. EPA for simulating atmospheric dispersion (CFR, 2005). Similar to the previous regulatory model (ISCST3; Pacific Environmental Services, Inc., 1995), AERMOD is based on the Gaussian plume model (Cimorelli et al., 2004). The following assumptions are applied to simplify eq 2-1: steady-state conditions ($\partial c/\partial t = 0$); mass is transported by convection in x-direction with constant downwind wind speed u_x; in both y- and z-directions, mass is transported mainly by diffusion (i.e., molecular and eddy) with constant diffusion coefficients (D_y, D_z); and no reaction/generation ($S = 0$) (Heinsohn and Kabel, 1999). The governing equation for the Gaussian plume model is given by:

$$u \frac{\partial C}{\partial x} = D_y \frac{\partial^2 C}{\partial y^2} + D_z \frac{\partial^2 C}{\partial z^2} \tag{2-2}$$

The analytical solution for eq 2-2 can be expressed as four separate factors:

$$C = Q \times F_{dw} \times F_{cw} \times F_v \tag{2-3}$$

where C is concentration ($\mu g/m^3$), Q is source emission rate, F_{dw} is downwind factor, which is the inverse of wind speed, (sec/m), and F_{cw} and F_v are crosswind and vertical factors, respectively (Turner, 1994). Eq 2-3 is commonly referred to as the Gaussian plume model since the last two factors, F_{cw} and F_v, are Gaussian (Heinsohn and Kabel, 1999; Turner, 1994). In reverse dispersion modeling, the emission flux is estimated using model-predicted and measured concentrations with the expression:

$$Q_O = \frac{Q_A}{C_A} \times C_O \tag{2-4}$$

where Q_o is calculated emission flux for the source ($\mu g/m^2$-sec), C_o is measured concentration downwind of the source ($\mu g/m^3$), Q_A is assumed emission flux in the modeling (e.g., 1.0 $\mu g/m^2$-sec), and C_A is concentration ($\mu g/m^3$) predicted in the modeling using Q_A, with the assumption that the emission rate (Q in eq 2-3) is independent of the other three factors (F_{dw}, F_{cw} and F_v) (Calder, 1977).

Similar to ISCST3, AERMOD is designed for modeling dispersion for point, area, and volume sources. Unlike in ISCST3, however, planetary boundary layer is well-characterized in

AERMOD (Cimorelli et al., 2004; Turner and Schulze, 2007). In ISCST3, only three boundary layer parameters (i.e., wind speed, mixing height, and stability class) are needed to run the modeling, whereas in AERMOD, several more parameters (i.e., friction velocity, convective velocity scale, potential temperature gradient, sensible heat flux) are required. For stable conditions, concentration distributions in both vertical and crosswind directions in AERMOD are Gaussian in form. For unstable conditions, the crosswind concentration distribution still has a Gaussian form but the vertical concentration distribution is represented with a bi-Gaussian form. This bi-Gaussian concept is assumed to be a more accurate approximation of actual vertical dispersion during unstable conditions (Cimorelli et al., 2004; Perry et al., 2005).

The performance of AERMOD in modeling point sources had been evaluated using field measurements on power plants with known emission rates (Perry et al., 2005). In these field studies, concentrations of either sulfur dioxide (SO_2) or atmospheric tracer were measured at several locations around the power plants, with downwind distances as far as 50 km (Perry et al., 2005). In general, AERMOD performed well in predicting the upper end of the observed concentration distributions downwind of point sources (Perry et al., 2005) and this capability of predicting the highest concentrations is one quality desired for a regulatory model (Hanna et al., 1999; Turner and Schulze, 2007). This success of AERMOD, which also performed better than ISCST3, is attributed to its better characterization of the atmospheric boundary layer, and its use of bi-Gaussian form to represent the vertical concentration distributions during unstable conditions (Perry et al., 2005).

On the other hand, the performance of AERMOD in modeling area sources, such as beef cattle feedlots, still has to be assessed. Evaluation of AERMOD's performance would require field measurements for area sources with known/measured emission rates, and measured downwind concentrations and meteorological conditions. However, having known emission rates would be formidable because direct measurement of air pollutant emissions for area sources is not feasible. Although static chambers and wind tunnels are indeed available, use of these direct techniques on area sources like cattle feedlots can have considerable uncertainties due to non-capture of emission spatial variability, and alteration of environment during measurement (National Research Council, 2003). Preliminary studies investigating AERMOD's performance in area source modeling used sources with several points of release; with all their points discharging emissions simultaneously, these sources were treated as area sources (Hanna et al.,

1999; Perry et al., 2005). For a refinery plant with several point releases, AERMOD produced better results by predicting concentrations that differed from measured concentrations by 2% only, compared to ISCST3, whose predicted concentrations were higher by almost a factor 2. But the performance of AERMOD was not always good; at another site, AERMOD under-predicted the concentration by a factor of 2, although it must be noted that it still performed better than ISCST3, which overpredicted the concentration by a factor of 3.

AERMOD and other Gaussian-based models have several limitations. One, AERMOD is not suitable for simulating low wind speed or calm conditions (Holmes and Morawska, 2006). And two, AERMOD does not give accurate downwind concentrations at locations less than 100 m away from the source (Holmes and Morawska, 2006). Drawback of placing sampler far away from the feedlot property line is that it may lead to inaccurate concentration measurements due to presence of sources (e.g., agricultural lands, unpaved roads) other than the feedlot (Faulkner et al., 2007), and may contribute to larger uncertainties in calculated emission rates.

2.2.2 WindTrax

WindTrax is based on a reduced mass transport equation that works with accumulation and bulk motion transport terms. The governing equation can be written as:

$$\frac{\partial C}{\partial t} + u_x \frac{\partial C}{\partial x} + u_y \frac{\partial C}{\partial y} + u_z \frac{\partial C}{\partial z} = 0 \qquad (2\text{-}5)$$

with the assumption that all wind speed components (u_x, u_y, u_z) are constant (Flesch and Wilson, 2005). To solve eq 2-5, the approach chosen by the developers of WindTrax is the Lagrangian stochastic technique. The Lagrangian stochastic technique is composed of particle equations that describe the particle position and velocity evolutions (Pope, 2000) and are given by:

$$du_i = a_i(\boldsymbol{x},\boldsymbol{u},t)dt + b_{i,j}(\boldsymbol{x},\boldsymbol{u},t)d\xi_j \qquad (2\text{-}6a)$$

$$dx_i = u_i dt \qquad (2\text{-}6b)$$

where x is particle position, u is particle velocity, a_i and $b_{i,j}$ are functions of ($\boldsymbol{x}$,$\boldsymbol{u}$,t), and $d\xi_j$ is a random parameter (Thomson, 1987). Equation for the concentration is based on particle trajectory, expressed in terms of its 'touchdown' location (x_o, y_o) and vertical 'touchdown' velocity (w_o, m/sec) (Flesch and Wilson, 2005). The concentration equation is given by:

$$C = Q\left(\frac{1}{N}\sum\left|\frac{2}{w_o}\right|\right) \quad (2\text{-}7)$$

where C is predicted concentration ($\mu g/m^3$) at a given location, Q is source emission rate ($\mu g/m^2$-sec), and N is total number of particles released from the specified location (Flesch et al., 2004; Flesch et al., 1995). The summation term in eq 2-7 is equivalent to the average concentration at the location (x, y, z). A backward time frame is also applied in solution, therefore the name backward Lagrangian stochastic (bLS) method.

WindTrax is a graphical dispersion tool developed based on the bLS technique described as an effective tool for modeling emissions from surface area sources (Flesch et al., 1995). Emission rate can be determined with WindTrax either by inverse dispersion modeling (eq 2-4), in which emission rate is estimated from WindTrax-predicted and corresponding measured concentrations, or just using the measured concentration as modeling input, from which WindTrax can directly estimate the emission rate (Crenna, 2006).

The performance of WindTrax in modeling area sources had been verified using a field experiment. Using a 36 m^2 PVC manifold as the area source, results showed that predicted concentrations were higher than observed concentrations by just 2% on the average, excluding conditions with either very stable or very unstable atmospheric conditions (Flesch et al., 2004). Results also revealed that WindTrax underpredicted (by 13%) the observed concentrations during unstable conditions, and overpredicted during near-neutral (by 12%) and stable (by 38%) conditions. The large inaccuracy in concentration predicted for stable conditions was attributed to uncertainties in meteorological measurements during these conditions (Flesch et al., 2004; Massman and Lee, 2002).

WindTrax has been used for cattle feedlot studies on gases (odor, Galvin et al., 2006; NH_3, Flesch et al., 2009; greenhouse gases, Leytem et al., 2011) and PM (PM_{10}, McGinn et al., 2010). WindTrax was also one of the techniques employed in NAEMS in computing gas emissions from waste storage structures in swine and dairy (Purdue Applied Meteorology Laboratory, 2009). In addition, WindTrax is designed to model downwind distances within 1 km of the area source (Crenna, 2006), therefore, unlike AERMOD, it can model downwind locations very close to the cattle feedlot. Another appealing quality of WindTrax is that it simulates dispersion based on wind and turbulence statistics of the atmosphere (Flesch et al., 2009). The

use of these statistics was described by Wilson and Sawford (1996) as a natural and effective approach of simulating atmospheric processes, such as pollutant transport.

2.2.3 Flux-Gradient Method

The transport of trace gases and aerosols between the surface and the atmosphere is a result of turbulent transfer processes near the surface (National Research Council, 2003). Micrometeorological techniques are considered the most direct, unobtrusive methods of measuring this surface-atmosphere exchange (Ham and Baum, 2007), which comprises of mass (e.g., trace gases) and energy (e.g., sensible heat) transfers between the surface and the atmosphere (Myles et al., 2011; Prueger et al., 2005). Different micrometeorological techniques include eddy covariace/eddy correlation, eddy accumulation, relaxed eddy accumulation, flux-gradient, integrated horizontal flux, and bowen ratio-energy balance methods (Kanemasu et al., 1979; Meyers and Baldocchi, 2005; National Research Council, 2003).

The flux-gradient method is a widely used emission estimation technique. The governing equation of this method can derived from eq 2-1 by accounting only the diffusion transport in *z*-direction (Prueger and Kustas, 2005), given by:

$$0 = \frac{\partial^2 (D_z C)}{\partial z^2} \tag{2-8}$$

Assuming that the effective diffusivity, D_z, is constant, integration with respect to *z* leads to Fick's first law of diffusion given by:

$$Q_z = -D_z \frac{dc}{dz} \tag{2-9}$$

where Q_z is vertical emission flux ($\mu g/m^2$-sec), D_z is effective diffusivity (m^2/sec), and *dc/dz* is vertical concentration gradient ($\mu g/m^3$-m) (Prueger and Kustas, 2005; Muller et al., 2009). Computation for the concentration gradient, *dc/dz*, requires concentration measurements from at least two different heights/levels (National Research Council, 2003), although use of more than two measurement heights is recommended to produce the essential flux profile (Meyers and Baldocchi, 2005). The effective diffusivity, D_z, is estimated from eddy diffusivity momentum that can in turn be estimated using eddy covariance measurements (Prueger et al, 2005).

Compared to the eddy correlation method, the most direct among the micrometeorological techniques (Kanemasu et al., 1979), one positive characteristic of the flux-gradient method is it does not require fast-response sensors (e.g., more than 1 Hz sampling frequency) in concentration measurements (National Research Council, 2003). And still, the flux-gradient method produced very similar results to the eddy correlation method if based on longer sampling intervals (e.g., less than 1 Hz sampling frequency) (Muller et al., 2009). One concern with this technique, however, is its sampling procedure. As mentioned, concentration measurements can be done at several heights. One way is to allocate one instrument for each height but the downside of having several instruments is it is costly, and requires cross-calibration among instruments to reduce sampling bias (Wagner-Riddle et al., 2005). Another approach to conduct sampling is to use a single instrument equipped with an air sampling system such that it can sample through different intake ports alternately; here, the instrument must have high sensitivity to detect small concentration differences (Wagner-Riddle et al., 2005).

The flux-gradient method has been used to determine gaseous emissions from agricultural soils; it has been used to calculate emissions for NH_3 (Myles et al., 2011), nitric acid (Myles et al., 2011), ozone (Muller et al., 2009), SO_2 (Myles et al., 2011), and pesticides (Prueger et al., 2005). Although rarely used, the flux-gradient technique had been applied in cattle feedlot studies estimating emissions of NH_3 (Todd et al., 2007) and nitrogen gases (Todd et al., 2005).

2.2.4 Turbulence Modeling with Computational Fluid Dynamics

Almost all flows in practical engineering applications are turbulent. Turbulence in a fluid develops when the fluid flows past an obstruction or when streamlines of the fluid pass or overlap one another; turbulence also develops as a consequence of the complex interaction between advection and diffusion processes involved in fluid transport (Wilcox, 1994). In analyzing turbulent fluid transport problems, the accepted technique is the use of turbulence models.

The general form for transport equation can be written as:

$$\frac{\partial}{\partial t}(\rho\phi) + \frac{\partial}{\partial x_i}\left(\rho u_i \phi\right) - \frac{\partial}{\partial x_i}\left(\Gamma_\phi \frac{\partial \phi}{\partial x_i}\right) = S_\phi \qquad (2\text{-}10)$$

where ϕ is fluid property being transported (e.g., mass, momentum, kinetic energy, dissipation rate), ρ is air density, i is subscript denoting x (downwind), y (crosswind) and z (vertical) directions, x_i is direction, u_i represents the velocity component in x_i direction, Γ_ϕ is diffusion coefficient, and S_ϕ is source term (Predicala and Maghirang, 2003). In eq 2-10, the first, second and third terms (at the left-hand side) are accumulation, convection and diffusion terms for ϕ, respectively. Definitions for Γ_ϕ and S_ϕ based on the fluid property, ϕ, are presented in detail by Predicala and Maghirang (2003). The Navier-Stokes equation is an equation of motion derived from eq 2-10 and is given by:

$$\rho \frac{\partial u_j}{\partial t} + \rho \frac{\partial}{\partial x_i}(u_i u_j) = -\frac{\partial P}{\partial x_j} + \frac{\partial \tau_{ij}}{\partial x_i} + \rho g_j \tag{2-11}$$

where i is subscript for all three directions (x, y, and z), j is subscript for the direction evaluated (x, y, or z), μ is air viscosity, P is pressure force in j-direction evaluated, τ_{ij} is viscous stress component, and g_j is gravitational force in j-direction (Glasgow, 2010). The viscous stress component, τ_{ij}, is given by (Feistauer et al. 2003; Ferziger and Peric, 2002):

$$\tau_{ij} = \mu \left(\frac{\partial u_j}{\partial x_i} + \frac{\partial u_i}{\partial x_j} \right) \tag{2-12}$$

In deriving the Navier-Stokes equation, both density and viscosity are assumed to be constant (Glasgow, 2010).

Turbulence can be incorporated in transport equations using Reynolds decomposition, in which the instantaneous value of ϕ is expressed in terms of its corresponding average and fluctuation components (Ferziger and Peric, 2002). The equation for Reynolds decomposition is given by:

$$\phi = \overline{\phi} + \phi' \tag{2-13}$$

where $\overline{\phi}$ is the average component, and ϕ' is the fluctuation component that represents turbulence. Applying Reynolds decomposition to the Navier-Stokes equation and averaging in terms of ϕ lead to the Reynolds-averaged Navier-Stokes (RANS) equation, from which a number of turbulence models are based (k-ε model, k-ω model; Ferziger and Peric, 2002).

Incorporating eq 2-13 into eq 2-11 and 2-12 and then averaging ϕ variables, RANS equations can be written as:

$$\rho \frac{\partial \overline{u_j}}{\partial t} + \frac{\partial}{\partial x_i}\left(\rho \overline{u_i}\ \overline{u_j}\right) = -\frac{\partial \overline{P}}{\partial x_j} + \frac{\partial}{\partial x_i}\left(\overline{\tau_{ij}} - \rho \overline{u_i' u_j'}\right) \tag{2-14}$$

with the average viscous stress component given by (Ferziger and Peric, 2002; Glasgow, 2010):

$$\overline{\tau_{ij}} = \mu \left(\frac{\partial \overline{u_j}}{\partial x_i} + \frac{\partial \overline{u_i}}{\partial x_j} \right) \tag{2-15}$$

Implementing the same steps described above, the resulting continuity equation is given by:

$$\frac{\partial \overline{u_i}}{\partial x_i} = 0 \tag{2-16}$$

The new terms, $\rho \overline{u_i' u_j'}$, in eq 2-14 are called Reynolds stresses and represent the turbulent momentum transport by turbulence itself (Glasgow, 2010). Addition of these new terms in the transport equations, however, leads to a closure problem as the number of unknown variables is now more than the number of available equations (Ferziger and Peric, 2002; Glasgow, 2010). Turbulence models, which are approximations involving Reynolds stresses and turbulent scalar fluxes, are developed to 'close' problems on turbulent flows.

Similar to transport equations presented above, turbulence models are defined by partial differential equations that are approximated numerically (Ferziger and Peric, 2002). This application of solving partial differential equations for transport problems numerically is referred to as computational fluid dynamics (CFD) (Feistauer et al., 2003). CFD has been used to simulate air transport within and outside CAFO buildings. CFD had been employed in studies that simulated air flow (Blanes-Vidal et al., 2008), and transport of gaseous (Bjerg et al., 2008; Li and Guo, 2006) and particulate (Maghirang and Manbeck, 1993; Predicala and Maghirang, 2003) emissions for CAFO facilities. The commonly-used turbulence model, as demonstrated by these studies, is the *k*-ε turbulence model (Wilcox, 1994). The *k*-ε turbulence model is a two-equation model composed of transport equations for turbulent kinetic energy, *k*, and dissipation rate, *e*, developed as closure for turbulent flow problems (Ferziger and Peric, 2002; Wilcox, 1994).

2.3 Summary

Air quality issues from CAFOs are becoming more important because of their adverse effects on human health and environment. More data are needed to establish air pollutant emission rates for CAFOs and improve emission estimation techniques. Additional research is needed to quantify PM emission rates from commercial beef cattle feedlots. The evaluation of the performance of AERMOD in determining emissions from area sources such as cattle feedlots is also important.

2.4 References

Alberta Cattle Feeders' Association. 2002. Other technologies and landscaping options. In Beneficial Management Practices – Environmental Manual for Feedlot Producers in Alberta. Alberta, CA.

Amosson, S.H., B. Guerrero, and L.K. Almas. 2006. Economic analysis of solid-set sprinklers to control dust in feedlots. Paper presented at Southern Agricultural Economics Association Annual Meetings, Orlando, FL. February 5 – 8, 2006.

Amosson, S.H., F. Bretz, L. New, and L.K. Almas. 2007. Economic analysis of a traveling gun for feedyard dust suppression. Paper presented at Southern Economics Association Meeting, Mobile, AL. February 3 – 6, 2007.

Auvermann, B.W., R. Bottcher, A. Heber, D. Meyer, C.B. Parnell Jr., B. Shaw, and J. Worley. 2006. Particulate matter emissions from animal feeding operations. In Animal Agriculture and the Environment: National Center for Manure and Animal Waste Management White Papers, 435-468. J.M. Rice, D.F. Caldwell, and F.J. Humenik, eds. St. Joseph, MI: ASABE

Blanes-Vidal, V., E. Guijarro, S. Balasch, and A.G. Torres. 2008. Application of computational fluid dynamics to the prediction of airflow in a mechanically ventilated commercial poultry building. *Biosystems Engineering* 100:105-116. doi:10.1016/j.biosystemeng.2008.02.004.

Bjerg, B., G. Zhang, and P. Kai. 2008. CFD investigation of a partly pit ventilation systems as a method to reduce ammonia emission from pig production units. Paper presented at Livestock Environment VIII Proceedings, Iguassu Falls, Brazil, August 31-September 4, 2008. ASABE Publication Number 701P0408.

Bonifacio, H.F., R.G. Maghirang, E.B. Razote, B.W. Auvermann, J.P. Harner III, J.P. Murphy, L. Guo, J.M. Sweeten, and W.L. Hargrove. 2011. Particulate control efficiency of a water sprinkler system at a beef cattle feedlot in Kansas. *Trans. ASABE* 54:295-304.

Calder, K.L. 1977. Multiple-source plume models of urban air pollution – Their general structure. *Atmos. Environ.* 11:403-414.

CFR. 2005. Code of Federal Regulations, 40 CFR, Part 51: Revision to the guideline of air quality models: Adoption of a preferred general purpose (flat and complex terrain) dispersion model and other revisions.

CFR. 2010. Code of Federal Regulations, 40 CFR, Part 50: National primary and secondary ambient air quality standards.

CFR, 2011. Code of Federal Regulations, 40 CFR, Part 60: Call for Information: Information related to the development of emission-estimating methodologies for animal feeding operations.

Cimorelli, A.J., S.G. Perry, A. Venkatram, J.C. Weil, R.J. Paine, R.B. Wilson, R.F. Lee, W.D. Peters, R.W. Brode, and J.O. Paumier. 2004. *AERMOD: Description of Model Formulation*, EPA-454/R-03-004. Research Triangle Park, NC: U.S. Environmental Protection Agency.

Cooper, C.D., and F.C. Alley. 2002. *Air Pollution Control – A Design Approach.* 3rd ed. Long Grove, IL: Waveland Press, Inc.

Crenna, B. 2006. *An Introduction to WindTrax.* Edmonton, AB: Department of Earth and Atmospheric Science, University of Alberta.

Duzgoren-Aydin. 2008. Health effects of atmospheric particulates: A medical geology perspective. *Journal of Environmental Science and Health, Part C* 26:1-39. doi:10.1080/10590500801907340.

Faulkner, W.B., J.M. Lange, J.J. Powell, B.W. Shaw, and C.B. Parnell. 2007. Sampler placement to determine emission factors from ground level area sources. ASABE Section Meeting Paper No. 074103. St. Joseph, MI: ASABE.

Feistauer, M., J. Felcman, and I. Straskraba. 2003. *Mathematical and Computational Methods for Compressible Flows.* Oxford, UK: Oxford University Press.

Ferziger, J.H. and M. Peric. 2002. *Computational Methods for Fluid Dynamics*. 3rd ed. Heidelberg, Germany: Springer-Verlag.

Flesch, T.K., L.A. Harper, J.M. Powell, and J.D. Wilson. 2009. Inverse-dispersion calculation of ammonia emissions from Wisconsin dairy farms. *Trans. ASABE* 52:253-265.

Flesch, T.K., and J.D. Wilson. 2005. Estimating tracer emission with a backward Lagrangian Stochastic technique. In *Micrometeorology in Agricultural Systems, Agronomy Monograph no. 47*. Madison, WI: American Society of Agronomy, Inc., Crop Science Society of America, Inc., Soil Science Society of America, Inc.

Flesch. T. K., J.D. Wilson, L.A. Harper, B.P. Crenna, and R.R. Sharpe. 2004. Deducing ground-to-air emissions from observed trace gas concentrations: a field trial. *J. Appl. Meteorol.* 43:487-502.

Flesch. T. K., J.D. Wilson, and E. Yee. 1995. Backward-time Lagrangian Stochastic models and their application to estimate gaseous emissions. *J. Appl. Meteorol*.34:1320-1332.

Galvin, G., C. Henry, D. Parker, R. Ormerod, P. D'Abreton, and M. Rhoades. 2006. Efficacy of Lagrangian and a Gaussian model for back calculating emission rates from feedyard area sources. Paper presented at the Workshop on Agricultural Air Quality, Potomac, MD, June 5-8, 2006.

Glasgow, L.A. 2010. *Transport Phenomena.* Hoboken, NJ: John Wiley & Sons, Inc.

Grant, R.H., and M.T. Boehm. 2010. *National Air Emissions Monitoring Study: Data from the southwest milk producer facility TX5A*, Final Report to the Agricultural Air Research Council. West Lafayette, IN: Purdue University. Available at www.epa.gov/airquality/agmonitoring/data.html. Accessed March 7, 2012.

Guo, L., R.G. Maghirang, E.B. Razote, and B.W. Auvermann. 2011. Laboratory evaluation of dust-control effectiveness of pen surface treatments for cattle feedlots. *J. Environ. Qual.* 40:1503-1509. doi:10.2134/jeq2010.0520.

Ham, J.M., and K.A. Baum. 2007. Measuring ammonia fluxes from cattle feedlots using time-averaged relaxed eddy accumulation. Paper presented at International Symposium on Air Quality and Waste Management for Agriculture, Broomfield, CO. September 16-19, 2007. ASABE Publication No. 701P0907cd.

Hanna, S.R., B.A. Egan, J. Purdum, and J. Wagler. 1999. Evaluation of the ADMS, AERMOD and ISC3 dispersion models with the OPTEX, Duke Forest, Kincaid, Indianapolis, and Lovett field data sets. *Int. J. of Environment and Pollution* 16:301-314.

Heinsohn, R. J., and R.L. Kabel. 1999. *Sources and Control of Air Pollution*. Upper Saddle River, NJ: Prentice-Hall, Inc.

Holmes, N.S., and L. Morawska. 2006. A review of dispersion modeling and its application to the dispersion of particles: An overview of different dispersion models available. *Atmos. Environ.* 40:5902-5928.

Kanemasu, E.T., M.L. Wesely, and B.B. Hicks. 1979. Techniques for calculating energy and mass fluxes. *Modification of the Aerial Environment of Crops, ASAE Monograph no. 2.* St. Joseph, MI: ASAE.

Kirkhorn, S.R., and M.B. Schenker. 2002. Current health effects of agricultural work: Respiratory disease, cancer, reproductive effects, musculoskeletal injuries, and pesticide-related illnesses. *J. Agric. Safety and Health* 8:199-214.

Lester, J.C. 2006. The evolution of agricultural air quality regulations. Paper presented at the Workshop on Agricultural Air Quality, Potomac, MD, June 5-8, 2006.

Leytem, A.B., R.S. Dungan, D.L. Bjorneberg, and A.C. Koehn. 2011. Emission of ammonia, methane, carbon dioxide, and nitrous oxide from dairy cattle housing and manure management systems. *J. Environ. Qual.* 40:1383-1394. doi:10.2134/jeq2009.0515.

Li, Y., and H. Guo. 2006. Comparison of odor dispersion predictions between CFD and CALPUFF models. *Trans. ASABE* 36:1915-1926.

Maghirang, R.G., and H.B. Manbeck. 1993. Modeling particle transport in slot-inlet ventilated airspaces. *Trans. ASAE* 36:1449-1459.

Massman, W.J., and X. Lee. 2002. Eddy covariance flux corrections and uncertainties in long-term studies of carbon and energy exchanges. *Agric. Forest Meteorol.* 113:121-144.

McGinn, S.M., T.K. Flesch, D. Chen, B. Crenna, O.T. Denmead, T. Naylor, and D. Rowell. 2010. Course particulate matter emissions from cattle feedlots in Australia. *J. Environ. Qual.* 39:791-798. doi:10.2134/jeq2009.0240.

Meyers, T.P., and D. D. Baldocchi. 2005. Current micrometeorological flux methodologies with applications in Agriculture. In *Micrometeorology in Agricultural Systems, Agronomy Monograph no. 47*. Madison, WI: American Society of Agronomy, Inc., Crop Science Society of America, Inc., Soil Science Society of America, Inc.

Midwest Plan Service. 2002. Outdoor air quality – Midwest Plan Service-18 Manure Management System Series 18. Section 18. Ames, IA: Midwest Plan Service.

Midwest Research Institute. 1988. *Gap Filling PM_{10} Emission Factors for Selected Open Area Dust Sources,* EPA-450/4-88-003. . Research Triangle Park, NC: U.S. Environmental Protection Agency.

Miller, D. N., and B. L. Woodbury. 2003. Simple protocols to determine dust potentials from cattle feedlot soil and surface samples. *J. Environ. Qual.* 32(5): 1634-1640.

Mitloehner, F.M. 2000. Behavioral and environmental management of feedlot cattle. Ph.D. dissertation. Lubbock, TX: Texas Tech University.

Mitloehner, F.M., and S.M. Calvo. 2008. Worker health and safety in Concentrated Animal Feeding Operations. *J. Agric. Safety and Health* 14:163-187.

Muller, J.B.A., M. Coyle, D. Fowler, M.W. Gallagher, E.G. Nemitz, and C.J. Percival. 2009. Comparison of ozone fluxes over grassland by gradient and eddy covariance technique. *Atmos. Sci. Let.* 10:164-169. doi:10.1002.asl.226.

Myles, L., J. Kochendorfer, M.W. Heuer, and T.P. Meyers. 2011. Measurement of trace gas fluxes over an unfertilized agricultural field using the flux-gradient technique. *J. Environ. Qual.* 40:1359-1369. doi:10.2134/jeq2009.0386.

National Research Council. 2003. *Air Emissions from Animal Feeding Operations: Current Knowledge, Future Needs*. Washington, D.C.: National Academy of Sciences.

Perry, S.G., A.J. Cimorelli, R.J. Paine, R.W. Brode, J.C. Weil, A. Venkatram, R.B. Wilson, R.F. Lee, and W.D. Peters. 2005. AERMOD: a dispersion model for industrial source applications. Part II: model performance against 17 field study databases. *J. Appl. Meteorol.* 44:694-708.

Pope, S.B. 2000. *Turbulent Flows.* Cambridge, UK: Cambridge University Press.

Predicala, B.Z., and R.G. Maghirang. 2003. Numerical simulation of particulate matter emissions from mechanically ventilated swine barns. *Trans. ASABE* 46:1685-1694.

Prueger, J.H., T.J. Gish, L.L. McConnell, L.G. McKee, J.L. Hatfield, and W.P. Kustas. 2005. Solar radiation, relative humidity, and soil water effects on Metolachlor volatilization. *Environ. Sci. Technol.* 39:5219-5226.

Prueger, J.H. and W. P. Kustas. 2005. Aerodynamic Methods for Estimating Turbulent Fluxes. In *Micrometeorology in Agricultural Systems, Agronomy Monograph no. 47.* Madison, WI: American Society of Agronomy, Inc., Crop Science Society of America, Inc., Soil Science Society of America, Inc.

Purdue Applied Meteorology Laboratory. 2009. *Qualtity Assurance Project Plan for the National Air Emissions Monitoring Study,* Revision No. 3. West Lafayette, IN: Purdue University.

Razote, E.B., R.G. Maghirang, B.Z. Predicala, J.P. Murphy, B.W. Auvermann, J.P. Harner III, and W.L. Hargrove. 2006. Laboratory evaluation of the dust-emission potential of cattle feedlot surfaces. *Trans. ASABE* 49:1117-1124.

Romanillos, A., and B.W. Auvermann. 1999. Effect of stocking density on fugitive PM_{10} emissions from a cattle feedyard. ASABE Section Meeting Paper No. 99-4192. St. Joseph, MI: ASABE.

Sweeten, J.M., C.B. Parnell, R.S. Etheredge, and D. Osborne. 1988. Dust emissions in cattle feedlots. *Vet. Clinics of North America, Food Animal Prac.* 4:557-578.

Thomson, D.J. 1987. Criteria for the selection of Stochastic models of particle trajectories in turbulent flows. *J. Fluid Mech.*180:529-556.

Todd, R.W., N.A. Cole, L.A. Harper, and T.K. Flesch. 2007. Flux-gradient estimates of ammonia emission from beef cattle feedyard pens. Paper presented at International Symposium on Air Quality and Waste Management for Agriculture, Broomfield, CO. September 16-19, 2007. ASABE Publication No. 701P0907cd.

Todd, R.W., N.A. Cole, L.A. Harper, T.K. Flesch, and B.H. Baek. 2005. Ammonia and gaseous nitrogen emissions from a commercial beef cattle feedyard estimated using the flux-gradient method and N:P ratio analysis. Paper presented at State of the Science Animal Manure and Waste Management, San Antonio, TX. January 4-7, 2005.

Turner, D. B. 1994. *Workbook of Atmospheric Dispersion Estimates – An Introduction to Dispersion Modeling.*2nd ed. Boca Raton, FL: Lewis Publishers.

Turner, D.B., and R.H. Schulze. 2007. *Practical Guide to Atmospheric Dispersion Modeling*. Dallas, TX: Trinity Consultants, Inc. and Air & Waste Management Association.

U.S. Environmental Protection Agency. 1995. *Compilation of Air Pollutant Emission Factors, Volume I: Stationary Point and Area Sources,* AP-42 Fifth edition. Research Triangle Park, NC: U.S. Environmental Protection Agency.

U.S. Environmental Protection Agency. 2001. *Procedures Document for National Emission Inventory, Criteria Air Pollutants 1985 – 1999,* EPA-454/R-01-006. Research Triangle Park, NC: U.S. Environmental Protection Agency.

U.S. Environmental Protection Agency. 2005. *Consent Agreement and Final Order*. Available at www.epa.gov/compliance/resources/agreements/caa/cafo-agr-050121.pdf. Accessed March 6, 2012.

Wagner-Riddle, C., G.W. Thurtell, and G.C. Edwards. 2005. Trace gas concentration measurements for micrometeorological flux quantification. In *Micrometeorology in Agricultural Systems, Agronomy Monograph no. 47*. Madison, WI: American Society of Agronomy, Inc., Crop Science Society of America, Inc., Soil Science Society of America, Inc.

Wang, H.E., S. Takle, and J. Shen. 2001. Shelterbelts and windbreaks: Mathematical modeling and computer simulations of turbulent flows. *Annual Review of Fluid Mechanics* 33:549-586.

Wilcox, D.C. 1994. *Turbulence Modeling for CFD.* La Canada, CA: DCW Industries, Inc.

Wilson, J.D., and B.L. Sawford. 1996. Review of Lagrangian stochastic models for trajectories in the turbulent atmosphere. *Boundary-Layer Meteorology* 78:191-210.

CHAPTER 3 - **Particulate Matter Emission Rates from Beef Cattle Feedlots in Kansas – Reverse Dispersion Modeling**[1]

3.1 Introduction

Open beef cattle feedlots face air quality challenges, including emissions of particulate matter (i.e., PM_{10} and $PM_{2.5}$), odorous volatile organic compounds, ammonia, and greenhouse gases. The long-term sustainability of feedlots and neighboring rural communities that are economically dependent on these operations will depend in part on overcoming these air quality challenges. In addition, open cattle feedlots may be subject to new regulations on air emissions. However, limited data on gaseous and PM emissions exist for large cattle feedlots (National Research Council, 2003), especially for those in the Great Plains region that comprises a large percentage of the U.S. beef cattle production. For example, as of July 2011, the Southern Great Plains states of Texas, Kansas, Nebraska, Colorado, Oklahoma, and New Mexico combined accounted for about 78% of the 10.5 million head of cattle on feed for feedlots with a capacity of 1,000 or more head (U.S. Department of Agriculture, 2011). Gaseous and PM emission rates need to be determined from large feedlots to provide realistic assessment of their environmental impacts. Estimates of emission rates are also critical in emission inventories and abatement measures development. As stated in the report on air emissions from animal feeding operations (AFOs) by the National Research Council (NRC) (2003): "While concern has mounted, research to provide the basic information needed for effective regulation and management of these emissions has languished… Accurate estimation of air emissions from AFOs is needed to gauge their possible adverse impacts and the subsequent implementation of control measures."

In response to the NRC report, the National Air Emissions Monitoring Study (NAEMS) was conducted on several swine, dairy, layer, and broiler facilities (National Research Council, 2003; Purdue Applied Meteorology Laboratory, 2009). There is also a need to measure and monitor air emissions from open beef cattle feedlots. Quantifying air emission rates from open feedlots is challenging, largely because of their unique characteristics, including surface heterogeneity, wide variation in source geometry, and temporal and spatial variability of

[1] Bonifacio, H.F., R.G. Maghirang, B.W. Auvermann, E.B. Razote, J.P. Murphy, and J.P. Harner III. 2012. Particulate matter emission rates from beef cattle feedlots in Kansas – reverse dispersion modeling. *J. Air & Waste Manage. Assoc*. 62:350-361. doi:10.1080/10473289.2011.651557.

emission rates. A widely used approach involves measuring upwind and downwind concentrations combined with reverse modeling with atmospheric dispersion models (National Research Council, 2003; Wanjura et a., 2004; McGinn et al., 2010; Faulkner et al., 2009; Goodrich et al., 2009). Currently, several dispersion models are available, with the American Meteorological Society/Environmental Protection Agency Regulatory Model (AERMOD) as the latest Gaussian model recommended by the U.S. Environmental Protection Agency (EPA) for regulatory purposes (CFR, 2005).

Several PM emission estimates for cattle feedlots are available from studies using dispersion models, including simple box models (e.g., San Joaquin Valley Air Pollution Control District, 2010), Gaussian dispersion models (e.g., Wanjura et al., 2004), and Lagrangian stochastic models (e.g., McGinn et al., 2010). For inventory purposes, U.S. EPA is currently using a PM_{10} emission factor of 17 tons/1,000 head (hd) throughput (equivalent to 82 kg/1,000 hd-day at 2 throughput/yr) (Midwest Research Institute, 1988); this factor was apparently obtained using a simple Gaussian model and PM measurements from California feedlots (Grelinger and Lapp, 1996; U.S. Environmental Protection Agency, 2001). California Air Resources Board (CARB) has recently published PM_{10} emission factor of 13.2 kg/1,000 hd-day for cattle feedlots (Countess Environmental, 2006; San Joaquin Valley Air Pollution Control District, 2010). The emission factor was determined by the San Joaquin Valley Air Pollution Control District (SJVAPCD) using Linear Profile model, Block Profile model, Logarithmic Profile model, and Box model (Countess Environmental, 2006; San Joaquin Valley Air Pollution Control District, 2010). Correspondence with SJVAPCD revealed that selection of model depended on the vertical profile of measured downwind concentrations. Wanjura et al.(2004) reported a PM_{10} emission factor of 19 kg/1,000 hd-day for a Texas feedlot using the Industrial Source Complex – Short Term (ISCST3) model; however, no information was given on inclusion of gravitational settling in the modeling. McGinn et al. (2010) calculated PM_{10} emission rates at two cattle feedlots in Australia using a Lagrangian stochastic (LS) dispersion model (i.e., WindTrax, Thunder Beach Scientific) modified to include effects of gravitational settling and surface deposition; PM_{10} emission rates were 31 kg/1,000 hd-day and 60 kg/1,000 hd-day for the two feedlots.

Most of the above emission rate values were based on relatively short-term measurements – usually only several days of measurement. Also, some were conducted during periods in which

pens were dry (i.e., Grelinger and Lapp, 1996), while others were based on measurement periods in which pens were relatively wet, due to either rain event or water sprinkling (i.e., Wanjura et al., 2004; San Joaquin Valley Air Pollution Control District, 2010). The U.S. EPA PM_{10} emission factor of 82 kg/1,000 hd-day (17 tons/1,000 hd- throughput) was also based on the assumption that PM emitted from cattle feedlot had the same size distribution as PM emitted from agricultural soils and that the PM_{10}/TSP ratio was equal to 0.64 (Midwest Research Institute, 1988). From field measurements on a cattle feedlot in Kansas (Gonzales, 2010), mean PM_{10}/TSP ratio was 0.35, suggesting that the size distribution assumed for the US EPA emission factor may not be suitable for cattle feedlots and the derived US EPA PM_{10} emission factor could be overestimated.

A limited number of studies have been carried out quantifying and characterizing PM_{10} emission rates from cattle feedlots, particularly for feedlots in Kansas; clearly, more research is needed. This research was conducted to determine PM_{10} emission rates from cattle feedlots by reverse modeling using AERMOD combined with extended measurement period for PM_{10} concentrations.

3.2 Materials and Methods

Emission rates of PM_{10} were determined using the following general procedure: (1) PM_{10} concentrations at the downwind and upwind edges of two cattle feedlots were monitored; (2) atmospheric dispersion modeling with AERMOD using a unit emission flux (i.e., 1.0 $\mu g/m^2$-sec) was used to predict PM_{10} concentrations in the feedlots; and (3) emission fluxes were calculated from measured concentrations and AERMOD-predicted concentrations. From emission fluxes and cattle population in the feedlots, emission factors (i.e., kg/1000 hd-day) were determined.

3.2.1 Field Measurements of PM_{10} Concentration

3.2.1.1 Feedlot Description

Two commercial cattle feedlots in Kansas, herein referred to as KS1 and KS2, were considered. Feedlots KS1 and KS2 are 35 km apart, surrounded by agricultural lands. Another feedlot is located about 3 km south-southwest of KS1 with several rows of trees separating the two feedlots. A feedlot is also located about 3 km east-southeast of KS2 with a row of trees between the two feedlots. Table 3-1 summarizes the general characteristics of feedlots KS1 and KS2. Prevailing wind directions at the feedlots were south-southeast during summer and north-

northwest during winter. Feedlot KS1 had approximately 30,000 head of cattle with total pen area of about 50 ha. It had a water sprinkler system with maximum application rate of approximately 5.0 mm/day. The water sprinkler system was normally operated during prolonged dry periods from April through October. Manure on pen surfaces were scraped and piled/compacted to one location in the pen (i.e., center mound) 2 to 3 times per year per pen, and were hauled from each pen at least once a year. Feedlot KS2, on the other hand, had approximately 25,000 head of cattle and total pen area of approximately 68 ha. For each pen, scraping/manure piling was done 5 to 6 times per year while manure hauling was scheduled 2 to 3 times per year.

Table 3-1. Description of feedlot KS1 and KS2

Parameter		Feedlot KS1	Feedlot KS2
Capacity, head		30,000	25,000
Area, ha		50	68
Dust control methods	Water sprinkler system	$\leq$ 5 mm/day	none
	Pen cleaning	2 to 3 times/year-pen	5 to 6 times/year-pen
Weather conditions	Prevailing wind Direction	South-southeast	South-southeast
	Average annual precipitation (mm)	679	757

Cattle were fed 3 times a day at both feedlots. For KS1, feeding periods were 6:00 a.m.-8:30 a.m., 11:00 a.m.-1:30 p.m., and 3:00 p.m.-5:30 p.m. For KS2, feeding periods were 5:30 a.m.-7:30 a.m., 9:30 a.m.-11:30 a.m., and 12:30 p.m.-4:30 p.m.

Table 3-1 indicates that KS2 received about 10% more precipitation than KS1 in 2007 and 2008. For KS1, the total amount of water applied through the sprinkler system and number of days the sprinkler system was operated varied from year to year depending on weather conditions. The total amounts of water used by the sprinkler system in 2007 and 2008 were 333 and 209 mm, respectively. The sprinkler system was operated for a total of 102 days in 2007 and 57 days in 2008.

3.2.1.2 Measurement of PM_{10} Concentration and Weather Conditions

PM_{10} mass concentrations were measured at the north and south edges of the feedlots. The north and south sampling locations for KS1 (Figure 3-1a) were approximately 5 m and 30 m, respectively, away from the closest pens; those for KS2 (Figure 3-1b) were approximately 40 m and 60 m, respectively, away from the closest pens. Note that the sampling locations at each feedlot were selected based on feedlot layout, power availability, and access.

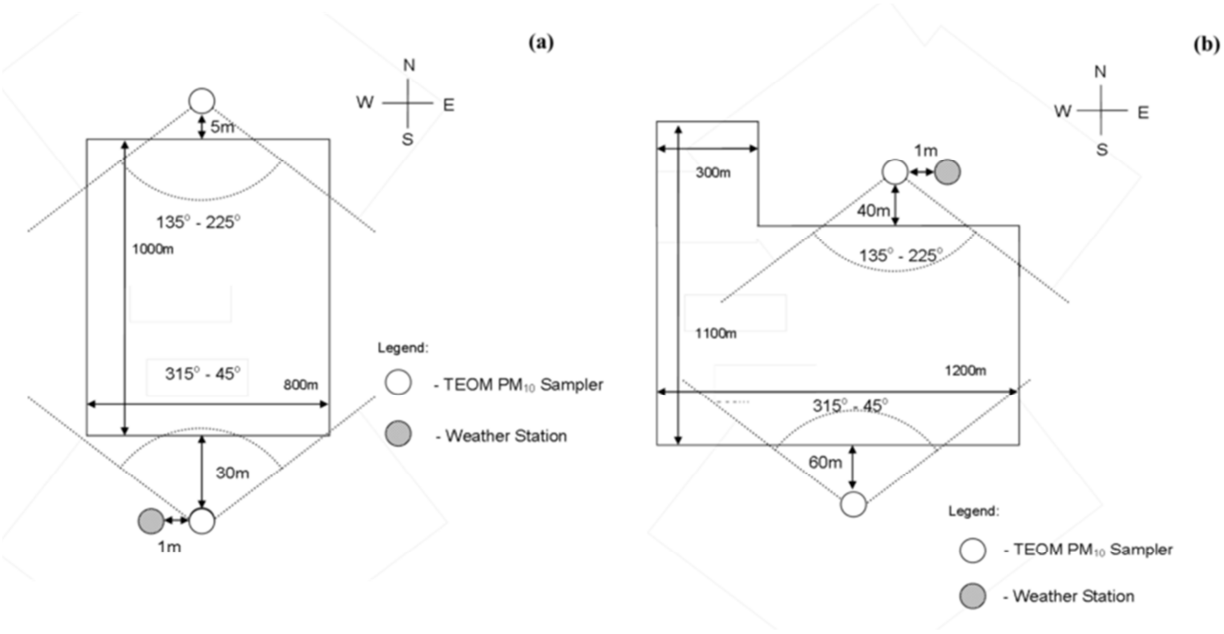

Figure 3-1. Schematic diagram showing locations of PM_{10} samplers and weather station at feedlots (a) KS1 and (b) KS2.

PM_{10} concentration at each sampling location was measured with a tapered element oscillating microbalance (TEOM) PM_{10} monitor (Series 1400a, Thermo Fisher Scientific, East Greenbush, NY; federal equivalent method designation No. EQPM-1090-079). The PM_{10} size-selective inlet was positioned 2.3 m above the ground. PM_{10} concentrations were recorded continuously at 20-min intervals. During sampling and measurement, the sampled air and TEOM filter were heated to 50°C. Maintenance of TEOMs (i.e., leak checks, flow audits, and inlet cleaning) was performed monthly. For cases of low flow audit results, either the TEOM pump was replaced or software calibration was done to correct the sampling flow rate. The TEOM

collection filters were replaced if the filter loading indicated by the TEOM reached the 90% value; TEOM in-line filters were replaced when the amount of dust collected was significant.

Each feedlot was equipped with a weather station (Campbell Scientific, Inc., Logan, Utah) to measure and record at 20-min intervals wind speed and direction (Model 05103-5), atmospheric pressure (Model CS100), precipitation (Model TE525), and air temperature and relative humidity (Model HMP45C).

The PM_{10} dataset from the TEOMs was screened based on wind direction. Datasets in which downwind was either the north sampling site (180° wind direction) or the south sampling site (0°/360° wind direction) were considered (Figures 3-1a and 3-1b). The working range for wind direction was set at $\pm$ 45° in accordance with guideline on air quality models (CFR, 2005). Data outside the acceptable range were then excluded from the analysis. Large negative 20-min PM_{10} concentrations (i.e., < -10 $\mu g/m^3$) were not used in the analysis in accordance with the TEOM manufacturer's recommendations. Only datasets with both concentrations (downwind, upwind) and complete meteorological data were considered in this study. The 20-min downwind and upwind PM_{10} concentrations were integrated to hourly averages before computing the hourly net concentrations (i.e., downwind concentration – upwind concentration). Negative net concentrations were also excluded in the analysis as they could indicate negligible PM_{10} emission from the feedlots. In this study, upwind (background) concentration was assumed to be uniformly distributed over the measurement time interval.

3.2.2 Reverse Dispersion Modeling

Modeling involved preparation of meteorological inputs, and then running AERMOD (version 09292, US EPA; www.epa.gov/ttn/scram) to predict concentrations downwind of each feedlot (Pacific Environmental Services, 2004; MACTEC Federal Programs, Inc., 2009). This version accounts for particle losses due to gravitational settling.

3.2.2.1 Meteorological Data

In AERMOD modeling, meteorological parameters should be specified and/or calculated that include the following: wind speed and direction, temperature, Monin-Obukhov length, friction velocity, sensible heat flux, mixing heights, and surface roughness length. Wind speed, wind direction, and temperature were obtained from measurements by the weather stations at the feedlots. The Monin-Obukhov length data were obtained from an Atmospheric Radiation

Measurement (ARM) research site approximately 16 km and 48 km away from feedlot KS1 and KS2, respectively. The 30-min eddy covariance measurements at the ARM research site were first averaged to be hourly values before computing Monin-Obukhov length. It was assumed that the same Monin-Obukhov length can be applied to the two feedlots. This assumption was based on a preliminary analysis of data from two other ARM sites about 80 km apart, with significantly different wind speeds ($p < 0.001$) that showed the two sites did not significantly differ ($p = 0.15$) in Monin-Obukhov length. Friction velocity, sensible heat flux, and mixing heights were calculated from the measured wind speed, measured temperature, and calculated Monin-Obukhov length using equations in AERMOD formulation (Cimorelli et al., 2004). Surface roughness length, defined to be related to the height of wind flow obstacles, was set at 5.0 cm based on the classification table by EPA (U.S. Environmental Protection Agency, 2008) and also on a study by Baum (2003) that reported a surface roughness value of 4.1 ± 2.2 cm for a cattle feedlot in Kansas. These parameters were then formatted as surface and profile data files that can be read by AERMOD. In addition, wind speed threshold was set at 1.0 m/sec based on the wind speed monitor's threshold sensitivity; data with wind speed less than the threshold were not considered in the modeling.

3.2.2.2 AERMOD Dispersion Modeling

The model used in this study was AERMOD, which is the current EPA preferred regulatory dispersion model (CFR, 2005). AERMOD is a steady-state Gaussian plume model that simulates dispersion based on a well-characterized planetary boundary layer structure (Cimorelli et al., 2004). For stable conditions, AERMOD applies Gaussian distribution to both vertical and lateral/horizontal distributions of concentrations (Cimorelli et al., 2004). For unstable conditions, Gaussian distribution still applies for lateral distribution of concentration; however, a bi-Gaussian distribution is now used by AERMOD to approximate the vertical concentration distribution (Cimorelli et al., 2004). This bi-Gaussian concept, which is a more accurate approximation of actual vertical dispersion, is another feature of AERMOD that makes it different from other models (Cimorelli et al., 2004; Perry et al., 2005). Based on AERMOD guidelines, the concentration can be expressed as:

$$C\{x,y,z\} = (Q/u)\ P_y P_z \tag{3-1}$$

where $C\{x,y,z\}$ is the concentration ($\mu g/m^3$) predicted for coordinate/receptor given by x (downwind distance from the source), y (lateral distance perpendicular to the plume downwind centerline) and z (height from the ground); Q is the source emission rate; u is the wind speed; and P_y and P_z are the probability density functions that describe the lateral and vertical distributions of concentration, respectively (Cimorelli et al., 2004). For dispersion modeling involving several area sources (e.g., pens in a feedlot), the total concentration is assumed equal to the sum of the concentrations predicted for each source (Calder, 1977).

The effects of gravitational settling of particles were considered (U.S. Environmental Protection Agency, 2009). Algorithms in AERMOD for modeling particle settling and removal are similar to those for ISCST3 (Pacific Environmental Services, Inc., 1995) U.S. Environmental Protection Agency, 2009). Settling velocity, V_g, is calculated using eq 3-2:

$$V_g = \frac{(\rho - \rho_{air}) g d_p^2 c_2}{18\mu} S_{CF} \tag{3-2}$$

where ρ is particle density (g/cm^3), ρ_{air} is air density (g/cm^3), g is the acceleration due to gravity (9.8 m/sec^2), μ is absolute air viscosity (g/cm-sec), c_2 is conversion constant, and S_{CF} is slip correction factor (U.S. Environmental Protection Agency, 2009). Particle deposition velocity (m/sec), V_d, is computed from V_g and is given by:

$$V_d = \frac{1}{R_a + R_p + R_a R_p V_g} + V_g \tag{3-3}$$

where R_a is aerodynamic resistance (sec/m) and R_p is quasi-laminar sublayer resistance (sec/m) (U.S. Environmental Protection Agency, 2009). From V_d, the source depletion factor, $F_q(x)$, is obtained, that is,

$$F_q(x) = \frac{Q(x)}{Q_o} = \exp\left[-\int_0^x \frac{V_d}{u} D(x) dx \right] \tag{3-4}$$

where $Q(x)$ is adjusted source strength at distance x (g/sec), Q_o is initial source strength (g/sec), u is transport wind speed (m/sec), and $D(x)$ is crosswind integrated diffusion function (1/m).

In this study, a unit emission flux (1.0 $\mu g/m^2$-sec) was used in AERMOD modeling to predict hourly concentrations at the downwind sampling location for each feedlot. The following assumptions were specified: (1) feedlots were area sources with flat terrain, (2) all pens had same

and constant emission flux for the 1-hr averaging time, (3) dry depletion of particles was the only removal mechanism (i.e., depletion due to precipitation not considered), and (4) concentration was the variable modeled. Inclusion of particle depletion required specifying particle size distribution (psd) in terms of particle size categories (as mass-mean aerodynamic diameters), their corresponding mass fractions, and particle densities (Cimorelli et al., 2004). The psd used in modeling was based on field measurements at KS1 using micro-orifice uniform deposit impactor (MOUDI, Model 100-R, MSP Corporation, Shoreview, MN) (Gonzales, 2010). For the 2-yr study period, there were 11 psd measurements at KS1, with 9 measurements for the May to November period and 2 measurements for the December to April period. From these measurements, considering particles that are smaller than approximately 10 µm to represent PM_{10}, mean mass percentages for the different particle size ranges were as follows: 52% for 6.20 µm – 9.90 µm; 27% for 3.10 µm – 6.20 µm; 7% for 1.80 µm - 3.10 µm; and 14% for < 1.80 µm. Other required inputs were SFC and PFL meteorological files, height (i.e., 2.3 m) and location of the receptor, and locations of area sources (i.e., pens). The locations of area sources and receptor in each feedlot were specified by encoding vertices of the area sources and receptor in the AERMOD runstream file. Vertices were determined using the DesignCAD 3M Max18 (IMSIDesign, Novato, CA) software.

3.2.3 Calculation of Emission Rates

Assuming that the emission rates are independent of P_y, P_z, and u in eq. 3-1 (Calder, 1977), the emission flux was calculated from the assumed emission flux (1.0 µg/m^2-sec) and predicted and measured net PM_{10} concentrations using eq 3-5:

$$Q_O = \frac{Q_A}{C_A} \times C_O \tag{3-5}$$

where Q_o is the calculated 1-hr emission flux (µg/m^2-sec), C_o is the measured 1-hr net PM_{10} concentration (µg/m^3), Q_A is 1.0 µg/m^2-sec, and C_A is the model-predicted 1-hr PM_{10} concentration (µg/m^3) for an emission flux of 1.0 µg/m^2-sec.

In computing emissions, only days with at least 50% of the hourly emission fluxes were considered (U.S. Environmental Protection Agency, 2003). For a given day, the average of hourly emission fluxes was used to represent the flux for that day. Medians were used to

represent the monthly and annual emission fluxes because of the non-normality of the data sets. Annual emission fluxes were converted to emission factors using the following relationship:

$$EF = \frac{Q_{yr} \times A}{10^3 \times N} \quad (3\text{-}6)$$

where EF is calculated emission factor (kg/1,000 hd-day), Q_{yr} is mean annual emission flux (g/m^2-day), A is total pen area (m^2), and N is number of cattle in thousands (i.e., 30 for KS1, 25 for KS2).

Data were analyzed with statistical tools of SAS software (SAS Institute Inc., 2004). Statistical tests on normality showed all of the data sets (i.e., wind speed, temperature, concentration, emission flux and factor) had non-normal distribution. Consequently, in comparing data sets of different groups (e.g., feedlot KS1 vs. KS2), nonparametric test (e.g., nonparametric one-way analysis of variance) was used and median values were then reported. Removal of outliers and computation of standard deviations were based on the procedure proposed by Schwertman et al. (2004) for data with non-normal distribution. A 5% level of significance was used in all comparisons.

3.3 Results and Discussion

3.3.1 Weather Conditions and PM_{10} Concentrations

During the study period (January 2007 to December 2008), 44% and 41% of the measurements at KS1 and KS2, respectively, had wind direction from the south (135° to 225°); 23% and 21% of the measurement had wind direction from the north (0° to 45°, 315° to 360°) at KS1 and KS2, respectively. Wind usually came from the south, particularly during the months of May to November (Figure 3-2). Non-parametric tests indicated that the two feedlots did not significantly differ in temperature ($p = 0.34$) but differed significantly ($p<0.05$) in wind speed.

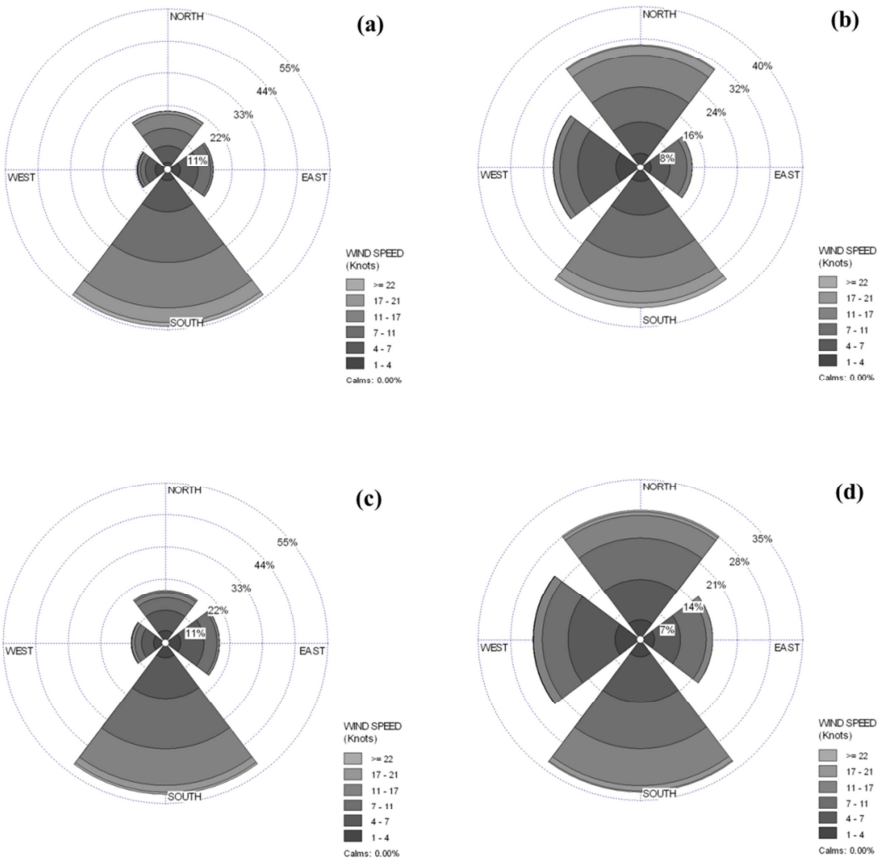

Figure 3-2. Wind speed and wind direction distributions at the feedlots for the 2-yr period: (a) KS1 May to November; (b) KS1 December to April; (c) KS2 May to November; (d) KS2 December to April.

For each feedlot, measured PM_{10} concentrations varied diurnally. Figure 3-3 plots the hourly concentrations for the two feedlots. The two feedlots showed similar diurnal trends: concentrations were generally lowest during the early morning period (2:00 a.m.-7:00 a.m.) and generally highest between 5:00 p.m. and 11:00 p.m. – in this study, this period was referred to as evening dust peak (EDP) period. The PM_{10} concentrations are summarized in Table 3-2 as medians of hourly concentrations for the EDP and non-EDP (12:00 a.m. – 4:00 p.m.) periods. Comparison of the two feedlots indicated that 24-hr PM_{10} concentrations at KS1 and KS2 were not significantly different ($p = 0.10$). Comparing non-EDP and EDP periods for each feedlot, the EDP period had significantly ($p < 0.001$) higher concentration. These higher concentrations

could be attributed to the high emission rate possibly due to high cattle activity (Mitloehner, 2000), low wind speed, and relatively stable atmospheric conditions during the EDP period (Auvermann et al., 2006).

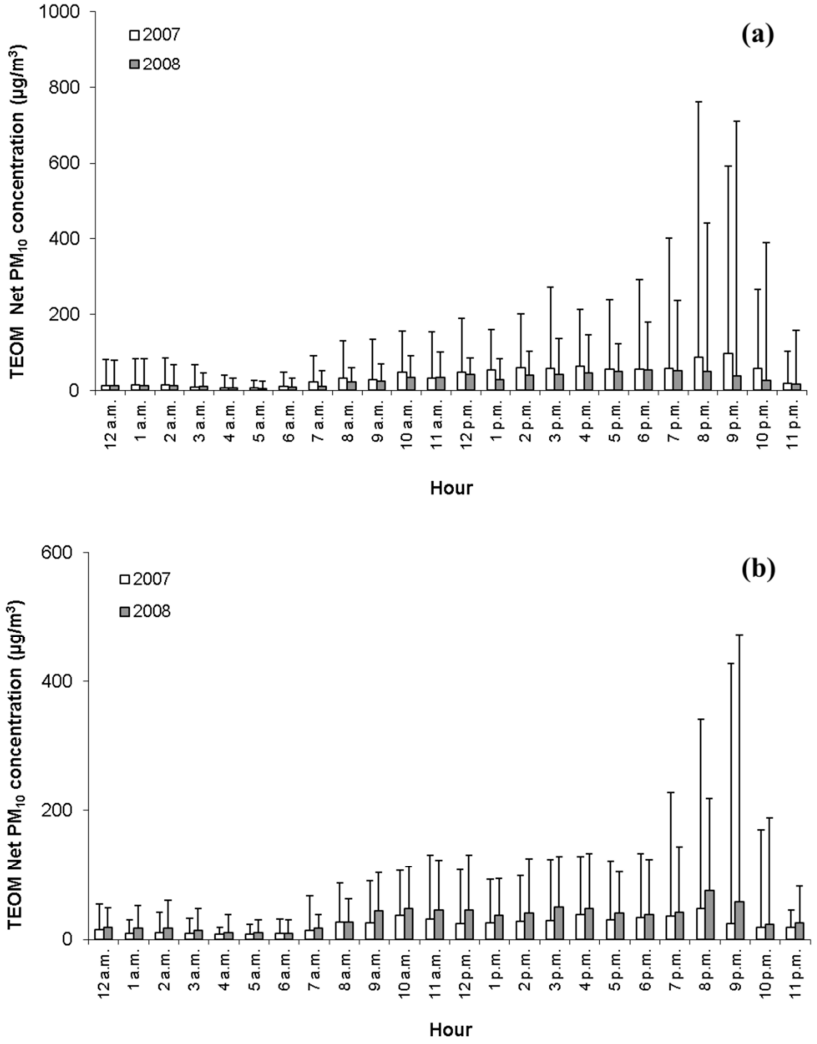

Figure 3-3. Median hourly net PM_{10} concentrations for feedlots (a) KS1 and (b) KS2. Median values were based on days with emission data. Error bars represent upper standard deviation estimates.

Table 3-2. Median PM_{10} concentrations at feedlot KS1 and KS2 for 2007 and 2008[a]

Concentrations ($\mu g/m^3$)	Feedlot KS1		Feedlot KS2	
	12a.m.-4p.m.	5p.m.-11p.m. (EDP)	12a.m.-4p.m.	5p.m.-11p.m. (EDP)
Number of Hourly Values	4,376	2,066	3,751	1,607
Downwind concentration	49	82	38	53
Upwind concentration	23	27	13	17
Net concentration	32	47	22	37

[a] For each feedlot (i.e., KS1, KS2) and location (i.e., downwind, upwind, net), median concentration values for the 12 a.m. – 4 p.m. and 5 p.m. – 11 p.m. periods are not significantly different at the 5% level of significance.

For the sampling days with at least 18 hourly PM_{10} concentration measurements, measured downwind concentrations exceeded US EPA National Ambient Air Quality Standards (NAAQS) for PM_{10} (150 $\mu g/m^3$ for 24-hr) (U.S. Environmental Protection Agency, 2008) 51 (out of 74) times in 2007 and 33 (out of 71) times in 2008 for KS1 and 19 (out of 62) times in 2007 and 14 (out of 50) times 2008 for KS2; if contribution of background (upwind) concentration was considered, the numbers of days in which the net concentrations exceeded the U.S. EPA NAAQS were fewer by 2 – 8 days. Higher non-attainment for KS1 could be explained by the difference in sampler location; as mentioned earlier, the sampler was closer to the pens at KS1 than at KS2. At the property lines, few hundred meters away from the pens, PM_{10} concentrations would likely be smaller than the PM_{10} NAAQS because of particle dispersion and settling.

3.3.2 Emission Rates

The two feedlots differed significantly ($p = 0.04$) in daily emission fluxes for the 2-yr period (Table 3-3), with KS1 having higher emission fluxes. In 2007, median PM_{10} emission fluxes were 1.68 g/m^2-day (101 days) and 1.08 g/m^2-day (91 days) for KS1 and KS2, respectively; in 2008, median PM_{10} emission fluxes were 1.58 g/m^2-day (140 days) for KS1 and 1.13 g/m^2-day (95 days) for KS2. Overall median emission fluxes were 1.60 g/m^2-day for KS1 and 1.10 g/m^2-day for KS2. Note that KS1 had a water sprinkler system for dust control and was expected to have smaller emission rate than KS2, which did not have any sprinkler water application. However, as stated earlier, pens were cleaned more frequently at KS2 than at KS1.

In addition, KS2 received more rain than KS1 (Table 3-1); during the 2-yr period, for KS1, 20% of the days with measurements had rainfall events; for KS2, on the other hand, 26% of the days with measurements received rainfall.

Equivalent PM_{10} emission factors for the 2-yr period were 27 kg/1,000 hd-day and 30 kg/1,000 hd-day for KS1 and KS2, respectively (Table 3-3). Unlike emission fluxes, the two feedlots did not differ significantly ($p = 0.53$) in emission factors. The computed emission factors for both feedlots were smaller than the US EPA PM_{10} emission factor (82 kg/1,000 hd-day) but were within the range of published values (Wanjura et al., 2004; Countess Environmental, 2006; McGinn et al., 2010). Compared to other studies, difference in calculated emission rates could be due to differences in measurement design (e.g., measurement period) and methods (e.g., samplers), measurement conditions (e.g., time of year, weather), meteorological data set (e.g., instrument, type), emission rate estimation technique (e.g., dispersion model), and feedlot characteristics (e.g., location, pen surface conditions).

Table 3-3. PM_{10} emission fluxes and factors at feedlot KS1 and KS2

Year	Parameters	Emission flux (g/m^2-day)		Emission factor (kg/1,000 hd-day)	
		KS1	KS2	KS1	KS2
January to December 2007	Number of Daily Values	101	91	101	91
	Minimum	0.04	0.09	1	2
	Maximum	9.70	6.84	162	187
	Median	1.68	1.08	28	30
January to December 2008	Number of Daily Values	140	95	140	95
	Minimum	0.07	0.06	1	2
	Maximum	9.04	6.86	151	188
	Median	1.58	1.13	26	31
Overall	Minimum	0.04	0.06	1	2
	Maximum	9.70	6.86	162	188
	Median[a]	1.60 a	1.10 b	27 c	30 c

[a] Overall median emission fluxes or emission factors followed by the same letters are not significantly different at the 5% level of significance.

Monthly emission rates are plotted with monthly average temperatures and monthly cumulative rain amounts in Figures 3-4a to 3-4d. Monthly consumption of water for the sprinkler system operation is also shown in Figure 3-4e. Statistical analysis showed that the temperature significantly ($p < 0.05$ for KS1and KS2) affected the emission rate whereas rainfall amount ($p = 0.47$ for KS1, $p = 0.77$ for KS2) and number of days with rainfall events ($p = 0.14$ for KS1, $p = 0.71$ for KS2) did not. Further analysis of the data for the May to November period (i.e., months with highest temperatures; 20 ± 9 °C for KS1, 21 ± 8 °C for KS2), however, revealed that the number of days with rainfall events significantly ($p = 0.03$) influenced emission fluxes for feedlot KS1. May to November period had relatively higher emission rates (2.55 ± 3.66 g/m^2-day for KS1, 2.35 ± 1.82 g/m^2-day for KS2) than the December to April period (0.43 ± 1.32 g/m^2-day for KS1, 0.50 ± 0.57 g/m^2-day for KS2), which had lower temperatures (2 ± 10 °C). This was expected since high temperatures should result in high evaporation of water from pen surfaces and consequently, dryer pen surfaces, which would then have higher PM emission potential (Miller and Berry, 2005; Razote et al., 2006). Cool months, with temperatures several degrees above freezing, could still have high emission rates. An example would be the month of November in 2007. Even with low temperature (6 ± 9 °C), it had an emission flux of 4.62 g/m^2-day. This emission flux was close to that of the month of August, which was the hottest month (27 ± 7 °C) and had the highest emission flux (5.69 g/m^2-day) for the year. High emission rates for the month of November could be due to prolonged dry periods; during this month, KS1 only had 0.25 mm (1 day) of precipitation and the sprinkler system was not used.

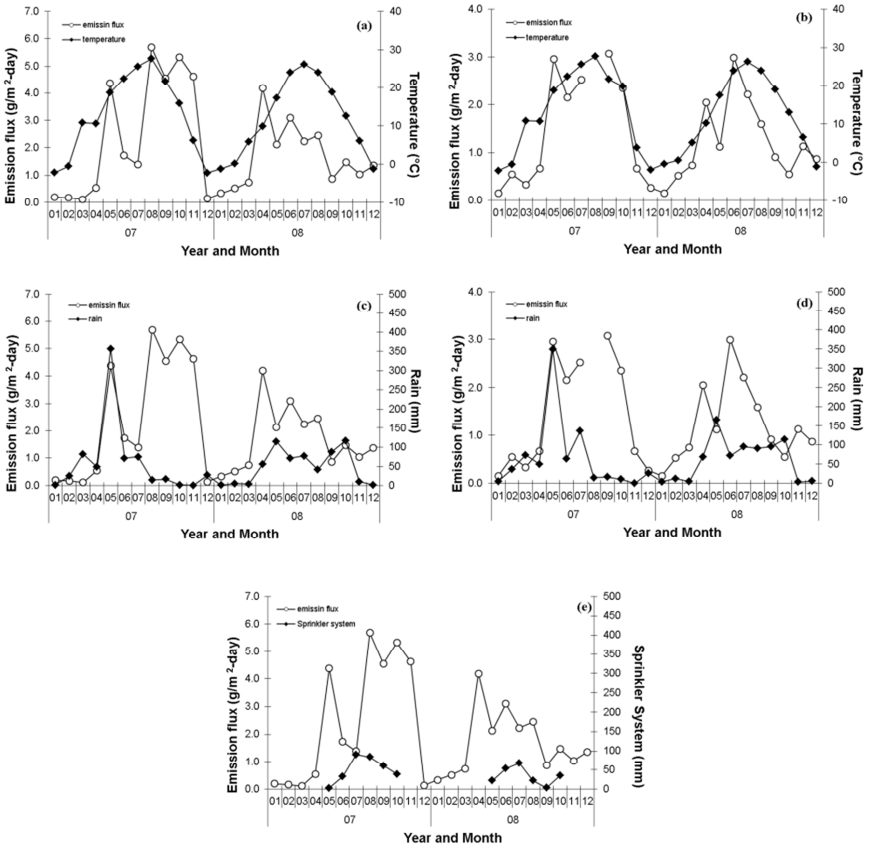

Figure 3-4. Monthly trends of emission flux plotted with temperature at feedlot (a) KS1 and (b) KS2; with amount of rain at (c) KS1 and (d) KS2; and with amount of sprinkler water at (d) KS1.

Hourly PM_{10} emission fluxes for KS1 and KS2 are shown in Figure 3-5. Highest PM_{10} concentrations of the day were measured during the EDP period for both KS1 (47 ± 243 µg/m^3) and KS2 (34 ± 125 µg/m^3). Relatively high concentrations can be brought about by three conditions: high emission rate, low wind speed, and/or stable atmosphere (Cimorelli et al., 2004). All these conditions were observed at the feedlots during the EDP period: (1) computed PM_{10} emission fluxes were relatively high during the EDP period for KS1 (16 ± 68 µg/m^2-sec) and KS2 (11 ± 38 µg/m^2-sec), specifically from 8:00 p.m. to 10:00 p.m.; (2) wind speed generally started to decrease around early evening (KS1: 3.5 ± 2.8 m/sec; KS2: 3.0 ± 2.2 m/sec); and (3) atmospheric conditions were generally stable during the EDP period based on the Monin-Obukhov length and on the classification by Seinfeld and Pandis (2006). High PM_{10} emission fluxes during this period were also calculated by McGinn et al. (2010) using a non-Gaussian

model (i.e., Lagrangian stochastic model). Although increase in emission rate was observed for both feedlots during the EDP period, emission fluxes at KS2 were relatively lower than at KS1. The degree of increase in emission rate could be affected by several factors such as PM control methods implemented (i.e., sprinkler system, pen cleaning) and management practice (i.e., stocking density). Even with a water sprinkler system, feedlot KS1 still had a higher emission flux than KS2, a non-sprinkled feedlot, possibly due to the greater amount of manure on the pen surface associated with less frequent pen cleaning/manure hauling at KS1. Water application would lower PM emission rate as shown previously for rainfall events; however, removal of manure from pen surfaces could also be effective in lowering PM emissions from feedlots.

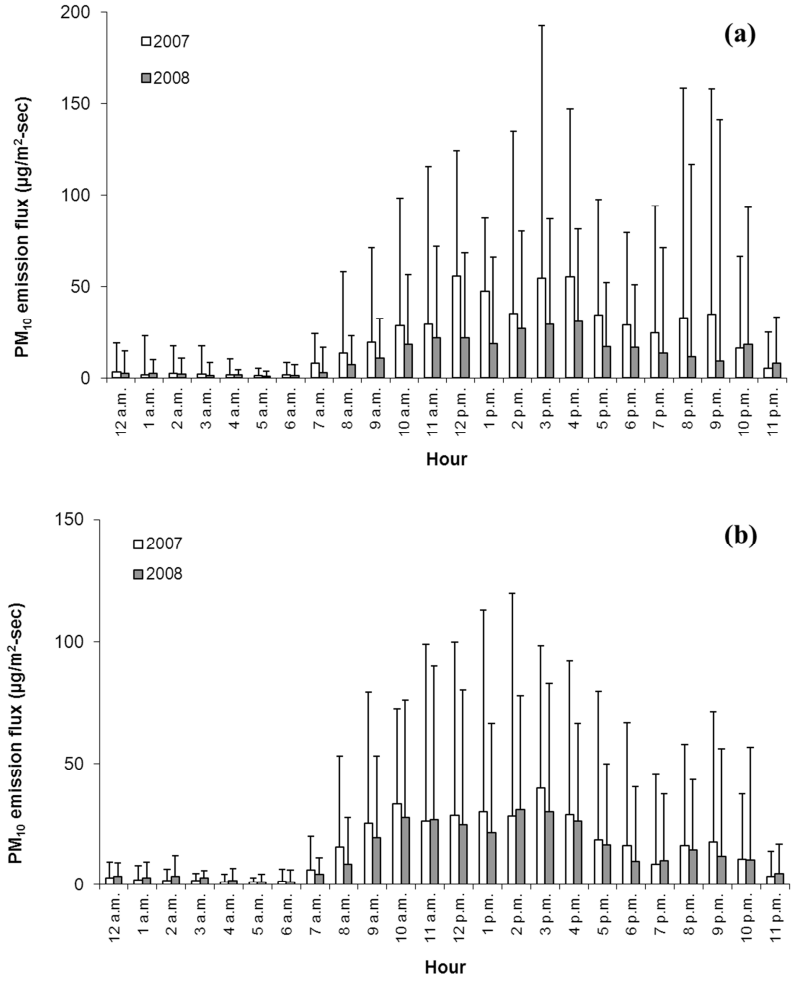

Figure 3-5. Median hourly PM_{10} emission fluxes at feedlots (a) KS1 and (b) KS2. Median values were based on days with emission data. Error bars represent upper standard deviation estimates.

For the late morning and afternoon periods (10:00 a.m.-5:00 p.m.), relatively lower PM_{10} concentrations (39 ± 95 $\mu g/m^3$ for KS1, 38 ± 79 $\mu g/m^3$ for KS2) were measured at the two feedlots. From dispersion modeling, PM_{10} emission fluxes were generally high during this period (27 ± 66 $\mu g/m^2$-sec for KS1 and 27 ± 59 $\mu g/m^2$-sec for KS2). For KS2, highest emission fluxes in the day were from this period. This high emission flux at KS2 could be due to feedlot set-up and activities. However, even with high PM_{10} emission fluxes in the afternoon period, PM_{10} concentrations were relatively low possibly because of unstable atmospheric conditions and higher wind speeds (KS1: 4.8 ± 2.9 m/sec; KS2: 4.0 ± 2.4 m/sec).

Figure 3-6 plots the mean percentage contribution of each hour to the daily PM_{10} emission flux. For KS1, the afternoon period had the highest contribution (average of 61%) to the overall daily PM_{10} emission flux; same was observed for KS2 (average of 66%). Average contributions of EDP period to the overall daily emission flux were 32% and 25% for KS1 and KS2, respectively. Still, emission flux for the EDP period was observed to increase during 8:00 p.m. to 10:00 p.m. period when the PM_{10} concentration reached its peak. For days with a least 18 hourly PM_{10} emission fluxes, non-parametric tests showed that emission fluxes during the afternoon period were higher than and significantly different ($p < 0.001$ for KS1 and KS2) from those for the EDP period.

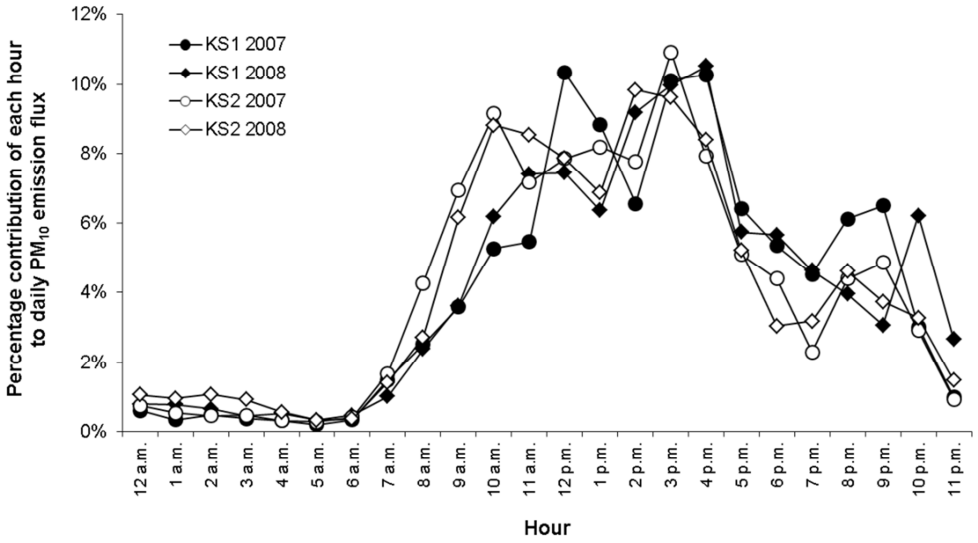

Figure 3-6. Percentage contribution of each hour to the daily PM_{10} emission flux for feedlots KS1 and KS2 based on mean hourly PM_{10} emission fluxes for the 2-yr period using days with emission data.

There were several limitations in this study that relate to PM monitoring and inherent weaknesses of atmospheric dispersion modeling. One limitation was the assumption that the emission flux was uniform throughout the feedlot and that the mass concentration, particularly on the downwind side of the feedlot, was also uniform so that a single point measurement of the concentration would be adequate. Another limitation is related to the atmospheric dispersion model (Holmes and Morawska, 2006; Turner and Schulze, 2007). Some studies have suggested that dispersion modeling results were model specific (Hall et al., 2002; Faulkner et al., 2007). In addition, due to limitations of on-site weather stations, atmospheric stability (i.e., Monin-Obukhov length) was obtained from a meteorological instrumentation tower located almost 50 km away from one of the feedlots. Despite these limitations, the emission rates presented here could serve as basis for estimating emission rates for cattle feedlots and for evaluating abatement measures.

3.4 Conclusions

PM_{10} emission rates at two cattle feedlots (KS1 and KS2) in Kansas were determined from measured PM_{10} concentrations using inverse dispersion modeling with AERMOD. For the 2-yr period, daily average PM_{10} concentration downwind exceeded 150 $\mu g/m^3$ 84 out of 145 days

for KS1 (downwind locations of 5 m and 30 m) and 33 out of 112 days for KS2 (downwind locations of 40 m and 60 m) for days with at least 18 hourly concentration measurements. Based on the 2-yr study period, feedlot KS1, equipped with a sprinkler system, had a median PM_{10} emission flux of 1.60 g/m^2-day (241 days) and emission factor of 27 kg/1,000 hd-day. KS2, a non-sprinkled feedlot but with more frequent pen cleaning, had a median PM_{10} emission flux of 1.10 g/m^2-day (186 days) and emission factor of 30 kg/1,000 hd-day. These emission factors were considerably smaller than published EPA PM_{10} emission factor for cattle feedlots.

Emission fluxes were greater during warm season and prolonged dry periods, generally because of the presence of dry, uncompacted manure layer on pen surfaces. Hourly emission rates varied during a given day. Highest emission fluxes were observed for the 10:00 a.m. to 5:00 p.m. period; possibly because of unstable atmospheric conditions, however, measured PM_{10} concentration during this period was not high. Emission flux also increased in the evening from 8:00 p.m. to 9:00 p.m., possibly due to greater animal activity during this period. Due to stable atmospheric conditions, very high PM_{10} concentration was measured for this period.

3.5 References

Auvermann, B., R. Bottcher, A. Heber, D. Meyer, C.B. Parnell Jr., B. Shaw, and J.Worley. 2006. Particulate matter emissions from animal feeding operations. In *Animal Agriculture and the Environment: National Center for Manure and Animal Waste Management White Papers*. Eds. J.M. Rice, D.F. Caldwell, F.J. Humenik. St. Joseph: ASABE.

Baum, K.A. 2003. Air emissions measurements at cattle feedlots. M.S. thesis, Kansas State University, Manhattan, KS.

Calder, K.L. 1977. Multiple-source plume models of urban air pollution – their general structure. *Atmospheric Environment* 11:403–414.

CFR. 2005. Revision to the guideline of air quality models: adoption of a preferred general purpose (flat and complex terrain) dispersion model and other revisions. *Code of Federal Regulations* Part 51(Title 40).

Cimorelli, A.J., S.G. Perry, A. Venkatram, J.C. Weil, R.J. Paine, R.B. Wilson, R.F. Lee, W.D. Peters, R.W. Brode, and J.O. Paumier. 2004. AERMOD: Description of Model Formulation. EPA-454/R–03–004., 68218–68261. Research Triangle Park, NC: U.S. Environmental Protection Agency.

Countess Environmental. 2006. *Western Regional Air Partnership (WRAP) Fugitive Dust Handbook*. Contract No. 30204-111. Denver, CO: Western Governors' Association.

Faulkner, W.B., L.B. Goodrich, V.S.V. Botlaguduru, S.C. Capareda, and C.B. Parnell. 2009. Particulate matter emission factors for almond harvest as a function of harvester speed. Journal of the Air and Waste Management Association 59:943–949. doi: 10.3155/1047-3289.59.8.943

Faulkner, W.B., J.J. Powell, J.M. Lange, B.W. Shaw, R.E. Lacey, and C.B. Parnell. 2007. Comparison of dispersion models for ammonia emissions from a ground-level area source. *Transactions of the ASABE* 50: 2189–2197.

Gonzales, H. 2010. Particulate emissions from cattle feedlots – particle size distribution and contribution of wind erosion and unpaved roads. M.S. thesis, Kansas State University, Manhattan, KS.

Goodrich, L.B., W.B. Faulkner, S.C. Capareda, C. Krauter, and C.B. Parnell. 2009. Particulate matter emissions from reduced-pass almond sweeping. *Transactions of the ASABE* 52:1669–1675.

Grelinger, M.A., and T. Lapp. 1996. An evaluation of published emission factors for cattle feedlots. In *Proceedings of International Conference on Air Pollution from Agricultural Operations*, Kansas City, MO, February 7–9, 1996. Ames, IA: MidWest Plan Service.

Hall, D.J., A.M. Spanton, M. Bennett, F. Dunkerley, R.F. Griffiths, B.E.A. Fisher, and R.J. Timmis. 2002. Evaluation of new generation atmospheric dispersion models. *International Journal of Environment and Pollution* 18:22–32.

Holmes, N.S., and L. Morawska. 2006. A review of dispersion modeling and its application to the dispersion of particles: an overview of different dispersion models available. *Atmospheric Environment* 40:5902–5928. doi: 10.1016/j.atmosenv.2006.06.003

MACTEC Federal Programs, Inc. 2009. Addendum – User's guide for the AMS/ EPA Regulatory Model – AERMOD. EPA-454/B-03-001. Research Triangle Park, NC: U.S. Environmental Protection Agency.

McGinn, S.M., T.K. Flesch, D. Chen, B. Crenna, O.T. Denmead, T. Naylor, and D. Rowell. 2010. Coarse particulate matter emissions from cattle feedlots in Australia. *Journal of Environmental Quality* 39:791–798. doi: 10.2134/jeq2009.0240

Midwest Research Institute. 1988. *Gap Filling PM_{10} Emission Factors for Selected Open Area Dust Sources*. EPA-450/4–88–003. Research Triangle Park, NC: U.S. Environmental Protection Agency.

Miller, D.N., and E.D. Berry. 2005. Cattle feedlot soil moisture and manure content: I. Impacts on greenhouse gases, odor compounds, nitrogen losses, and dust. *Journal of Environmental Quality* 34:644–655.

Mitloehner, F.M. 2000. Behavioral and environmental management of feedlot cattle. Ph.D. dissertation, Texas Tech University, Lubbock, TX.

National Research Council. 2003. *Air Emissions from Animal Feeding Operations: Current Knowledge, Future Needs*. Washington, DC: National Academy of Sciences.

Pacific Environmental Services, Inc. 1995. *User's Guide for the Industrial Source Complex (ISC3) Dispersion Models*. EPA-454/B-95-003b. Research Triangle Park, NC: U.S. Environmental Protection Agency.

Pacific Environmental Services, Inc. 2004. *User's Guide for the AMS/EPA Regulatory Model – AERMOD*. EPA-454/B-03-001. Research Triangle Park, NC: U.S. Environmental Protection Agency.

Perry, S.G., A.J. Cimorelli, R.J. Paine, R.W. Brode, J.C.Weil, A. Venkatram, R.B. Wilson, R.F. Lee, and W.D. Peters. 2005. AERMOD: a dispersion model for industrial source applications. Part II: model performance Against 17 field study databases. *Journal of Applied Meteorology* 44:694–708.

Purdue Applied Meteorology Laboratory. 2009. *Quality Assurance Project Plan for the National Air Emissions Monitoring Study*, Revision No. 3. West Lafayette: Purdue University.

Razote, E.B., R.G. Maghirang, B.Z. Predicala, J.P. Murphy, B.W. Auvermann, J.P. Harner, and W.L. Hargrove. 2006. Laboratory evaluation of the dust emission potential of cattle feedlot surfaces. *Transactions of the ASABE* 49: 1117–1124.

San Joaquin Valley Air Pollution Control District. 2006. Dairy and feedlot PM_{10} emission factors: draft office memo. http://www.valleyair.org/ (accessed March 5, 2010).

SAS Institute Inc. 2004. *SAS System for Windows, Release 9.1.3*. Cary: SAS Institute Inc.

Schwertman, N.C., M.A. Owens, and R. Adnan. 2004. A simple more general boxplot method for identifying outliers. *Computational Statistics and Data Analysis* 47:165–174. doi: 10.1016/j.csda.2003.10.012

Seinfeld, J.H., and S.N. Pandis. 2006. *Atmospheric Chemistry and Physics— From Air Pollution to Climate Change*, 2nd ed. Hoboken, NJ: John Wiley & Sons.

Turner, D.B., and R.H. Schulze. 2007. *Practical Guide To Atmospheric Dispersion Modeling*. Dallas, TX: Trinity Consultants, Inc. and Air & Waste Management Association.

U.S. Department of Agriculture. 2011. *Cattle on Feed*. Washington, DC: National Agricultural Statistics Service, U.S. Department of Agriculture.

U.S. Environmental Protection Agency. 2001. *Procedures Document for National Emission Inventory, Criteria Air Pollutants 1985–1999*. EPA-454/R–01–006. Research Triangle Park, NC: U.S. Environmental Protection Agency.

U.S. Environmental Protection Agency. 2003. *National Air Quality and Emissions Trends Report – 2003 Special Studies Editio*n. EPA-454/R–03–005. Research Triangle Park, NC: U.S. Environmental Protection Agency.

U.S. Environmental Protection Agency. 2008a. *AERSURFACE User's Guide*. EPA-454/B-08-001. Research Triangle Park, NC: U.S. Environmental Protection Agency.

U.S. Environmental Protection Agency. 2008b. *Integrated Review Plan for the National Ambient Air Quality Standards for Particulate Matter*. EPA-452/R-08-004. Research Triangle Park, NC: U.S. Environmental Protection Agency.

U.S. Environmental Protection Agency. 2009. *AERMOD Deposition Algorithms– Science Document (Revised Draft)*. Research Triangle Park, NC: U.S. Environmental Protection Agency.

Wanjura, J.D., C.B. Parnell, B.W. Shaw, and R.E. Lacey. 2004. A Protocol for determining a fugitive dust emission factor from a ground level area source. In *American Society of Agricultural Engineers (ASAE) Proceedings*, Ontario, Canada, August 1–4, 2004. St. Joseph: ASAE. Paper 044018.

CHAPTER 4 - **Comparison of AERMOD and WindTrax Dispersion Models in Determining PM_{10} Emission Rates from a Beef Cattle Feedlot**[2]

4.1 Introduction

Air emissions from animal feeding operations (AFOs) have been a primary interest of research because of their potential impact on human health and the environment. Particulate matter (PM) from AFOs has been cited as both a health and environmental hazard (Mitloehner and Calvo, 2008; National Research Council, 2003; Von Essen and Auvermann, 2006). Assessing the full impact of PM emissions from AFOs on local communities is difficult, due to the lack of data and the cost of monitoring programs. Open cattle feedlots make monitoring efforts even more challenging because of their size and the variable nature of emissions from open sources. Reverse-dispersion modeling is a potential tool to solve this problem; it estimates emissions from open sources by measuring only upwind and downwind concentrations followed by back-calculation of emission rates using an atmospheric dispersion model.

Two dispersion models that have been applied in recent cattle feedlot emission studies are AERMOD, the choice for the American Meteorological Society and the U.S. EPA's preferred regulatory model (CFR, 2005), and WindTrax (Flesch and Wilson, 2005). WindTrax, a backward Lagrangian stochastic-based (bLS) model, has been used to estimate emission rates for PM_{10} (McGinn et al., 2010), odor (Galvin et al., 2006), ammonia (Faulkner et al., 2007; McGinn et al., 2007; Price et al., 2004), and greenhouse gases (Denmead et al., 2008) from cattle feedlots. AERMOD, a Gaussian-based model, has also been used for simulating feedlot emissions on PM_{10} (Bonifacio et al., 2012) and ammonia (Faulkner et al., 2007).

A concern on estimating emission rates from area sources is that calculated values maybe model-specific, that is, emission rates determined with one model (e.g., WindTrax) may not be suitable for other models (e.g., AERMOD). For example, a feedlot study (Faulkner et al., 2007)

[2] Bonifacio, H.F., R.G. Maghirang, E.B. Razote, S.L. Trabue, and J.H. Prueger. 2013. Comparison of AERMOD and WindTrax dispersion models in determining PM_{10} emission rates from a beef cattle feedlot. *J. Air & Waste Manage. Assoc*. doi:10.1080/10962247.2013.768311.

reported that AERMOD and WindTrax modeling results were significantly different, with AERMOD predicting higher emission rates than WindTrax during daytime and lower during nighttime. The said study indicated that developing conversion factors between models was not feasible.

A vital component of dispersion modeling is the type of meteorological data because they can significantly affect modeling results (Dai et al., 2003). Although several approaches to specifying meteorological measurements in WindTrax are available, using sonic anemometer measurements is recommended to achieve higher accuracy. Many more meteorological parameters are required to characterize the atmospheric boundary layer in AERMOD. Because on-site measurement of all these parameters can be expensive, a number of them can be obtained from National Oceanic and Atmospheric Administration (NOAA) stations (U.S. EPA, 2009) and/or generated using prognostic meteorological models (Touma et al., 2007).

Evidently, more research is needed to evaluate and compare AERMOD and WindTrax in determining emission rates for ground-level area sources such as open cattle feedlots. This research was conducted to compare AERMOD and WindTrax in terms of their back-calculated PM_{10} emission rates for a beef cattle feedlot in Kansas using an extended measurement period. The effect of the type of meteorological data on the performance of both models was also verified.

4.2 Materials and Methods

The reverse dispersion modeling technique in this study involved three major steps in computing PM_{10} emission flux. As shown in Figure 4-1a, the first step involved field measurements of PM_{10} concentrations and weather conditions; the second step was dispersion modeling using either AERMOD or WindTrax for an assumed unit emission flux ($1 \mu g/m^2$-sec) to calculate unit-flux concentrations; and in the last step, PM_{10} emission flux was back-calculated using values obtained from the first two steps (i.e., measured and calculated unit-flux concentrations from the first and second steps, respectively).

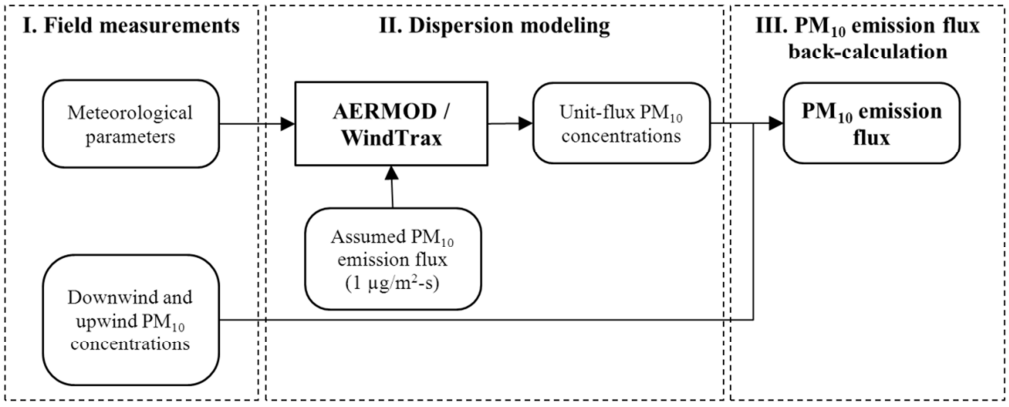

Figure 4-1. Reverse dispersion modeling technique steps.

4.2.1 Field Measurements

4.2.1.1 Feedlot Description

Field measurements were conducted at a commercial cattle feedlot that was surrounded by agricultural lands in Kansas from May 2010 through September 2011. The feedlot had approximately 30,000 head of cattle with a total pen area of about 59 ha. Manure on pen surfaces was scraped two to three times per year per pen and was hauled from each pen at least once a year. During prolonged dry periods, water was applied to unpaved roads, alleys, and/or pens using water trucks to control dust emission.

4.2.1.2 Micrometeorological Conditions

A 5.3-m tower equipped with micrometeorological and eddy covariance (EC) instrumentations was installed inside the feedlot. The pen in which the tower was installed was approximately 0.4 km and 1.3 km away from north and south edges of the feedlot, respectively (Figure 4-2). The EC instrumentation included a 3D sonic anemometer (CSAT3, Campbell Scientific, Inc., Logan, UT) for measuring the three orthogonal wind velocity components (*u*, *v*, *w*) and temperature, and an infrared hygrometer (Model LI-7500A, LICOR, Inc., Lincoln, NE) for measuring water vapor density. The sampling frequency for the EC instrumentation was 20 Hz. A data logger (Model CR5000, Campbell Scientific, Inc., Logan, UT) was used to record the EC measurements as 15-min averages and was programmed to compute and record friction velocity, sensible heat, resultant horizontal wind speed, wind direction, and variances and covariances of wind components and temperature.

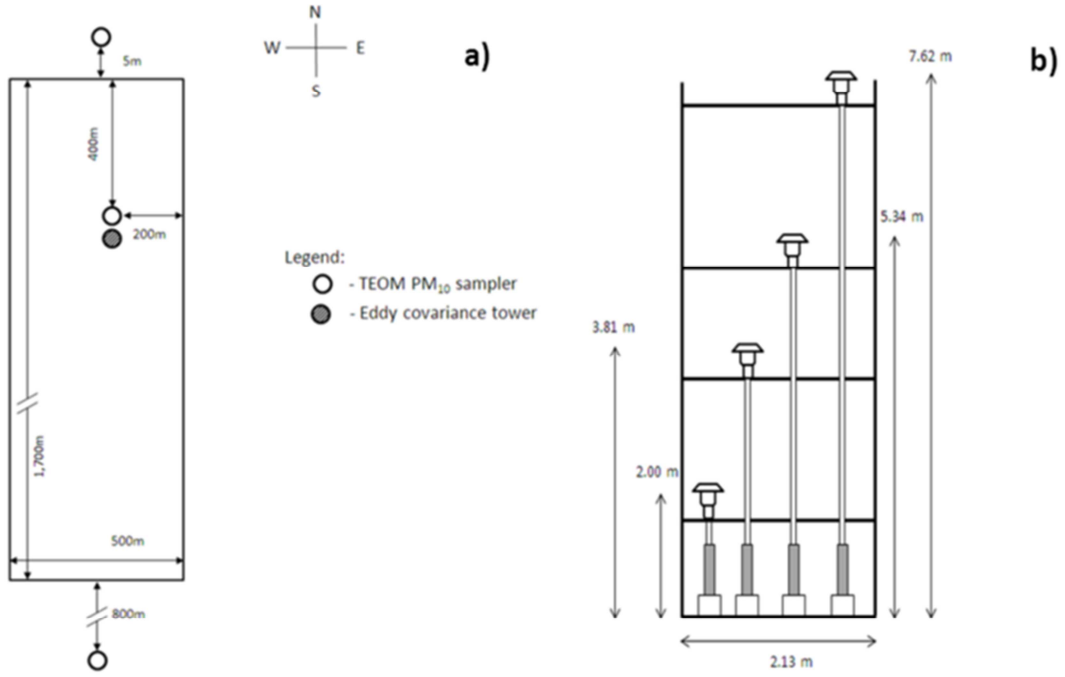

Figure 4-2. Locations of PM_{10} samplers and eddy covariance tower at the feedlot.

4.2.1.3 PM_{10} Concentrations

Tapered element oscillating microbalance (TEOM) PM_{10} monitors (Series 1400a, Thermo Fisher Scientific, East Greenbush, NY; federal equivalent method designation No. EQPM-1090-079) were used to measure PM_{10} mass concentration at three locations simultaneously: (1) within the feedlot, approximately 5.5 m north of the EC tower; (2) 5 m away from the north edge of the feedlot; and (3) 800 m away from the feedlot south edge (Figure 4-2). For the sampling location within the feedlot, PM_{10} concentrations were measured at four heights (i.e., 2.0, 3.81, 5.34, and 7.62 m), as shown in Figure 4-1b. For the north and south edge sampling locations, PM_{10} concentration was measured at 2.0 m. TEOM PM_{10} monitor's recording interval was set at 20 min. PM_{10} concentrations measured within the feedlot were used as downwind concentrations, whereas PM_{10} concentrations at the north and south edges of the feedlot were used as upwind concentrations, depending on the wind direction (i.e., upwind at north site if wind was coming from the north, south site if wind was from the south). Selection of sampling locations was based on feedlot layout, power availability, and feedlot management approval.

4.2.1.4 Data Screening

Measured values were screened based on the following: (1) accuracy of the measured meteorological parameters; (2) wind direction; and (3) completeness of meteorological and PM_{10} concentration data. The first screening was based on the criteria suggested by Flesch et al. (2005). Measurements made during periods with very strong stability (absolute value of L, $|L|$, $\leq$ 10 m), low wind speed (friction velocity, u_*, $\leq$ 0.15 m/sec), and/or unrealistic wind profile (surface roughness, $z_{o,} \geq$ 1 m) were removed because they could have been unreliable.

Second, data points were screened based on wind direction. Because upwind PM_{10} samplers were located at the north and south edges of the feedlot, only data points with north wind (wind from north) or south wind (from south) were considered. In addition, the north and south wind direction ranges were optimized to resolve data completeness issues due to several equipment problems (Table 4-1). From preliminary analysis using EC measurements, it was determined that wind directions within 0° $\pm$ 67.5° (north wind) and 180° $\pm$ 67.5° (south wind) met the fetch requirement based on the sampler location inside the feedlot and the feedlot layout. Therefore, only data points with wind directions within these ranges were included in the analysis.

Table 4-1. Completeness of eddy covariance (EC) and TEOM PM_{10} concentration measurements[a]

		EC	TEOM PM_{10} concentration			Reasons for lack of data
			Inside the feedlot [b, c]	North site [c]	South site [c]	
2010	May	66%	14%	12%	*no data*	Severe weather in April resulting in late monitoring in May
	June	100%	58%	*no data*	58%	Equipment availability issue as a result of severe weather in April
	July	100%	84%	*no data*	90%	
	August	96%	11%	*no data*	12%	Experimental set-up and equipment damaged by severe storms.
	September	100%	*no data*	*no data*	*no data*	Equipment repair and calibration after severe weather
	October	100%	36%	1%	*no data*	Start of PM_{10} monitoring late October; equipment availability issue
	November	54%	77%	89%	*no data*	Equipment availability issue
	December	91%	91%	50%	35%	Equipment availability issue
2011	January	96%	100%	44%	75%	Remote connection problem for the N and S sites
	February	92%	94%	98%	98%	
	March	59%	58%	98%	99%	Power supply problem for the sampling site inside the feedlot
	April	98%	77%	76%	78%	
	May	98%	96%	92%	98%	
	June	99%	82%	97%	100%	
	July	100%	98%	48%	52%	Remote connection problem for the N and S sites
	August	66%	40%	70%	97%	Hot weather – temperature control issue for the samplers inside the feedlot
	September	73%	14%	14%	54%	Hot weather – temperature control issue for the samplers inside the feedlot
Overall		87%	61%	46%	55%	

[a] Completeness based on hourly measurements; [b] equipped with remote connection for downloading data; [c] data points with negative net concentrations already removed.

For the last screening, only data points with complete meteorological and PM_{10} concentration (downwind, upwind) data were included in the analyses. TEOM PM_{10} concentration data were missing/incomplete in several months as shown in Table 4-1. Data points with large negative 20-min PM_{10} concentrations (< -10 µg/m^3) were also not used in accordance with the TEOM manufacturer's recommendations (Rupprecht & Patashnick Co., Inc., 2011). The 20-min downwind and upwind sampler concentrations were integrated into hourly averages before computing the hourly net concentrations (i.e., downwind concentration – upwind concentration). Prior to data screening, the four heights had more than 4,000 hourly data points with a complete set of downwind and upwind PM_{10} concentrations; however, an average of 21% (n = 855) of the data points had negative net PM_{10} concentrations. Forty-five percent (45%) of these negative values had net concentrations ranging from 0 to -10 µg/m^3; 28% from -10 to -50 µg/m^3; 12% from -50 to -100 µg/m^3; and 15% were lower than -100 µg/m^3. Negative net PM_{10} concentrations were excluded in the analyses because they could indicate presence of a significant PM_{10} emission source outside the feedlot. Also, they could be due to negligible PM_{10} emissions from the feedlot; based on precipitation data (rain gage TE525, Campbell Scientific, Inc., Logan, UT), close to 40% of the negative net concentrations could be due to effects of rainfall on PM emissions.

4.2.2 AERMOD Modeling

4.2.2.1 Dispersion Modeling

AERMOD is a Gaussian plume model based on the general equation for concentration, *c*, given by:

$$u\ \frac{\partial c}{\partial x} = D_y \frac{\partial^2 c}{\partial y^2} + D_z \frac{\partial^2 c}{\partial z^2} \qquad (4\text{-}1)$$

where the overall mass transport is defined by the convective mass transport in *x*-direction (downwind) with constant wind speed *u*, and the diffusion (i.e., molecular and eddy) transport in *y* (crosswind) and *z* (vertical) directions with constant effective diffusion coefficients (D_y, D_z) (Heinsohn and Kabel, 1999). The general analytical solution to eq 4-1 is commonly referred to as the Gaussian plume model (Heinsohn and Kabel, 1999). AERMOD, however, is different from other Gaussian models in way it simulates dispersion as it uses a well-characterized planetary boundary layer structure, and applies a bi-Gaussian distribution to represent vertical

concentration distribution for unstable conditions rather than a Gaussian distribution (Cimorelli et al., 2004; Perry et al., 2005).

In this study, the following were applied in AERMOD modeling: an emission flux of 1.0 $\mu g/m^2$-sec was assumed in the simulation, the feedlot was treated as a flat terrain, and all pens had same and constant emission for the 1-hr averaging period. Particle settling was not considered because the available WindTrax version does not include the gravitational settling of particles. From preliminary analysis (n = 4,161 hourly data points) using PM_{10} particle size distribution for the feedlot (55% for 6.20 µm–9.90 µm; 26% for 3.10 µm–6.20 µm; 8% for 1.80 µm–3.10 µm; and 11% for <1.80 µm) measured with a micro-orifice uniform deposit impactor (MOUDI, Model 100-R, MSP Corporation, Shoreview, MN), concentrations calculated with AERMOD would be higher by 4% if settling effects were neglected.

4.2.2.2 Meteorological Data

A critical component of dispersion modeling is the meteorological data applied in the simulation. Two approaches of generating meteorological files required in AERMOD were evaluated in this study. The first approach, herein referred to as AERMOD-PD, utilized AERMET, which is the AERMOD meteorological preprocessor (U.S. EPA, 2009). Three meteorological data sets (i.e., upper air, surface hourly, on-site) were provided to AERMET. Upper air and surface hourly data were obtained from the NOAA sites, which were about 90 km and 29 km, respectively, from the feedlot, and were described as pseudo data (Dai et al., 2003). On-site data consisted of wind speed, wind direction, and temperature measured by the EC instrumentation at the feedlot. Values for the three site characteristics required in estimating other meteorological parameters, such as friction velocity (u_*), sensible heat and Monin-Obukhov length (L) were as follows: albedo (0.2) and Bowen ratio (2.0) were based on the U.S. EPA (2008) classification table; and surface roughness, z_o, was set at 5.0 cm based on the U.S. EPA classification table and on a previous study on the same feedlot by Baum (2003).

In the second approach, herein referred to as AERMOD-EC, u_*, and sensible heat measured by EC instrumentation were now used in addition to wind speed, wind direction, and temperature. Without the need for albedo and Bowen ratio, other parameters necessary in running AERMOD were derived using equations discussed by Cimorelli et al. (2004). The 15-min averages of the measured parameters were first integrated into hourly averages before using them in the modeling.

4.2.3 WindTrax Modeling

4.2.3.1 Dispersion Modeling

WindTrax is based on a reduced transport equation given by:

$$\frac{\partial c}{\partial t} + u\ \frac{\partial c}{\partial x} + v\ \frac{\partial c}{\partial y} + w\ \frac{\partial c}{\partial z} = 0 \qquad (4\text{-}2)$$

where the overall mass transport is defined by the convective mass transport in all directions (*x*, *y*, *z*) with constant wind speeds (*u*, *v*, *w*) and the accumulation term (*dc/dt*) (Flesch and Wilson, 2005). The method selected to solve eq 4-2 is the bLS approach that describes the evolution of particle position and particle velocity in a backward time frame. The derivation of concentration equation for the bLS approach is explained in detail by Flesch et al. (1995) and Flesch and Wilson (2005).

This study used WindTrax version 2.0.8.4. Similar to AERMOD, a unit emission flux (1.0 µg/m^2-sec) was used in the modeling; modeling inputs (receptor heights and location, pen locations) were similar to the inputs in AERMOD modeling. The number of particles released was set at 50,000, which is the default value to shorten simulation time. Based on preliminary analysis (n = 192) comparing particle number settings of 50,000 and 1 million, the mean percentage difference in predicted concentration was less than 1% (maximum of 5%).

4.2.3.2 Meteorological Data

In simulating dispersion, WindTrax requires seven meteorological parameters to characterize the surface boundary layer. These include u_*, wind direction, z_o, L, and the standard deviations for the three wind components (σ_u for u, σ_v for v, σ_w for w) (Crenna, 2006a, 2006b). Two of the four basic approaches to providing meteorological parameters in WindTrax were evaluated in this study. The first approach (WindTrax-SD) was using the sonic anemometer data and was input as mean products of *u*, *v*, *w*, and temperature. Expression for the mean product is given by:

$$\langle v_i \times v_j \rangle = \langle v'_i v'_j \rangle + \langle v_i \rangle \langle v_j \rangle \qquad (4\text{-}3)$$

where $\langle v_i \times v_j \rangle$ is the mean product, $\langle v'_i\ v'_j \rangle$ is the covariance (or variance if $i = j$), and $\langle v_i \rangle$ and $\langle v_j \rangle$ are the averages of parameters v_i and v_j (wind components, temperature). All seven parameters could be derived by WindTrax from the sonic anemometer data following equations

in Flesch et al. (2004). Use of sonic anemometer data in WindTrax is described as the most accurate.

The second approach (WindTrax-3V), which was based on the Monin-Obukhov length theory, applied a 3-variable meteorological data set composed of wind speed, z_o, and L. Wind speed and wind direction were derived from the sonic anemometer data; z_o was set at 5.0 cm, similar to AERMOD modeling in this study; and L was computed using the original Monin-Obukhov length equation (Cimorelli et al., 2004). The rest of the parameters were then computed by WindTrax: u_* was derived from wind speed and L, and σ_u, σ_v, and σ_w were estimated using empirical relationships shown below:

$$\frac{\sigma_u}{u_*} = \begin{cases} 2.5\ , & L>0 \\ \sqrt{0.35\ w_*^2+2.5^2}, & L<0 \end{cases} \tag{4-4a}$$

$$\frac{\sigma_v}{u_*} = \begin{cases} 2.0\ , & L>0 \\ \sqrt{0.35\ w_*^2+2.0^2}, & L<0 \end{cases} \tag{4-4b}$$

and

$$\frac{\sigma_w}{u_*} = \begin{cases} 1.25\ , & L>0 \\ 1.25\left(1.0\ -3.0\frac{z}{L}\right)^{\frac{1}{3}}, & L<0 \end{cases} \tag{4-4c}$$

where z is measurement height, and w_* is convective velocity scale calculated from L and height of boundary layer during unstable conditions, H, using eq 4-5 (Crenna, 2006b; Flesch et al., 2004).

$$\frac{w_*}{u_*} = \left(\frac{-H}{0.4L}\right)^{\frac{1}{3}} \tag{4-5}$$

4.2.4 Modeling Height

For one height with at least 10,000 15-min data points, WindTrax simulation (using PC with 2.99 GHz processor and 1.99 GB RAM) took approximately 31 days using sonic anemometer and 7 days using 3-variable data sets. AERMOD, on the other hand, only took a few seconds in modeling the whole measurement period (17 months, ~12,000 hourly data points). Due to extremely long modeling time required in running WindTrax, comparison between the two models was completed using only one receptor height. With the capability of giving modeling results instantly, AERMOD was used to determine which receptor height would be best used in the comparisons. Data used in the preliminary analysis were from January through August 2011, and meteorological parameters in the modeling were from the EC measurement. Given that the area source was ground-level and the downwind samplers were located within the area source, data points were further screened using the criteria $PM_{10,2.0m} > PM_{10,3.81m} > PM_{10,5.34m} > PM_{10,7.62m}$ (i.e., the higher the receptor height, the lower the concentration). Using 376 hourly data points from 2011, the back-calculated PM_{10} emission fluxes are plotted in a scatter plot matrix (Figure 4-3). Linearity in back-calculated emission fluxes existed among the receptor heights, with the highest linearity ($R^2 \geq 0.86$) observed between adjacent heights. In terms of PM_{10} emission fluxes, statistical comparison showed that the 2.0-m receptor height was significantly different ($P < 0.05$) from the other heights, whereas the other three heights were not significantly different ($P \geq 0.14$) from each other. Combination of sampler placement (i.e., inside a feedlot pen) and short receptor height could have contributed to higher PM_{10} emission fluxes (28 to 49%) estimated for the 2.0-m height.

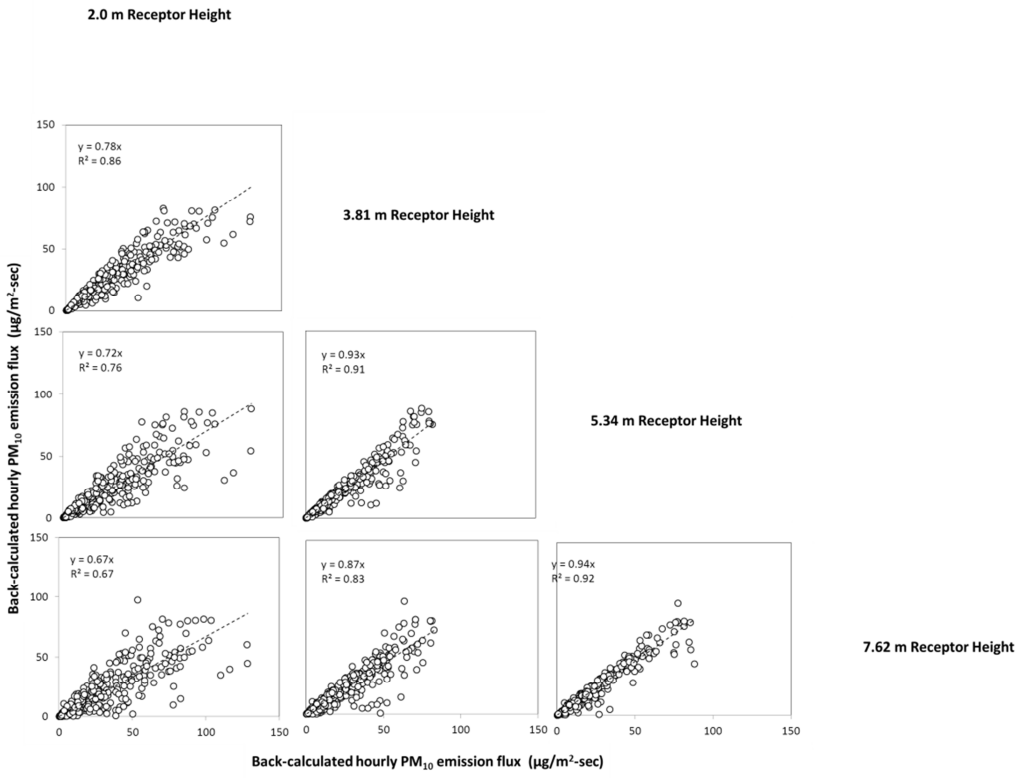

Figure 4-3. Back-calculated PM_{10} emission fluxes ($\mu g/m^2$-sec, n = 376) for the four receptor heights using AERMOD and eddy covariance meteorological data.

Therefore, in comparing AERMOD and WindTrax, the receptor height was set at 3.81 m. The 3.81-m setting was not significantly different from 5.34- and 7.62-m heights and had the lowest percentage difference (22%) with the 2.0-m height setting (27% for 5.34 m, 33% for 7.62 m) in terms of back-calculated emission fluxes.

4.2.5 Calculation of Emission Flux

Based on the reverse dispersion modeling technique, the emission flux was calculated from the assumed emission flux (1.0 $\mu g/m^2$-sec), unit-flux concentrations, and measured net PM_{10} concentrations using the equation:

$$Q_O = \frac{Q_A}{C_A} \times C_O \tag{4-8}$$

where Q_o is calculated 1-hr emission flux (µg/m^2-sec), C_o is measured 1-hr net PM_{10} concentration (µg/m^3), Q_A is 1.0 µg/m^2-sec, and C_A is calculated unit-flux PM_{10} concentration (µg/m^3). Turner and Schulze (2007) indicated that dispersion modeling can be conducted in situations with at least 50% of the period with measurements; thus, in this study, daily emission fluxes were derived for days with at least 12 hourly emission fluxes, and overall PM_{10} emission fluxes were then computed using derived daily emission fluxes.

Data were analyzed using SAS (2004). Normality tests showed that all data sets (i.e., measured PM_{10} concentrations, unit-flux PM_{10} concentrations, and back-calculated PM_{10} emission fluxes) had non-normal distributions. Accordingly, nonparametric test (e.g., nonparametric one-way analysis of variance) was used in all comparisons (5% level of significance), and median values were reported. Standard deviation computation followed the procedure by Schwertman et al. (2004) for non-normal distributed data. Removal of outliers in the emission flux data sets was based on the boxplot method applicable for non-normal data distribution (Schwertman et al., 2004). Variation between PM_{10} emission fluxes was measured using interquartile range (IQR). In this study, four dispersion model-meteorological data combinations were evaluated: (1) AERMOD using the on-site EC measurement data (AERMOD-EC); (2) AERMOD using the AERMET-generated data (pseudo data) (AERMOD-PD); (3) WindTrax using the sonic anemometer data (WindTrax-SD); and (4) WindTrax using the three variable (wind, z_o, L)-data (WindTrax-3V).

4.3 Results and Discussion

4.3.1 Measured PM_{10} Concentrations

Based on hourly data points that had net PM_{10} concentration values for the four measurement heights (n = 2,612), PM_{10} concentrations at the feedlot generally followed a diurnal trend (Figure 4-4). For all receptor heights, PM concentrations were generally highest during the early evening period (7:00 p.m. to 9:00 p.m.), possibly due to high cattle activity and stable atmospheric conditions during that period. Concentrations were generally lowest from the 2:00 a.m. to 5:00 a.m. period. Overall hourly net PM_{10} concentrations were as follows: 102 $\pm$ 208 µg/m^3 for the 2.0-m receptor height; 81 $\pm$ 152 µg/m^3 for the 3.81-m height; 61 $\pm$ 128 µg/m^3 for the 5.34-m height; and 53 $\pm$ 112 µg/m^3 for the 7.62-m height. These values are similar to those previously reported in the literature for net PM_{10} concentrations (2.0 m height) at cattle feedlots

ranging from 16 to 233 µg/m^3, with the lowest value associated with rain events (Sweeten et al., 1988; McGinn et al., 2010). Although the 2.0-m height-net PM_{10} concentration presented was well within the range of published values, comparing these PM_{10} concentrations would not be meaningful due to considerable differences in measurement design (i.e., PM_{10} sampler used, sampler downwind location, length of measurement period, feedlot characteristics, etc.).

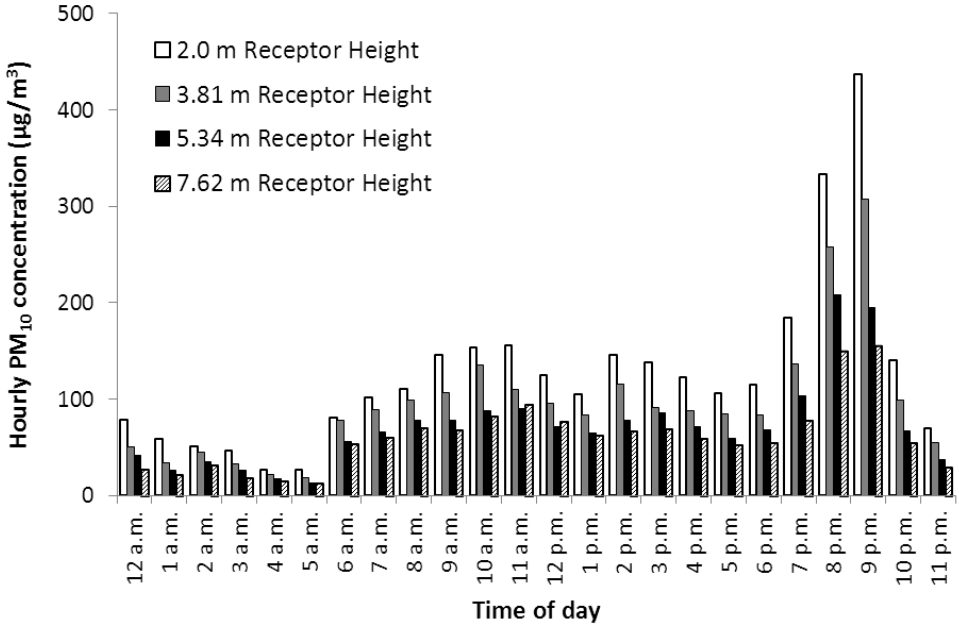

Figure 4-4. Hourly median net PM_{10} concentrations (n = 2,612) for the four receptor heights. Concentrations were measured with a tapered element oscillating microbalance (TEOM) PM_{10} monitor.

4.3.2 AERMOD-WindTrax Comparison

4.3.2.1 Meteorological Conditions

Based on the EC measurement, 66% and 34% of the hourly data points accepted for the analysis (n = 2,269) had wind coming from the south (180° $\pm$ 67.5°) and the north (0° $\pm$ 67.5°), respectively. Hourly meteorological parameters for these hourly data points were as follows: overall wind speed was 5.24 $\pm$ 2.23 m/sec, with the highest wind speed observed in the month of June (5.71 $\pm$ 1.76 m/sec in 2010, 6.09 $\pm$ 2.21 m/sec in 2011); overall temperature was 13 $\pm$ 15 °C, with July and August (28 $\pm$ 5 °C) as the warmest months, and December, January and February (-5 $\pm$ 9 °C) as the coldest months; overall friction velocity was 0.42 $\pm$ 0.17 m/sec, with the highest friction velocity observed in May and June 2011 (0.47 $\pm$ 0.17 m/sec); overall sensible

heat flux was 63 W/m^2 (range: -1,425 to 2,802 W/m^2), with the highest sensible heat flux measured for the month of July (mean values of 101 and 90 W/m^2 in 2010 and 2011, respectively) and the lowest for the November through February period (mean value of 28 W/m^2). Based on the atmospheric stability classification for L (Seinfeld and Pandis, 2006), 36% of the data points had very unstable conditions (-100 m < L < 0 m), 30% had unstable conditions (-10^5 m $\leq L \leq$ -100 m), 17% had very stable conditions (0 m < L < 100 m), 16% had stable conditions (100 m $\leq L \leq 10^5$ m), and 1% had neutral conditions ($|L| > 10^5$ m).

4.3.2.2 Calculated Unit-Flux PM_{10} Concentrations

After data screening, a total of 2,553 hourly data points had all four emission flux values; approximately 260 hourly data points were not included due to missing/incomplete upper air/surface hourly data files for June and December in 2010 and February through September in 2011. After removing the outliers, 2,269 hourly data points remained for analyses. Calculated unit-flux PM_{10} concentrations from the four dispersion model-meteorological data combinations are plotted in a scatter plot matrix (Figure 4-5). Based on linear regression, WindTrax calculated higher concentrations than AERMOD, with the difference ranging from 4 to 28% depending on meteorological data sets implemented in the dispersion simulations.

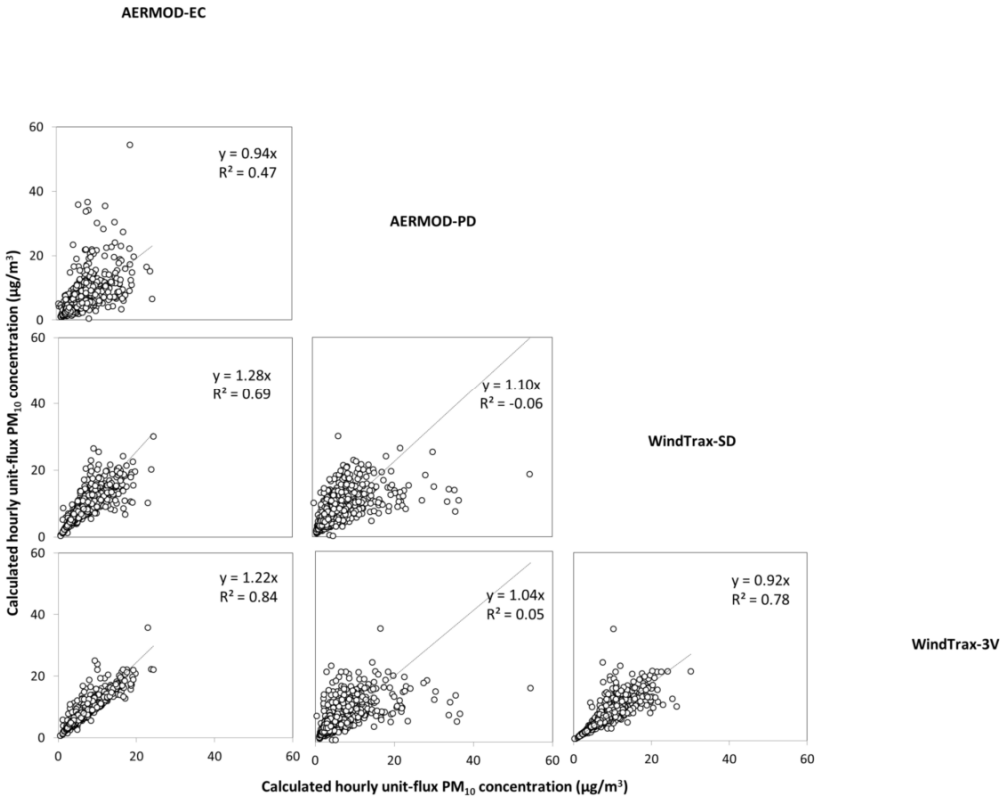

Figure 4-5. Hourly calculated unit-flux PM_{10} concentrations ($\mu g/m^3$, n = 2,269) for the four dispersion model-meteorological data combinations.

Nonparametric tests indicated that the calculated unit-flux concentrations of the dispersion model-meteorological data combinations were significantly different ($P < 0.05$) from each other. Between the two dispersion models, higher concentrations were obtained with WindTrax. Based on the comparison, 96% and 90% of the data points had WindTrax-SD predicting higher concentrations than AERMOD-EC and AERMOD-PD, respectively; 97% and 88% had WindTrax-3V having higher concentrations than AERMOD-EC and AERMOD-PD, respectively. This relationship between concentrations of AERMOD and WindTrax could be explained by the difference in their governing equations. In WindTrax (eq 4-2), mass is transported mainly by convection in all directions (downwind, crosswind, vertical). In AERMOD (eq 4-1), downwind mass transport is by convection, but crosswind and vertical mass transports are both governed by diffusion, a much slower transport process (Glasgow, 2010).

4.3.2.3 Back-Calculated PM_{10} Emission Rates.

Hourly median PM_{10} emission fluxes obtained by the four dispersion model-meteorological data combinations are shown in Figure 4-6. A similar trend was obtained for all combinations. The trend was comparable to those from a previous cattle feedlot study. Emission fluxes obtained with AERMOD-EC and AERMOD-PD were both higher than those with WindTrax-SD and WindTrax-3V, particularly in the daytime (e.g., 7:00 a.m. to 7:00 p.m.), when atmospheric conditions were normally unstable due to solar radiation.

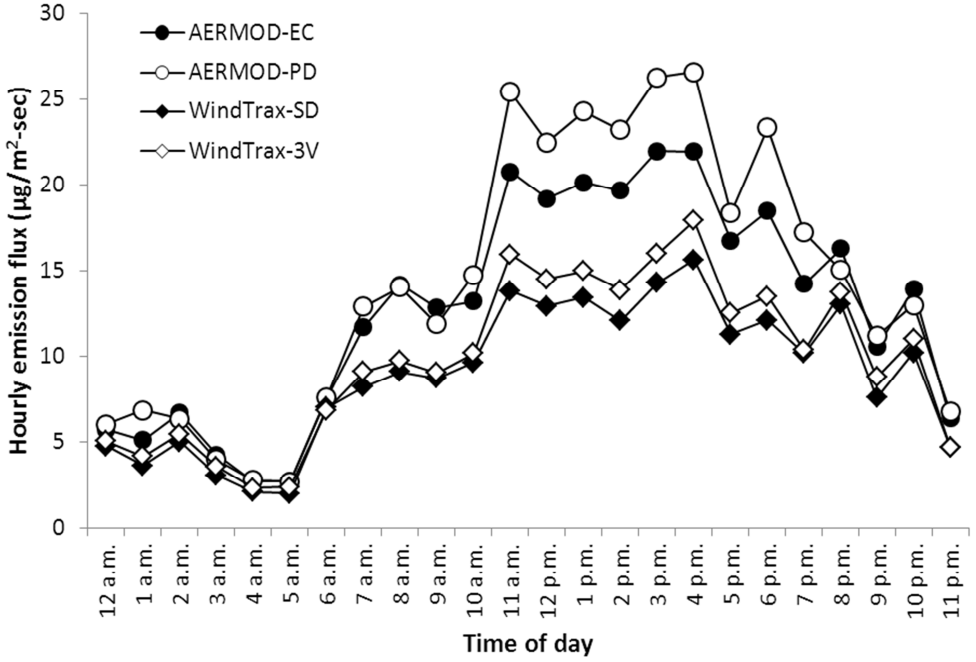

Figure 4-6. Hourly median PM_{10} emission fluxes estimated for the feedlot using the four dispersion model-meteorological data combinations.

Figure 4-7 is the scatter plot matrix for PM_{10} emission fluxes from the four dispersion model-meteorological data combinations. Based on the scatter plots, PM_{10} emission fluxes back-calculated with AERMOD were higher by 32 to 69% compared with those estimated with WindTrax. In terms of PM_{10} emission fluxes, there was a strong linear relationship ($R^2 \geq 0.88$) among the four combinations (i.e., AERMOD-EC and AERMOD-PD, AERMOD-EC, and WindTrax-SD, etc.). This high linearity in back-calculated emission fluxes suggests the possibility of developing conversion factors between: (1) two meteorological data sets evaluated for each model (i.e., locally measured and pseudo data sets for AERMOD; sonic anemometer and wind-z_o-L data sets for WindTrax); and (2) the two dispersion models. Linearity among

combinations as a function of atmospheric stability was also verified. In general, linearity between any two combinations was similar for all atmospheric stability conditions (Table 4-2).

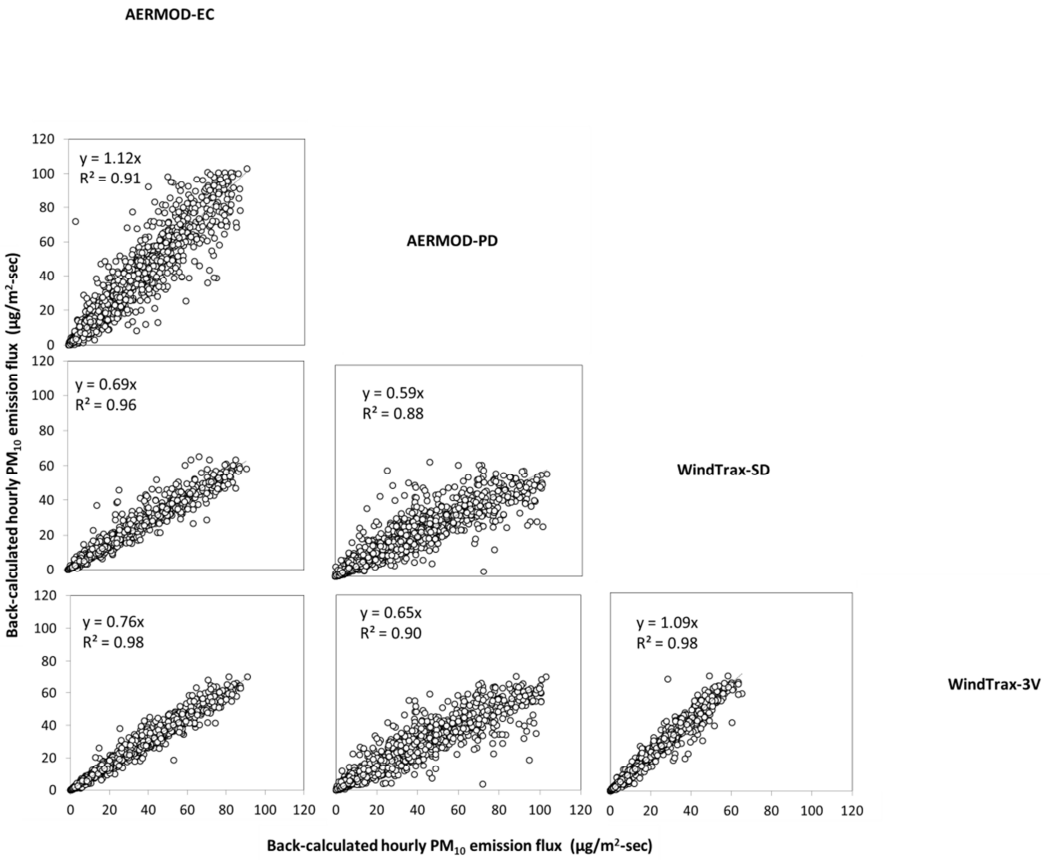

Figure 4-7. Back-calculated PM_{10} emission fluxes ($\mu g/m^2$-sec, n = 2,269) for the four dispersion model-meteorological data combinations.

Table 4-2. Linear regression between AERMOD and WindTrax back-calculated emission fluxes as a function of atmospheric stability[a]

		AERMOD-EC	AERMOD-PD	WindTrax-SD
All data (n = 2,269)	AERMOD-PD	1.12 (0.91)	-	-
	WindTrax-SD	0.69 (0.96)	0.59 (0.88)	-
	WindTrax-3V	0.76 (0.98)	0.65 (0.90)	1.09 (0.98)
Stable (n = 366)	AERMOD-PD	1.08 (0.91)	-	-
	WindTrax-SD	0.70 (0.98)	0.62 (0.89)	-
	WindTrax-3V	0.77 (0.98)	0.68 (0.90)	1.09 (0.99)
Very Stable (n = 386)	AERMOD-PD	1.09 (0.86)	-	-
	WindTrax-SD	0.70 (0.93)	0.59 (0.77)	-
	WindTrax-3V	0.79 (0.97)	0.67 (0.86)	1.08 (0.97)
Unstable (n = 674)	AERMOD-PD	1.12 (0.94)	-	-
	WindTrax-SD	0.68 (0.97)	0.59 (0.91)	-
	WindTrax-3V	0.75 (0.99)	0.65 (0.93)	1.09 (0.99)
Very Unstable (n = 821)	AERMOD-PD	1.14 (0.91)	-	-
	WindTrax-SD	0.70 (0.96)	0.58 (0.87)	-
	WindTrax-3V	0.77 (0.97)	0.64 (0.89)	1.09 (0.97)
Neutral (n = 22)	AERMOD-PD	1.01 (0.97)	-	-
	WindTrax-SD	0.79 (0.95)	0.77 (0.94)	-
	WindTrax-3V	0.76 (1.00)	0.74 (0.97)	0.93 (0.97)

[a] Values presented are slopes; values in parentheses are R^2 values.

Statistical analyses suggested that PM_{10} emission fluxes derived using same dispersion model but different meteorological data sets were not significantly different (P = 0.12 for AERMOD-EC and AERMOD-PD and P = 0.30 for WindTrax-SD and WindTrax-3V). Variation in PM_{10} emission fluxes, however, was smaller between WindTrax-SD and WindTrax-3V (IQR = 2 $\mu g/m^2$-sec) than between AERMOD-EC and AERMOD-PD (IQR = 5 $\mu g/m^2$-sec). In general, PM_{10} emission fluxes derived by AERMOD were significantly different (P < 0.05) from those by WindTrax; differences in PM_{10} emission fluxes were smallest between AERMOD-EC and WindTrax-3V (IQR = 6 $\mu g/m^2$-sec) and largest between AERMOD-PD and WindTrax-SD (IQR = 12 $\mu g/m^2$-sec). Correlation analysis indicated the potential to develop conversion factors for any pair of dispersion model-meteorological data sets. Within models, AERMOD-EC/AERMOD-PD factor had a mean value of 0.9 (range of 0.05 to 9.5), whereas WindTrax-SD/WindTrax-3V factor had a mean value of 0.9 (range of 0.4 to 3.5). Although the factors between meteorological data sets in each model were close to 1.0, one must always consider the difference resulting from the use of pseudo meteorological data in AERMOD (20 $\pm$ 22%) and the use of empirically derived parameters in WindTrax (10 $\pm$ 10%). Between models, mean AERMOD/WindTrax factors derived in this study ranged from 1.3 to 1.6 (Table 4-3). The smallest AERMOD/WindTrax factor was obtained between AERMOD-EC and WindTrax-3V, the pair with the smallest PM_{10} emission flux difference. Aside from measured wind speed and assumed z_o, AERMOD-EC and WindTrax-3V both used L determined at the facility rather than derived within the models (i.e., using pseudo data in AERMOD, sonic anemometer measurements in WindTrax).

Table 4-3. AERMOD/WindTrax factor as a function of AERMOD and WindTrax meteorological data sets in the modeling[a]

	AERMOD-EC	AERMOD-PD
WindTrax-SD	1.4	1.6
	(0.4 to 7.0)	(0.1 to 25.8)
WindTrax-3V	1.3	1.4
	(0.6 to 5.3)	(0.1 to 20.8)

[a] Values in parentheses are ranges.

The hourly trend of AERMOD/WindTrax factor within the day was also examined. Using AERMOD-EC and WindTrax-SD, hourly mean AERMOD/WindTrax factors within the day ranged from 1.2 to 1.5 ($R^2 \geq 0.90$), with the highest factors occurring from 7:00 a.m. to 7:00 p.m. Slightly lower AERMOD/WindTrax factors (range of 1.1 to 1.4, $R^2 \geq 0.94$) were observed if WindTrax-3V was used.

Based on days with at least 12 hourly emission fluxes (n = 89), overall PM_{10} emission fluxes were 1.85 g/m^2-day for AERMOD-EC, 2.10 g/m^2-day for AERMOD-PD, 1.32 g/m^2-day for WindTrax-SD, and 1.43 g/m^2-day for WindTrax-3V. These values were within the range of published PM_{10} emission fluxes for cattle feedlots. Using AERMOD, Bonifacio et al. (2012) reported PM_{10} emission fluxes of 1.10 and 1.60 g/m^2-day for two Kansas cattle feedlots. If effects of particle settling were incorporated, PM_{10} emission flux derived with AERMOD-EC would be approximately 1.92 g/m^2-day. Higher emission flux was expected, because pens at the studied feedlot were neither consistently watered nor frequently scraped as at feedlots presented in the previous study. Using WindTrax, McGinn et al. (2010) derived PM_{10} emission fluxes of 1.45 g/m^2-day and 1.61 g/m^2-day for two cattle feedlots in Australia, which were slightly higher than figures derived for WindTrax-SD (similar procedure). Notably, effects of particle settling were not incorporated in WindTrax-SD. Difference of PM_{10} emission fluxes presented in this study from published values can easily be explained by differences in feedlot characteristics (feedlot layout and design, feedlot practices), design of study (sampler type and locations, meteorological instrumentations), and length of measurement period (days with measurements).

Limitations in this study were related to measurements and dispersion modeling. Instrument-related biases due to PM_{10} samplers and micrometeorological instrumentation would likely introduce some uncertainties in PM_{10} emission fluxes presented. Although cross-calibration of PM samplers indicated slight variations between measured concentrations, it was conducted only at PM_{10} concentrations less than 120 µg/m^3. Dispersion models also had inherent limitations due to their many assumptions. Values derived with Gaussian modeling could differ from true values by at least a factor of two (National Research Council, 2003; Turner, 1994); this could also be the case for WindTrax modeling (Flesch et al., 2004). Effects of gravitational settling as dry and wet depositions were not incorporated in estimating PM_{10} emission fluxes in this study. Estimated emission rates may also differ among different measurement heights; as shown, emission rates derived for the 3.81-m height varied from those for other heights by at

least 22%. Note that AERMOD/WindTrax factors presented may be applicable only to modeling with meteorological data sets derived in similar manners.

4.4 Conclusions

AERMOD and WindTrax were compared in terms of unit flux PM_{10} concentrations and back-calculated PM_{10} emission fluxes using PM_{10} concentration and micrometeorological measurements from a beef cattle feedlot in Kansas. From the comparisons, the following conclusions were made.

- In general, for the same emission flux, PM_{10} concentrations calculated by WindTrax were higher than those by AERMOD, with mean percentage difference between the two models ranging from 4 to 28%. Conversely, for the same measured concentration, AERMOD gave higher back-calculated PM_{10} emission fluxes than WindTrax, with mean percentage difference ranging from 32 to 69%.
- For AERMOD, modeling results derived using pseudo data (i.e., NOAA) differed by 20 $\pm$ 22% from those determined using eddy covariance measurements. For WindTrax, use of empirically derived meteorological parameters resulted in 10 $\pm$ 10% difference in modeling results compared with the use of sonic anemometer measurements.
- In terms of back-calculated PM_{10} emission fluxes, high linearity was observed between the two dispersion models ($R^2 \geq 0.88$), and between the two meteorological data sets evaluated for each model ($R^2 = 0.91$ for AERMOD, $R^2 = 0.98$ for WindTrax). As such, conversion factors can be developed between the two models and between meteorological data sets. In this study, mean conversion factors between models (i.e., AERMOD/WindTrax factors) ranged from 1.3 to 1.6, with the smallest factor observed if same set of wind speed, surface roughness, and atmospheric stability were implemented in both models. For each model, mean conversion factor between the two meteorological data sets was 0.9.

With limited study of AERMOD and WindTrax models, it is left to the user's judgment which model provides the most accurate emission flux computation for area sources such as beef cattle feedlots. Nevertheless, this study indicated that development of conversion factors between

AERMOD and WindTrax is feasible. The procedure and results presented in this study could serve as basis for developing conversion factors between AERMOD and WindTrax.

4.5 References

Baum, K.A. 2003. Air emissions measurements at cattle feedlots. M.S. thesis, Kansas State University, Manhattan, KS.

Bonifacio, H.F., R.G. Maghirang, B.W. Auvermann, E.B. Razote, J.P. Murphy, and J.P. Harner III. 2012. Particulate matter emission rates from beef cattle feedlots in Kansas – reverse dispersion modeling. *J. Air & Waste Manage. Assoc*. 62:350-361. doi:10.1080/10473289.2011.651557.

CFR. 2005. Code of Federal Regulations, 40 CFR, Part 51: Revision to the guideline of air quality models: Adoption of a preferred general purpose (flat and complex terrain) dispersion model and other revisions.

Cimorelli, A. J., S.G. Perry, A. Venkatram, J.C. Weil, R.J. Paine, R.B. Wilson, R.F. Lee, W.D. Peters, R.W. Brode, and J.O. Paumier. 2004. *AERMOD: Description of Model Formulation,* EPA-454/R-03-004. Research Triangle Park, NC: U.S. Environmental Protection Agency.

Crenna, B. 2006a. *An Introduction to WindTrax*. Edmonton, AB: Department of Earth and Atmospheric Science, University of Alberta.

Crenna, B. 2006b. *Atmospheric Data in WindTrax*. Edmonton, AB: Department of Earth and Atmospheric Science, University of Alberta.

Dai, W., C. Otto, and D. Reeves. 2003. Performing CALPUFF analyses with pseudo-station data derived from MM5 data. Paper presented at the Proceedings of the 96th Annual Conference of the Air & Waste Management Association, San Diego, CA, June 22-26, 2003.

Denmead, O.T., D. Chen, D.W.T. Griffith, Z.M. Loh, M. Bai, and T. Naylor. 2008. Emissions of the indirect greenhouse gases NH_3 and NO_x from Australian beef cattle feedlots. *Austr. J. Exp. Agric.* 48:213-218.

Faulkner, W. B., J.J. Powell, J.M. Lange, B.W. Shaw, R.E. Lacey, and C.B. Parnell. 2007. Comparison of dispersion models for ammonia emissions from a ground-level area source. *Trans. ASABE* 50:2189-2197.

Flesch, T.K., and J.D. Wilson. 2005. Estimating tracer emission with a backward Lagrangian Stochastic technique. *Micrometeorology in Agricultural Systems, Agronomy Monograph no. 47*. Madison, WI: American Society of Agronomy, Inc., Crop Science Society of America, Inc., Soil Science Society of America, Inc.

Flesch. T. K., J.D. Wilson, L.A. Harper, and B.P. Crenna. 2005. Estimating gas emissions from a farm with an inverse-dispersion technique. *Atmos. Envrion.* 39:4863-4874. doi:10.1016/j.atmosenv.2005.04.032.

Flesch. T. K., J.D. Wilson, L.A. Harper, B.P. Crenna, and R.R. Sharpe. 2004. Deducing ground-to-air emissions from observed trace gas concentrations: a field trial. *J. Appl. Meteorol.* 43:487-502.

Flesch. T. K., J.D. Wilson, and E. Yee. 1995. Backward-time Lagrangian Stochastic models and their application to estimate gaseous emissions. *J. Appl. Meteorol.*34:1320-1332.

Galvin, G., C. Henry, D. Parker, R. Ormerod, P. D'Abreton, and M. Rhoades. 2006. Efficacy of Lagrangian and a Gaussian model for back calculating emission rates from feedyard area sources. Paper presented at the Workshop on Agricultural Air Quality, Potomac, MD, June 5-8, 2006.

Glasgow, L.A. 2010. *Transport Phenomena.* Hoboken, NJ: John Wiley & Sons, Inc.

Heinsohn, R. J., and R.L. Kabel. 1999. *Sources and Control of Air Pollution*. Upper Saddle River, NJ: Prentice-Hall, Inc.

Leytem, A.B., R.S. Dungan, D.L. Bjorneberg, and A.C. Koehn. 2011. Emission of ammonia, methane, carbon dioxide, and nitrous oxide from dairy cattle housing and manure management systems. *J. Environ. Qual.* 40:1383-1394. doi:10.2134/jeq2009.0515.

McGinn, S. M., T.K. Flesch, D. Chen, B. Crenna, O.T. Denmead, T. Naylor, and D. Rowell. 2010. Coarse particulate matter emissions from cattle feedlots in Australia. *J. Environ. Qual.* 39:791-798. doi:10.2134/jeq2009.0240.

McGinn, S.M., T.K. Flesch, B.P. Crenna, K.A. Beauchemin, and T. Coates. 2007. Quantifying ammonia emissions from a cattle feedlot using a dispersion model. *J. Environ. Qual.* 36:1585-1590.

Mitloehner, F. M. and S.M. Calvo. 2008. Worker health and safety in concentrated animal feeding operations. *J. Agric. Safety and Health* 14:163-187.

National Research Council. 2003. *Air Emissions from Animal Feeding Operations: Current Knowledge, Future Needs.* Washington, D.C.: National Academy of Sciences.

Perry, S.G., A.J. Cimorelli, R.J. Paine, R.W. Brode, J.C. Weil, A. Venkatram, R.B. Wilson, R.F. Lee, and W.D. Peters. 2005. AERMOD: a dispersion model for industrial source applications. Part II: model performance against 17 field study databases. *J. Appl. Meteorol.* 44:694-708.

Price, J. E., R.E. Lacey, B.W. Shaw, N.A. Cole, R. Todd, S. Capareda, and C.B. Parnell. 2004. A comparison of ammonia emission rates from an agricultural area source using dispersion modeling: Gaussian versus backward-Lagrangian Stochastic. Paper presented at the American Society of Agricultural Engineers (ASAE), Ontario, Canada, August 1-4, 2004.

Rupprecht & Patashnick Co., Inc. 2011. *Procedure for Operating the Rupprecht & Patashnick TEOM Series 1400ab - Section II: Tapered Element Oscillating Microbalance (TEOM) Site Operator's Quality Assurance Plan and Standard Operating Procedure (QAP/SOP),* TEOM QAP/SOP 2.27.2, 6th revision. New York, NY: Thermo Fisher Scientific.

SAS Institute, Inc. 2004. *SAS system for Windows*, release 9.1.3. Cary, NC: SAS Institute, Inc.

Schwertman, N.C., M.A. Owens, and R. Adnan. 2004. A simple more general Boxplot method for identifying outliers. *Comput. Statist. Data Anal.* 47:165-174. doi:10.1016/j.csda.2003.10.012.

Seinfeld, J.H., and S.N. Pandis. 2006. Meteorology of the Local Scale. *Atmospheric Chemistry and Physics - from Air Pollution to Climate Change*. 2nd ed. Hoboken, NJ: John Wiley & Sons.

Sweeten, J.M, C.B. Parnell, R.S. Etheredge, and D. Osborne. 1988. Dust emissions in cattle feedlots. *Vet. Clinics of North America, Food Animal Prac.* 4:557-578.

Touma, J.S., V. Isakov, A.J. Cimorelli, R.W. Brode, and B. Anderson. 2007. Using prognostic-model generated meteorological output in the AERMOD dispersion model: An illustrative application in Philadelphia, PA. *J. Air & Waste Manage. Assoc.* 57:586-595. doi:10.3155/1047-3289.57.5.586.

Turner, D. B. 1994. *Workbook of Atmospheric Dispersion Estimates – An Introduction to Dispersion Modeling*.2nd ed. Boca Raton, FL: Lewis Publishers.

Turner, D.B., and R.H. Schulze. 2007. *Practical Guide to Atmospheric Dispersion Modeling*. Dallas, TX: Trinity Consultants, Inc. and Air & Waste Management Association.

U.S. Environmental Protection Agency. 2008. *AERSURFACE User's Guide,* EPA-454/B-08-001. Research Triangle Park, NC: U.S. Environmental Protection Agency.

U.S Environmental Protection Agency. 2009. *User's Guide for the AERMOD Meteorological Preprocessor (AERMET),* EPA-454/B-03-002Research Triangle Park, NC: U.S Environmental Protection Agency.

Von Essen, S. G., and B.W. Auvermann. 2006. Health effects from breathing air near CAFOs for feeder cattle or hogs. *J. Agromed.* 10:55-64. doi:10.1300/J096v10n04_08.

CHAPTER 5 - **Simulating Particulate Emissions from Area Sources Using AERMOD and WindTrax: Effects of Meteorological Parameters**

5.1 Introduction

Air emissions from animal feeding operations (AFOs), including open-lot beef cattle feedlots, and other ground-level area sources, can adversely affect human health and the environment. Previous studies have characterized and estimated air pollutant emissions from AFOs. In 2005, the U.S. Environmental Protection Agency (EPA) established the National Air Emissions Monitoring Study (NAEMS) to gather pollutant emission data from AFOs and to develop emission estimating methodologies for AFOs (CFR, 2011; Purdue Applied Meteorology Laboratory, 2009). In the NAEMS, one of the methodologies was WindTrax (Thunder Beach Scientific, Alberta, Canada), a dispersion model based on backward Lagrangian stochastic (bLS) method (Crenna, 2006a; Flesch and Wilson, 2005).

For cattle feedlots, WindTrax has been used on emission studies on odor (Galvin et al., 2006), gases (Denmean et al., 2008; McGinn et al., 2007), and particulate matter (McGinn et al., 2010). This model also has been employed on emission studies on broiler (Harper et al., 2010), swine (Flesch et al., 2005), and dairy cattle (Bjorneberg et al., 2009; Leytem et al., 2011). WindTrax is appealing as it has a graphical interface and can process modeling inputs such as concentration and meteorological parameters in several ways. One major shortcoming of this model is relatively long simulation time. Several techniques have been advanced to possibly reduce the computational time for WindTrax (Crenna, 2006a). For example, the number of particles released in the simulation can be fewer; however, this introduces higher uncertainty in modeling results. In addition, data from previous simulations, referred to as touchdown catalogs, can be saved; however, this consumes at lot of computer memory.

The current U.S. EPA preferred dispersion model is the American Meteorological Society/Environmental Protection Agency Regulatory Model or AERMOD (CFR, 2005), which is Gaussian-based. AERMOD can model emission dispersion for point, area and volume sources (Turner and Schulze, 2007). AERMOD has been extensively evaluated for simulating emissions from industrial area sources (Hanna et al., 2001; Perry et al., 2005); however, its performance on

modeling ground-level area sources still needs to be evaluated. Several studies have utilized this model to calculate emission rates from area sources – AERMOD had been used to calculate ammonia (Faulkner et al., 2007b) and particulate (Bonifacio et al., 2012) emission rates from cattle feedlots, to assess dispersion of ammonia and odor emissions from a swine facility (Sarr et al., 2010), and to estimate particulate emission rates from almond farms (Faulkner et al., 2009; Goodrich et al., 2009). Notably, the computational time period for AERMOD is relatively short.

This study was conducted to evaluate the performance of AERMOD and WindTrax in estimating concentrations downwind of ground-level area sources, such as cattle feedlots. These two dispersion models were compared based on their sensitivity to changes in modeling inputs, including meteorological parameters, area source and receptor locations.

5.2 Methods

5.2.1 Dispersion Modeling

5.2.1.1 AERMOD

As a Gaussian plume model (Cimorelli et al., 2004), AERMOD is based on several assumptions that include steady-state conditions, downwind (*x*-direction) mass transport through convection with constant wind speed, crosswind (*y*-direction) and vertical (*z*-direction) mass transport through diffusion with constant effective diffusion coefficients for crosswind and vertical, and no reaction/generation (Heinsohn and Kabel, 1999). The general expression for Gaussian plume models is given by:

$$u\ \frac{\partial c}{\partial x} = D_y \frac{\partial^2 c}{\partial y^2} + D_z \frac{\partial^2 c}{\partial z^2} \qquad (5\text{-}1)$$

where c is concentration, u is wind speed along-wind (i.e., downwind) direction, and D_y and D_z are diffusion coefficients for crosswind and vertical directions, respectively. The general solution for equation 5-1 is referred to as the Gaussian plume model.

The planetary boundary layer in AERMOD is well-characterized using a number of meteorological parameters such as sensible heat, friction velocity, and Monin-Obukhov length (Turner and Schulze, 2007; U.S. EPA, 2009). For stable conditions (i.e., defined by positive Monin-Obukhov lengths), concentration in both vertical and crosswind directions has

Gaussian/normal distribution (Cimorelli et al., 2004). For unstable conditions (i.e., negative Monin-Obukhov lengths), concentration in crosswind direction still has Gaussian distribution; however, concentration in vertical direction has a bi-Gaussian distribution (Cimorelli et al., 2004). Similar to other Gaussian-based models, AERMOD is not suitable for modeling low wind speed or calm conditions as it tends to overestimate concentrations (Holmes and Morawska, 2006). Furthermore, AERMOD is considered ideal for middle-scale (100 – 500 m) and large-scale (500 m - tens of kilometer) modeling; it is not recommended for predicting concentrations at locations close to the source (< 100 m) (Holmes and Morawska, 2006; CFR, 2010). As such, if AERMOD were applied in reverse dispersion modeling to quantify emission rates, sampler placement of at least 100 m downwind of the source might be required. This could be a challenge if applied as an emission estimation tool for ground-level area sources like AFOs. For sources such as cattle feedlots, placing samplers far downwind could result in concentration measurements contaminated by outside sources, such as unpaved roads and agricultural lands (Faulkner et al., 2007a).

In this study, AERMOD (version 09292, U.S. EPA; www.epa.gov/ttn/scram) was run using a unit emission flux (1.0 $\mu g/m^2$-sec) to calculate hourly concentrations at specified receptor locations downwind of a feedlot-like area source with several pens. Assumptions of flat terrain and constant emission flux (for the 1-hr averaging period) were applied in the modeling.

5.2.1.2 WindTrax

For WindTrax, mass transport in all directions (*x*, *y*, *z*) is governed by convection or bulk motion, and is therefore expressed by the mass continuity equation:

$$\frac{\partial c}{\partial t} + u\ \frac{\partial c}{\partial x} + v\ \frac{\partial c}{\partial y} + w\ \frac{\partial c}{\partial z} = 0 \qquad (5\text{-}2)$$

where *t* is time, and *u*, *v*, and *w* are wind velocities in *x*-, *y*-, and *z*-directions, respectively (Flesch and Wilson, 2005). The first term on the left-hand side of equation 5-2 stands for accumulation and the last three terms represent convective transport in the *x*-, *y*-, and *z*-directions. Wind speeds (*u*, *v* and *w*) are assumed constant during the averaging period. For WindTrax, the method used to solve equation 5-2 is the Lagrangian stochastic technique that described the evolution of particle position and velocity in a backward timeframe.

WindTrax can predict concentrations downwind of an area source using known emission rates; alternatively, it can be used to estimate emission rates from concentrations measured downwind of the source. The recommended modeling downwind distance for WindTrax is within 1 km from the area source (Crenna, 2006a). As such, WindTrax is ideal for micro- (less than 100 m) and middle- (100 – 500 m) scale modeling (CFR, 2010). Compared to AERMOD, WindTrax may be more suitable for emission studies on AFOs especially if sampler placement was restricted to locations near the sources.

Similar to AERMOD modeling, a unit emission flux (1.0 $\mu g/m^2$-sec) was used to predict downwind concentrations. Pen and receptors locations were similar to AERMOD inputs. To shorten simulation time, the number of particles released was set at the default value (50,000) (Crenna, 2006a).

5.2.2 Meteorological Parameter Inputs

AERMOD and WindTrax use different sets of meteorological parameters to characterize the atmospheric boundary layer, with AERMOD having the larger meteorological data requirement. Required meteorological parameters common for the two models are wind speed, temperature, surface roughness, and Monin-Obukhov length. Meteorological inputs evaluated in this study were wind speed (u), surface roughness (z_o), and Monin-Obukhov length (L). Temperature was not considered as preliminary analysis revealed it had little effects on calculated concentration in this study.

To simulate meteorological conditions at ground-level area sources, year-long measurements at cattle feedlots were used as reference in setting values for u, z_o, and L used in the comparison. Wind speed measurements were from a 2.5-m high anemometer installed at a Kansas cattle feedlot where u ranged from 0.5 to 14.6 m/sec and had an overall value of 4.7 m/sec in 2008 (Table 5-1). Values for z_o and L were derived from eddy covariance measurements obtained at another Kansas cattle feedlot from May 2010 to April 2011. Overall z_o value computed was 4.1 cm (Table 5-1). Summarized in Table 5-2 are hourly L values classified using the atmospheric stability grouping presented in Seinfeld and Pandis (2006) (i.e., -10^5 m $\leq L \leq$ -100 m for unstable, -100 m $< L <$ 0 m for very unstable, 0 m $< L <$ 100 m for very stable, 100 m $\leq L \leq 10^5$ m for stable, and $L > 10^5$ m, $L < -10^5$ m for neutral).

Table 5-1. Wind speed (u) and surface roughness (z_o) measurements at cattle feedlots

	u [a, c] (m/sec)	z_o [b, d] (cm)
# of hourly data points	8,734	7,463
Overall	4.7	4.1
Lowest	0.5	~ 0.0
Highest	14.6	22.4

[a] From 2.5-m high wind anemometer measurement
[b] From eddy covariance measurements
[c] Normally distributed data, with average as overall value, minimum as lowest value and maximum as highest value
[d] Non-normally distributed data with median as overall value, lower fence/limit as lowest value and upper fence/limit as highest value

Table 5-2. Atmospheric stability classification of hourly feedlot measurements[a]

	Unstable	Very Unstable	Very Stable	Stable	Neutral
L values	-10^5 to 100 m	-100 to 0 m	0 to 100 m	100 to 10^5 m	$>10^5$ m, $<-10^5$ m
# of hourly data points	1,859	2,850	1,503	1,082	169
Percentage	25%	38%	20%	14%	2%

[a] Stability classification based on Seinfeld and Pandis (2006).

Settings for u, z_o, and L in this study are shown in Table 5-3. Each parameter had several values specified, namely minimum, maximum, and base values. When assessing how the calculated concentration responded to a specific parameter, settings evaluated for that parameter included its base, minimum, and maximum values while settings applied for other parameters were their corresponding base values. For u and z_o, a number of values within the range of their minimum and maximum values were also tested. Values for u and z_o evaluated were based on feedlot meteorological measurements shown in Table 5-1. The base, minimum, and maximum values of u were 5.0, 0.5 and 15.0 m/sec, respectively, with the measurement height for u set at 2.5 m. From the measured value of 4.1 cm, the base value of z_o was set at 5.0 cm, whereas its minimum (2.5 cm) and maximum (20.0 cm) values were based on the computed lower and upper limits, respectively. Influence of atmospheric stability on the calculated concentration was examined using the five atmospheric stability conditions mentioned. Settings of L for four of the

atmospheric stability conditions were based on the mean of their defined ranges: -5,000 m for unstable, -50 m for very unstable, 50 m for very stable, and 5,000 m for stable. For neutral condition, in which L can have either a very large positive value ($L > 10^5$ m) or a very large negative value ($L < -10^5$ m), L was arbitrarily set at 500,000 m. Its corresponding negative value (L = -500,000 m) was not evaluated as AERMOD does not simulate conditions with $L \leq$ -99,999. Note that evaluation of u and z_o were performed using L = 5,000 m and L = -5,000 m to demonstrate difference in calculated concentrations between stable (i.e., $L > 0$ m) and unstable (i.e., $L < 0$ m) conditions. In total, there were 23 test cases. A fixed setting of 180° removed the influence of wind direction in the simulation.

Table 5-3. Wind speed (u), surface roughness (z_o) and Monin-Obukhov length (L) settings for AERMOD and WindTrax comparison

	u (m/sec)	z_o (cm)	L (m)	
			$L > 0$ m	$L < 0$ m
Minimum	0.5	2.5	50[b]	-50[c]
Maximum	15.0	20.0	500,000[d]	N/A
Base value[a]	5.0	5.0	5,000[e]	-5,000[f]
Resolution	0.5 for 0.5 – 1.0 1.0 for 1.0 – 5.0 2.5 for 5.0 – 15.0	2.5	N/A	N/A
# of test cases	10	8	3	2

N/A = not applicable

[a] Value used when evaluating a specific parameter. In evaluating effects of L, atmospheric stability conditions considered were: [b] very stable condition; [c] very unstable condition; [d] neutral condition; [e] stable condition; [f] unstable condition.

WindTrax can be run using only u, z_o, L, and temperature (Crenna, 2006a; 2006b). AERMOD, on the other hand, requires a lot more meteorological parameters to characterize the atmospheric boundary layer (U.S. EPA, 2004a; 2004b). AERMOD requires two meteorological files called profile data file (PFL) and surface data file (SFC). Parameter u is specified in PFL, together with wind direction and temperature. In SFC, a much larger data file, u, z_o, and L are all

included with other parameters, such as wind direction, temperature, sensible heat, friction velocity, and mixing height. For this evaluation, other parameters in SFC were derived from *u*, *L*, and temperature using formulations in AERMOD (Cimorelli et al., 2004).

5.2.3 Area Source Layout

Prior to evaluating calculated concentration's sensitivity to changes in *u*, z_o, and *L*, effects of downwind and crosswind distances between the area source and the receptor were first assessed. Two feedlot-area source layouts were initially evaluated. The first layout had five 200 m x 200 m adjoining feedlot pens aligned along the north-south direction parallel to the wind direction set in the simulation, with Pen 1 as the southernmost pen and Pen 5 as the northernmost pen (Figure 5-1a). In this layout, downwind distances of the pens to a receptor varied while their corresponding crosswind distances were negligible as all pens lie directly upwind of the receptor. The second layout had five 200 m x 200 m adjoining feedlot pens aligned in west-east direction perpendicular to wind direction, with Pen 1 as the westernmost pen and Pen 5 as the easternmost pen (Figure 5-1b). Here, crosswind distances of the pens to a receptor varied while their downwind distances were the same. Influence of area source-receptor downwind and crosswind distances on downwind concentrations were assessed using first and second layouts, respectively. At a given receptor location, the contribution of each pen on the total concentration was determined by computing its corresponding predicted concentration and weighing it against the sum of concentrations contributed by all pens (Calder, 1977).

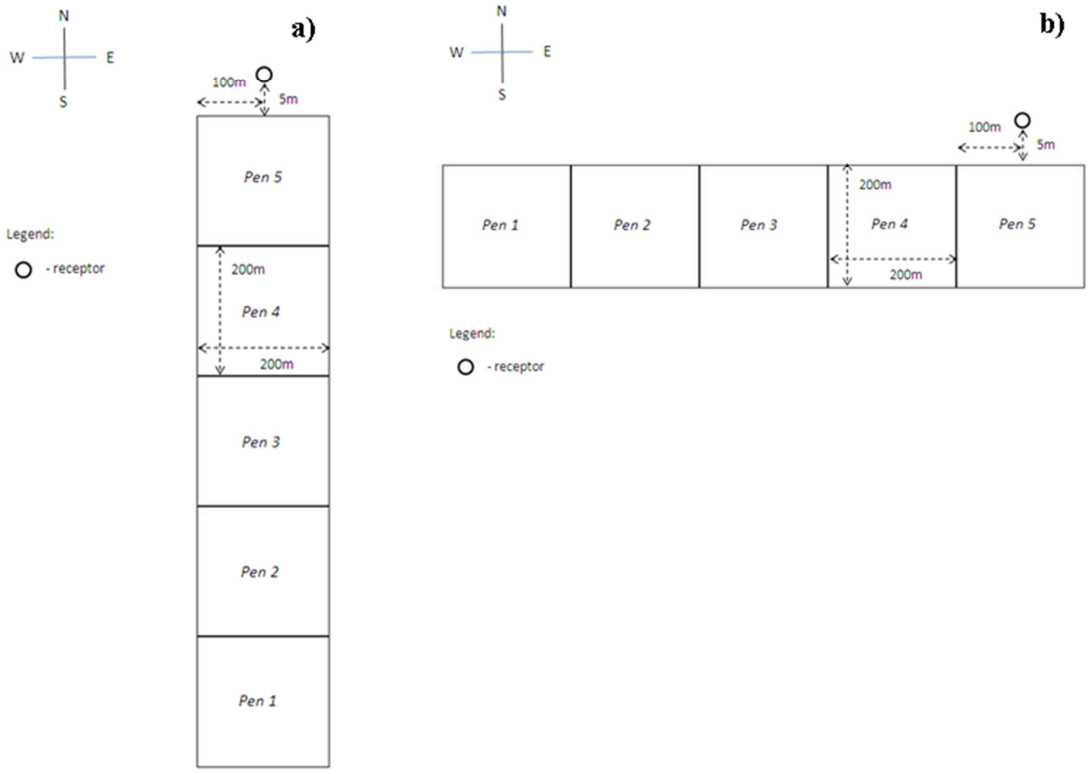

Figure 5-1. Area source layouts: a) pens aligned along wind direction (north-south); and b) pens aligned across wind direction (east-west). Wind direction was set at 180° from the north in the modeling.

In both layouts, receptors were specified for three different downwind distances north of Pen 5. Shortest downwind distance was 5 m from the north edge of Pen 5; this represented the sampler placement near the source to minimize effects of outside sources. Next distance was 100 m, which is the recommended minimum downwind distance for Gaussian models like AERMOD. Farthest distance was 1,000 m, which is the longest modeling distance for WindTrax.

In analyses of area source-receptor downwind and crosswind distances, receptor height was set at 7 m, a monitoring height valid for all three downwind distances evaluated (CFR, 2010). Meteorological parameters were set at their base values (Table 5-3). The area source configuration for analyses of meteorological parameters would then be based on results of this analysis.

5.2.4 Receptor Heights

AERMOD and WindTrax were also compared in terms of resulting vertical concentration profiles. Vertical concentration profile was obtained for two downwind distances, 5 and 100 m. Receptor heights specified for each downwind distance were based on recommendation by CFR (2010). For the 5-m downwind distance, receptor heights of 2 to 7 m, at 1-m interval, were used in profiling concentrations. For the 100-m downwind distance, heights of 7 to 15 m, also with 1-m interval, were applied. In profiling concentration, settings for meteorological parameters were their respective base values (Table 5-3).

5.2.5 Data Analysis

Data were analyzed using SAS (release 9.1.3., SAS Institute Inc., NC). Paired t-test was used in comparing calculated concentrations between the two dispersion models. Linear regression was applied to determine the influence of u, z_o, and L on calculated concentrations and was used to measure the linearity in concentrations predicted by the two dispersion models. A 5% level of significance was implemented in all statistical analyses.

5.3 Results

5.3.1 Effects of Area Source-Receptor Downwind and Crosswind Distances

For the first feedlot-area source layout (i.e., north-south direction), contributions of each pen to concentrations calculated for receptors at three downwind distances are summarized in Table 5-4. In both AERMOD and WindTrax modeling, close to 90% of the total concentrations calculated for the three 7-m high downwind receptors was contributed by Pens 2 to 5, with Pen 5 expectedly having the highest contribution. At 5, 100, and 1,000-m downwind distances, contributions of Pen 5 were 30%, 34%, and 24%, respectively, as modeled by AERMOD; with WindTrax, contributions were 38%, 40%, and 29%, respectively. The difference on how AERMOD and WindTrax simulate stable and unstable conditions was also notable. With AERMOD, pen contributions differed between stable and unstable conditions. Contributions of farthest pens on calculated concentrations increased with unstable atmosphere; Pen 1, which only had 10% contribution for stable condition, had a higher contribution, close to 20%, for unstable condition. On the other hand, there was no difference in results between stable and unstable conditions in WindTrax modeling.

Table 5-4. Pen contributions on predicted concentrations – Pens aligned along wind direction

Downwind distance	Stability	Model	Pen 5 [a]	Pen 4	Pen 3	Pen 2	Pen 1 [b]
5 m	Stable	AERMOD	34%	27%	17%	12%	10%
		WindTrax	38%	25%	17%	12%	8%
	Unstable	AERMOD	26%	20%	18%	18%	18%
		WindTrax	38%	25%	17%	12%	8%
100 m	Stable	AERMOD	41%	23%	15%	12%	9%
		WindTrax	40%	23%	17%	11%	9%
	Unstable	AERMOD	25%	19%	19%	19%	18%
		WindTrax	40%	23%	17%	11%	9%
1,000 m	Stable	AERMOD	27%	23%	19%	17%	14%
		WindTrax	29%	24%	16%	17%	14%
	Unstable	AERMOD	21%	20%	20%	20%	19%
		WindTrax	29%	24%	16%	17%	14%

[a] Closest to receptors; [b] farthest from receptors.

Pen contributions computed for the second area source layout (i.e., east-west direction) are shown in Table 5-5. Contributions obtained in both AERMOD and WindTrax modeling were relatively the same. Pen 5, the pen closest to the receptors, was the only source of concentration calculated for receptors at downwind distances of 5 and 100 m. Pen 5 also was the main contributor (99% and 94% based on AERMOD and WindTrax, respectively) of concentration derived for the 1,000-m downwind distance receptor. Even the next closest pen (Pen 4), which had only 100-m crosswind distance from the receptor (measured from Pen 4's edge), had no significant influence on calculated concentration.

Table 5-5. Pen contributions on predicted concentrations – Pens aligned across wind direction

Downwind distance	Stability	Model	Pen 5 [a]	Pen 4	Pen 3	Pen 2	Pen 1 [b]
5 m	Stable	AERMOD	100%	-	-	-	-
		WindTrax	100%	-	-	-	-
	Unstable	AERMOD	100%	-	-	-	-
		WindTrax	100%	-	-	-	-
100 m	Stable	AERMOD	100%	-	-	-	-
		WindTrax	100%	-	-	-	-
	Unstable	AERMOD	100%	-	-	-	-
		WindTrax	100%	-	-	-	-
1,000 m	Stable	AERMOD	99%	1%	-	-	-
		WindTrax	94%	6%	-	-	-
	Unstable	AERMOD	99%	1%	-	-	-
		WindTrax	94%	6%	-	-	-

[a] Closest to receptors; [b] farthest from receptors.

Based on these findings, the first feedlot-area source layout, in which pens were aligned along the wind direction (180°), was used in analyzing sensitivity of the two models to changes in meteorological parameters.

5.3.2 Effects of Meteorological Parameters

5.3.2.1 Wind Speed

Figure 5-2 shows calculated concentrations as a function of *u* for the three downwind distances evaluated. For stable conditions, AERMOD and WindTrax produced similar concentration profiles with respect to *u* and were highly correlated ($R^2 = 1.00$) for all downwind distances. However, concentrations predicted during stable conditions were significantly different ($P < 0.05$) between AERMOD and WindTrax, with the latter generating higher concentrations. The ratio of calculated concentrations, expressed as WindTrax/AERMOD ratio, ranged from 1.13 to 1.24, 1.09 to 1.23, and 1.00 to 1.89 for the 5, 100, and 1,000 m downwind distances, respectively. Average WindTrax/AERMOD ratios as functions of *u* were as follows:

for the 5-m downwind distance, 1.13 for 1.0 m/sec $\leq u \leq$ 3.0 m/sec and 1.20 for $u \geq$ 4.0 m/sec; and for the 100-m downwind distance, 1.11 for 0.5 m/sec $\leq u \leq$ 5.0 m/sec and 1.21 for $u \geq$ 7.5 m/sec. For the 1,000-m distance, no average value was obtained as WindTrax/AERMOD ratio was highly variable with respect to *u*.

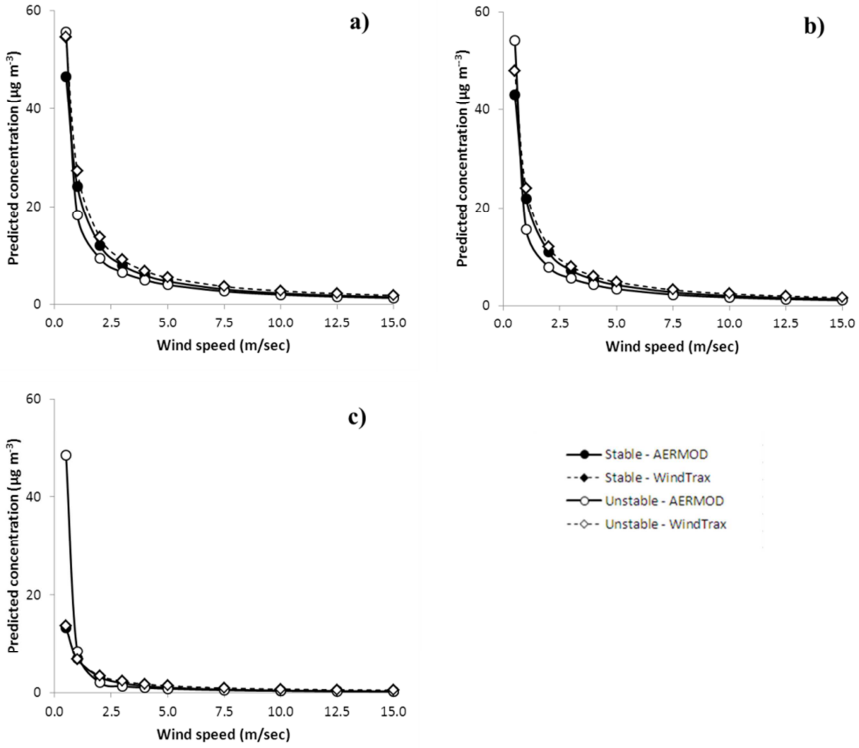

Figure 5-2. Calculated concentration as function of wind speed for downwind distances of: (a) 5 m, (b) 100 m, and (c) 1,000 m.

Calculated concentrations of AERMOD and WindTrax for unstable conditions were also highly correlated. Unlike for stable conditions, however, correlation decreased as downwind distance increased, with R^2 of 0.96, 0.93, and 0.77 for 5, 100, and 1,000-m downwind distances, respectively. This decrease in correlation could be attributed to lower *u* settings included the evaluation. If $u < 1.0$ m/sec was not included in concentration comparison for the 100-m distance, R^2 would be close to 1.0. For the 1000-m distance, R^2 would increase if $u < 2.0$ m/sec were excluded in the analysis. Higher difference between AERMOD and WindTrax was also observed for unstable conditions, with the latter producing higher concentrations ($P < 0.05$): WindTrax/AERMOD ratios of 0.98 to 1.50, 0.89 to 1.54, and 0.28 to 2.18 were computed for 5,

100, and 1,000-m distances, respectively. In terms of u, average WindTrax/AERMOD ratios for unstable conditions were as follows: for the 5-m downwind distance, 1.48 for 1.0 m/sec $\leq u \leq$ 2.0 m/sec and 1.39 for $u \geq$ 3.0 m/sec; and for the 100-m downwind distance, 1.53 for 1.0 m/sec $\leq u \leq$ 2.0 m/sec and 1.44 for $u \geq$ 3.0 m/sec. Similar to what was observed for stable conditions, WindTrax/AERMOD ratio at the 1,000-m downwind distance, with respect to u, was highly variable.

5.3.2.2 Surface Roughness

Figure 5-3 shows that calculated concentrations decreased with increasing values of z_o for both stable and unstable conditions. Also, higher concentrations ($P < 0.05$) were predicted by WindTrax, and high linearity between AERMOD and WindTrax concentrations were modeled. WindTrax/AERMOD concentration ratios for stable and unstable conditions were as follows: at downwind distance of 5 m, ratios of 1.14 to 1.20 and 1.35 to 1.39, respectively; at 100 m, 1.12 to 1.19 and 1.39 to 1.43, respectively; at 1,000 m, 1.36 to 1.65 and 1.64 to 1.86, respectively. Excluding the 1,000-m distance, WindTrax/AERMOD concentration ratio remained relatively stable with average values for stable and unstable conditions of 1.18 and 1.37, respectively, for the 5-m downwind distance, and 1.15 and 1.41, respectively, for the 100-m distance. Even though WindTrax gave higher concentrations, the two models' concentrations still had high linear relationship: regression analyses between calculated concentrations showed R^2 values greater than 0.96 for stable and 0.98 for unstable conditions.

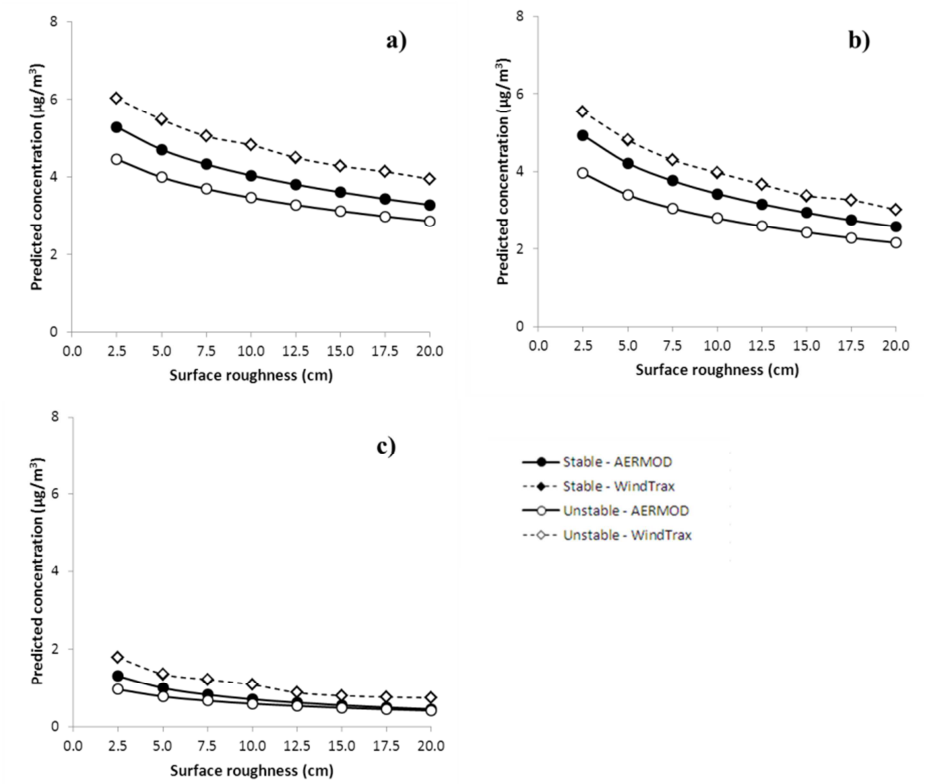

Figure 5-3. Calculated concentration as function of surface roughness for downwind distances of: (a) 5 m, (b) 100 m, and (c) 1,000 m.

Rates of decrease in concentration with respect to z_o were relatively similar between AERMOD and WindTrax, and were much faster for longer downwind distances (Figure 5-3). When z_o increased from 2.5 to 20 cm, concentration at the closest receptor was reduced by 36%; at the next receptor (100-m distance), concentration decreased by 46%; and at the farthest receptor, the decrease was about 60%. Regression analyses indicated high linearity ($0.96 \geq R^2 \geq 0.88$) between predicted concentration and z_o, the lowest linearity ($0.91 \geq R^2 \geq 0.88$) determined at the farthest sampler placement.

5.3.2.3 Atmospheric Stability

Influence of atmospheric stability on concentration was determined by evaluating several stability conditions. Plots of calculated concentration as a function of Monin-Obukhov length, *L*, are illustrated in Figure 5-4. High linearity ($R^2 \geq 0.89$) in calculated concentrations was again observed between AERMOD and WindTrax. The smallest difference between the two models (WindTrax/AERMOD concentration ratio of 1.02 to 1.23) was observed for very stable condition

(L = 50 m) whereas the highest difference (ratio of 1.37 to 1.75) was observed for unstable condition (L = -5,000 m). The 100-m downwind distance had the lowest difference between the two models for conditions with $L > 0$: WindTrax/AERMOD ratios for very stable, stable, and near-neutral, stable conditions were 1.02, 1.14, and 1.16, respectively. The lowest difference for unstable and very unstable conditions was obtained for 5-m (ratio of 1.37) and 1,000-m (ratio of 1.11) downwind distances, respectively.

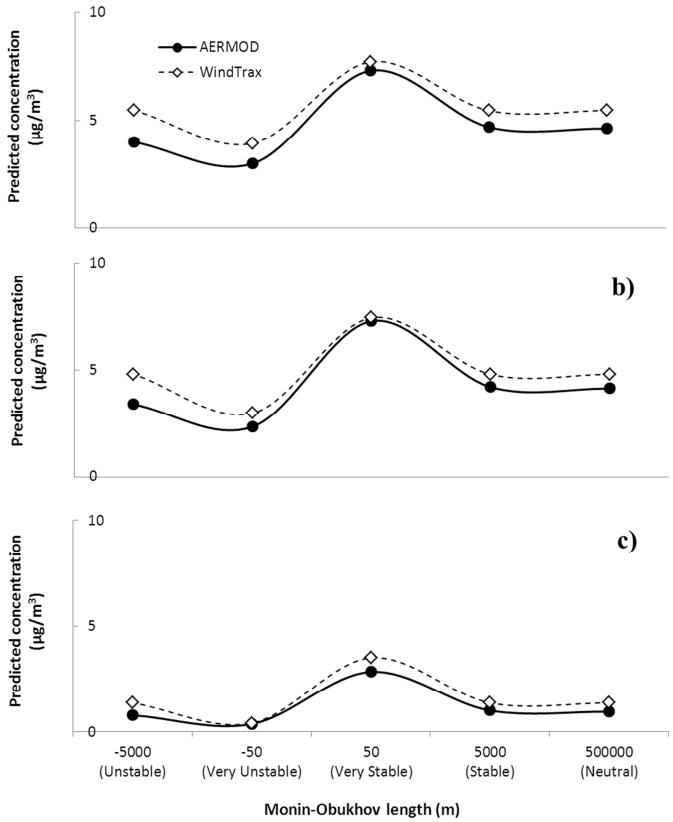

Figure 5-4. Calculated concentration as function of Monin-Obukhov length for downwind distances of: (a) 5 m, (b) 100 m, and (c) 1,000 m.

Effects of atmospheric stability were further evaluated using additional L values (Figure 5-5). This evaluation was done at the 100-m downwind distance to obtain the lowest difference between AERMOD and WindTrax. The lowest difference between the two models was again observed for stable conditions ($L > 0$ m), with WindTrax predicting significantly higher concentrations ($P < 0.05$). As a function of atmospheric stability, average WindTrax/AERMOD ratios were 1.05 (0.98 to 1.08) for 5 m $\leq L \leq$ 1,000 m and 1.17 (1.16 to 1.18) for $L >$ 1,000 m.

Unstable conditions (L < 0 m) had larger WindTrax/AERMOD ratios, implying larger difference in concentrations between the two models. For $L \geq$ -50 m, WindTrax/AERMOD ratio ranged from 0.61 to 1.30, and starting $L \leq$ -100 m, the ratio remained above 1.40 and had an average value of 1.44 (1.40 to 1.49).

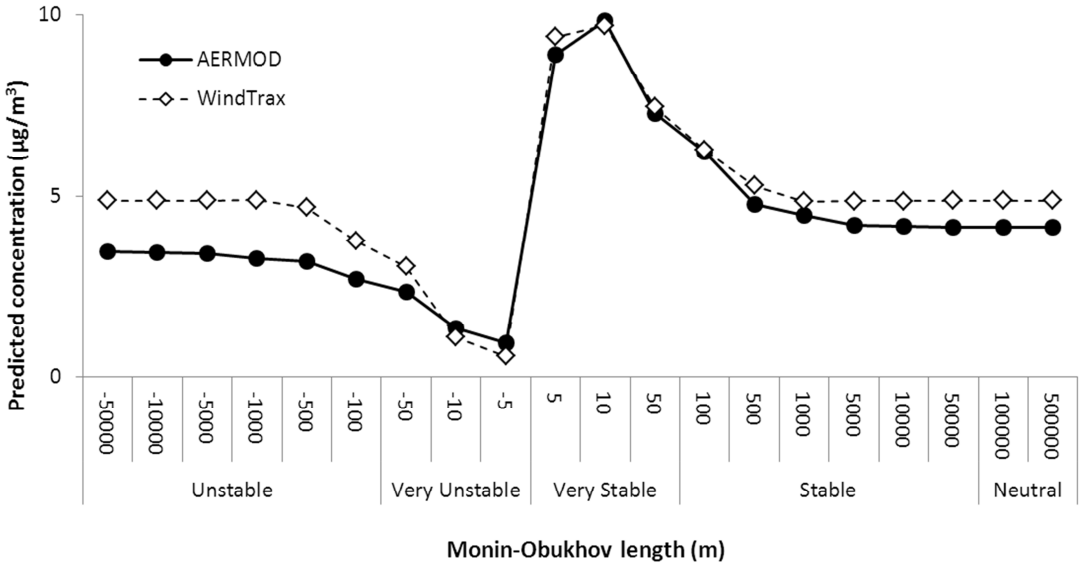

Figure 5-5. Calculated concentration as function of Monin-Obukhov length for the 100-m downwind distance – Higher resolution.

Relationship between L and concentration was also checked. From regression analyses, high linearity existed between L and the logarithm of concentration. R^2- values were 0.76 and 0.71 for AERMOD and WindTrax, respectively, for stable conditions (L > 0 m), and were 0.83 and 0.78, respectively, for unstable conditions (L < 0 m). Comparing stable and unstable conditions with same absolute values of L, AERMOD calculated higher concentrations for stable conditions. However, this was not the case for WindTrax. For $|L| \leq$ 100 m, WindTrax modeled higher concentrations (at least 66%) for stable conditions. The difference in calculated concentration between stable and unstable conditions in WindTrax decreased as the value of $|L|$ increased: for $|L|$ = 500 m, concentration for stable condition (L = 500 m) was higher by just 13% than that of unstable condition (L = -500 m); and starting $|L|$ > 500 m, concentrations for stable (L > 500 m) and unstable (L < -500 m) conditions were relatively the same (~ 0.15% difference).

5.3.3 Vertical Concentration Profile

Vertical concentration profiles for downwind distances of 5 and 100 m are shown in Figure 5-6. Findings drawn from preceding analyses were also observed in evaluation of vertical concentration profile: (1) higher concentrations were calculated by WindTrax; (2) AERMOD calculated higher concentrations for stable conditions than for unstable conditions; and (3) with $|L|$ = 5,000 m, WindTrax modeled almost same concentrations for both stable and unstable conditions.

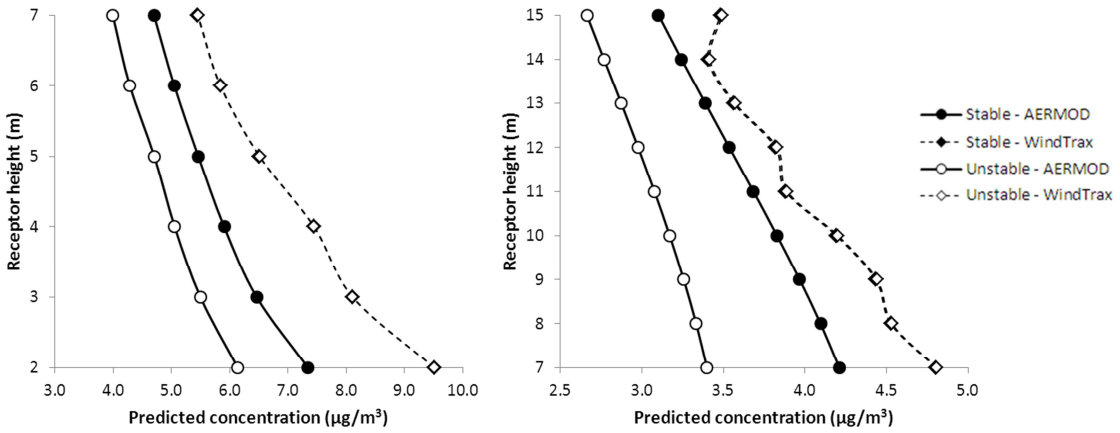

Figure 5-6. Vertical profiles of calculated concentrations at: (a) 5-m downwind distance, with 2 to 7-m height settings, and (b) 100-m downwind distance, with 7 to 15-m height settings.

For the 5-m downwind distance, WindTrax/AERMOD ratio was smaller for stable condition (L = 5,000 m) than for unstable condition (L = -5,000 m). As a function of height, average ratios were 1.27 (1.26 to 1.30) for heights of 2 to 4 m and 1.17 (1.16 to 1.19) for heights of 5 to 7 m for stable condition; for unstable condition, ratios were 1.50 (1.47 to 1.55) for heights of 2 to 4 m and 1.37 (1.36 to 1.38) for heights of 5 to 7 m. WindTrax/AERMOD ratio was also smaller during stable condition for the 100-m downwind distance. During stable condition, the ratio remained relatively constant with height at this distance, with an average value of 1.09 (1.05 to 1.14). On the other hand, the ratio changed with height during unstable condition: for 7 to 9-m heights, the ratio was 1.38 (1.36 to 1.41); for 10 to 12-m heights, the ratio was 1.29 (1.26 to 1.33); for heights 13 to 14 m, the ratio was 1.24 (1.23 to 1.24); and the 15-m height had a ratio of 1.31. Based on these results, WindTrax/AERMOD ratio decreased with height in general.

As mentioned, WindTrax requires longer simulation time. Using a meteorological data set composed of u, z_o, and L, and setting the number of particles released at 50,000, the average WindTrax simulation time for each data point (i.e., one set of meteorological data, one receptor) in this study was 2 min. Considerably longer simulation time should be expected if sonic anemometer measurements and/or higher number of particles released were used. Whereas the length of simulation was not a concern in AERMOD; as observed in this study, only a few seconds was required to complete a simulation.

5.4 Discussion

Difference in simulating dispersion might explain why AERMOD calculated lower concentrations than WindTrax. In WindTrax, mass transport in all directions (downwind, crosswind and vertical) is by convection (eq 5-2). In AERMOD, downwind mass transport is also by convection; however, both crosswind and vertical mass transports are by diffusion (eq 5-1). As diffusion is a much slower transport process compared to convection (Glasgow, 2010), overall mass dispersion in AERMOD is modeled at a lower transport rate than in WindTrax resulting in lower downwind concentrations calculated with AERMOD modeling.

In AERMOD, the concentration difference between stable (i.e., stable, very stable) and unstable (i.e., unstable, very unstable) conditions was expected as simulation of the vertical concentration distribution depends on atmospheric stability. The concentration in vertical direction for stable and unstable conditions has Gaussian and bi-Gaussian distributions, respectively (Cimorelli et al., 2004); given the same emission rate, AERMOD modeled lower concentrations for unstable conditions. On the other hand, WindTrax simulates dispersion in stable and unstable conditions similarly as only one set of concentration formulations is applied (Flesch et al., 1995). In WindTrax, atmospheric stability is used only to decide which equations will be used in characterizing wind flow; these include equations for Monin-Obukhov universal function, vertical velocity fluctuation stability correction function and dissipation rate stability correction factor (Flesch et al., 1995; Flesch et al., 2004). The difference in concentration between stable and unstable conditions in WindTrax simply depends on the degree of stability of the atmosphere. With L as the atmospheric stability parameter, the concentration difference was very large between very stable and very unstable conditions (e.g., 66% for $|L| \leq 100$ m) but was

almost negligible between stable and unstable atmospheric conditions (e.g., 0.15% for $|L| > 500$ m).

The rates of concentration decrease with height in AERMOD and WindTrax could explain why the concentration difference between the two models decreased with height. Overall, concentration decreased much faster with height in WindTrax than in AERMOD. Results showed that the rates of decrease for WindTrax-derived concentrations were approximately 0.83 and 0.19 $\mu g/m^3$-m for 5 and 100-m downwind distances, respectively, for both stable and unstable conditions. The rates of decrease for AERMOD-derived concentrations during stable condition were 0.53 and 0.14 $\mu g/m^3$-m for 5 and 100-m distances, respectively; during unstable conditions, the rates of decrease were 0.43 $\mu g/m^3$-m for the 5-m downwind distance and 0.09 $\mu g/m^3$-m for the 100-m distance. Based on these results, the rate of concentration decrease with height in WindTrax was faster than in AERMOD by at least 30%. Thus, this implies that smaller difference in calculated concentrations between the two models could be attained at higher receptor height settings.

Perhaps, more important, concentrations calculated by AERMOD and WindTrax have high linear correlation. This suggests that correction/conversion factors between these two dispersion models can be developed. Still, several things can be considered to improve working with conversion factors. One is that development of new and use of available conversion factors can be based on sampler placement, as sampler's downwind location and sampling height affect the degree of concentration difference between the two models. As shown in this study, difference between AERMOD and WindTrax modeling results was lowest if the sampler was located close to the area source and placed at higher height settings. Other considerations may include using wind speed and atmospheric stability as criteria for conversion factors.

5.5 Conclusions

The performance of AERMOD and WindTrax in calculating concentrations downwind of ground-level area sources was evaluated by comparing their sensitivity to variations in modeling inputs. The following conclusions were drawn from this study:

- AERMOD calculated lower concentrations than WindTrax, possibly due to the difference in their treatment of mass transport. Mass transport in WindTrax is based mainly on convection whereas in AERMOD, mass transport consisted of both convection and

diffusion. The two models also differ on how they model concentrations during stable and unstable conditions. AERMOD applies Gaussian and bi-Gaussian forms to model vertical concentration distribution for stable and unstable conditions, respectively. In contrast, WindTrax uses just one set of concentration formulations regardless of atmospheric stability.

- Concentrations calculated by AERMOD and WindTrax responded similarly to area source and receptor/sampler locations, and to changes in wind speed, surface roughness, and atmospheric stability. In both models, a downwind receptor was mainly impacted by area sources directly upwind of its location. Profiles of calculated concentration as functions of wind speed, surface roughness, and atmospheric stability were highly comparable between the two models. Their modeled vertical concentration profiles were also similar. More important, concentrations calculated by these two models were highly linear.

Indications are development of conversion factors between these two dispersion models is feasible. Results presented in this study can also be used as guidelines in designing studies aimed to develop factors between AERMOD and WindTrax, and/or to compare any other dispersion models.

5.6 References

Bjorneberg, D.L., A.B. Leytem, D.T. Westermann, P.R. Griffiths, L. Shao, and M.J. Pollard. 2009. Measurement of atmospheric ammonia, methane, and nitrous oxide at a concentrated dairy production facility in Southern Idaho using open-path FTIR spectrometry. *Trans. ASABE* 52:1749-1756.

Bonifacio, H.F., R.G. Maghirang, B.W. Auvermann, E.B. Razote, J.P. Murphy, and J.P. Harner III. 2012. Particulate matter emission rates from beef cattle feedlots in Kansas – reverse dispersion modeling. *J. Air & Waste Manage. Assoc*. 62:350-361.

Calder, K.L. 1977. Multiple-source plume models of urban air pollution – their general structure. *Atmos. Environ.* 11:403-414.

CFR. 2005. Code of Federal Regulations, 40 CFR, Part 51: Revision to the guideline of air quality models: Adoption of a preferred general purpose (flat and complex terrain) dispersion model and other revisions.

CFR. 2010. Code of Federal Regulations, 40 CFR, Part 58: Ambient Air Quality Surveillance.

CFR. 2011. Code of Federal Regulations, 40 CFR, Part 60: Call for Information: Information related to the development of emission-estimating methodologies for animal feeding operations.

Cimorelli, A. J., S.G. Perry, A. Venkatram, J.C. Weil, R.J. Paine, R.B. Wilson, R.F. Lee, W.D. Peters, R.W. Brode, and J.O. Paumier. 2004. *AERMOD: Description of Model Formulation,* EPA-454/R-03-004. Research Triangle Park, NC: U.S. Environmental Protection Agency.

Crenna, B. 2006a. *An Introduction to WindTrax*. Edmonton, AB: Department of Earth and Atmospheric Science, University of Alberta.

Crenna, B. 2006b. *Atmospheric Data in WindTrax*. Edmonton, AB: Department of Earth and Atmospheric Science, University of Alberta.

Denmead, O.T., D. Chen, D.W.T. Griffith, Z.M. Loh, M. Bai, and T. Naylor. 2008. Emissions of the indirect greenhouse gases NH3 and NOx from Australian beef cattle feedlots. *Austr. J. Exp. Agric.* 48:213-218.

Faulkner W.B., L.B. Goodrich, V.S.V. Botlaguduru, S.C. Capareda, and C.B. Parnell. 2009. Particulate matter emission factors for almond harvest as a function of harvester speed. *J. Air & Waste Manage. Assoc.* 59:943-949.

Faulkner, W. B., J. M. Lange, J. J. Powell, B. W. Shaw, and C. B. Parnell. 2007a. Sampler placement to determine emission factors from ground level area sources. ASABE Paper No. 074103. St. Joseph, MI:ASABE

Faulkner, W. B., J.J. Powell, J.M. Lange, B.W. Shaw, R.E. Lacey, and C.B. Parnell. 2007b. Comparison of dispersion models for ammonia emissions from a ground-level area source. *Trans. ASABE* 50:2189-2197.

Flesch, T.K., and J.D. Wilson. 2005. Estimating tracer emission with a backward Lagrangian Stochastic technique. In *Micrometeorology in Agricultural Systems, Agronomy Monograph no. 47.* Madison, WI: American Society of Agronomy, Inc., Crop Science Society of America, Inc., Soil Science Society of America, Inc.

Flesch. T. K., J.D. Wilson, L.A. Harper, and B.P. Crenna. 2005.Estimating gas emissions from a farm with an inverse-dispersion technique. *Atmos. Environ.* 39:4863-4874.

Flesch. T. K., J.D. Wilson, L.A. Harper, B.P. Crenna, and R.R. Sharpe. 2004. Deducing ground-to-air emissions from observed trace gas concentrations: a field trial. *J. Appl. Meteorol.* 43:487-502.

Flesch. T. K., J.D. Wilson, and E. Yee. 1995. Backward-time Lagrangian Stochastic models and their application to estimate gaseous emissions. *J. Appl. Meteorol.* 34:1320-1332.

Galvin, G., C. Henry, D. Parker, R. Ormerod, P. D'Abreton, and M. Rhoades. Efficacy of Lagrangian and a Gaussian model for back calculating emission rates from feedyard area sources. In *Workshop on Agricultural Air Quality,* Potomac, MD.

Glasgow, L.A. 2010. *Transport Phenomena.* Hoboken, NJ: John & Wiley & Sons, Inc.

Goodrich, L.B., W.B. Faulkner, S.C. Capareda, C. Krauter, and C.B. Parnell. 2009. Particulate matter emissions from reduced-pass almond sweeping. *Trans. ASABE* 52:1669-1675.

Hanna, S.R., B.A. Egan, J. Purdum, and J. Wagler. 2001. Evaluation of the ADMS, AERMOD and ISC3 dispersion models with the OPTEX, Duke Forest, Kincaid, Indianapolis, and Lovett field data sets. *Int. J. of Environment and Pollution* 16:301-314.

Harper, L.A., T.K. Flesch, and J.D. Wilson. 2010. Ammonia emissions from broiler production in the San Joaquin Valley. *Poultry Science* 89:1802-1814.

Heinsohn, R. J., and R.L. Kabel. 1999. *Sources and Control of Air Pollution*. Upper Saddle River, NJ: Prentice-Hall, Inc.

Holmes, N.S., and L. Morawska. 2006. A review of dispersion modeling and its application to the dispersion of particles: An overview of different dispersion models available. *Atmos. Environ.* 40:5902-5928.

Leytem, A.B., R.S. Dungan, D.L. Bjorneberg, and A.C. Koehn. 2011. Emission of ammonia, methane, carbon dioxide, and nitrous oxide from dairy cattle housing and manure management systems. *J. Environ. Qual.* 40:1383-1394.

McGinn, S. M., T.K. Flesch, D. Chen, B. Crenna, O.T. Denmead, T. Naylor, and D. Rowell. 2010. Coarse particulate matter emissions from cattle feedlots in Australia. *J. Environ. Qual.* 39:791-798.

McGinn, S.M., T.K. Flesch, B.P. Crenna, K.A. Beauchemin, and T. Coates. 2007. Quantifying ammonia emissions from a cattle feedlot using a dispersion model. *J. Environ. Qual.* 36:1585-1590.

Perry, S.G., A.J. Cimorelli, R.J. Paine, R.W. Brode, J.C. Weil, A. Venkatram, R.B. Wilson, R.F. Lee, and W.D. Peters. 2005. AERMOD: a dispersion model for industrial source applications. Part II: model performance against 17 field study databases. *J. Appl. Meteorol.* 44:694-708.

Purdue Applied Meteorology Laboratory. 2009. *Quality Assurance Project Plan for the National Air Emissions Monitoring Study*, Revision No. 3. West Lafayette, IN: Purdue University.

Sarr, J.H., K. Goita, and C. Desmarais. 2010. Analysis of air pollution from swine production by using air dispersion model and GIS in Quebec. *J. Environ. Qual.* 39:1975-1983.

SAS Institute Inc. 2004. *SAS system for Windows, release 9.1.3*. Cary, NC: SAS Institute Inc.

Seinfeld, J.H., and S.N. Pandis. 2006. *Meteorology of the Local Scale. Atmospheric Chemistry and Physics - from Air Pollution to Climate Change.* 2nd ed. Hoboken, NJ: John Wiley & Sons.

Turner, D. B. 1994. *Workbook of Atmospheric Dispersion Estimates – An Introduction to Dispersion Modeling.* 2nd ed. Boca Raton, FL: Lewis Publishers.

Turner, D.B., and R.H. Schulze. 2007. *Practical Guide to Atmospheric Dispersion Modeling.* Dallas, TX: Trinity Consultants, Inc. and Air & Waste Management Association.

U.S Environmental Protection Agency. 2009. *User's Guide for the AERMOD Meteorological Preprocessor (AERMET).* EPA-454/B-03-002. Research Triangle Park, NC: U.S Environmental Protection Agency.

U.S. Environmental Protection Agency. 2004a. *User's Guide for the AMS/EPA Regulatory Model – AERMOD.* EPA-454/B-03-001. Research Triangle Park, NC: U.S. Environmental Protection Agency.

U.S. Environmental Protection Agency. 2004b. *User's Guide for the AERMOD Meteorological Preprocessor (AERMET).* EPA-454/B-03-002. Research Triangle Park, NC: U.S. Environmental Protection Agency.

CHAPTER 6 - **Particulate Emissions from a Beef Cattle Feedlot Using Flux-gradient Technique**

6.1 Introduction

Air pollutant emissions from concentrated animal feeding operations (CAFOs) such as open-lot beef cattle feedlots can adversely affect air quality locally in downwind areas. Emissions also may affect air quality on a regional basis in certain areas like the San Joaquin Valley of California. Emissions from CAFOs generally include ammonia (NH_3), methane (CH_4), greenhouse gases (GHGs), volatile organic compounds, and particulate matter (PM). The National Research Council (2003) stated the need for accurate pollutant emissions estimates for CAFOs that can be used to assess their impact on the environment and regulate them effectively. In 2005, the U. S. Environmental Protection Agency (U.S. EPA) initiated the National Air Emissions Monitoring Study (NAEMS), a two-year study to continuously measure the emissions of regulated pollutants from different types of CAFOs and to develop and improve available emission quantifying techniques (CFR, 2011; Purdue Applied Meteorology Laboratory, 2009). Participating CAFOs in NAEMS represented the layer, broiler, swine and dairy industries but none came from the beef industry (Purdue Applied Meteorology Laboratory, 2009). In 2011, the U.S. EPA solicited quality-assured CAFO emissions data to supplement that collected through NAEMS (CFR, 2011). Requested data included emissions of PM ($PM_{2.5}$, PM_{10}, and TSP), hydrogen sulfide (H_2S), NH_3, and VOCs from broiler, layer, turkey, swine, dairy and beef operations (CFR, 2011). Clearly, more gaseous and PM emission estimates are needed for CAFOs, particularly for open-lot beef cattle feedlots.

Techniques appropriate for estimating emission rates from area sources include micrometeorological techniques, mass balance techniques, atmospheric dispersion models and atmospheric tracers (National Research Council, 2003). Recently published pollutant emission rates for beef cattle feedlots were determined using atmospheric dispersion models such as WindTrax, a backward Lagrangian stochastic-based (bLS) model (Flesch and Wilson, 2005), and AERMOD, a Gaussian-based and the current U.S. EPA preferred regulatory model (CFR, 2005). WindTrax has been used in quantifying emission rates for NH_3 (Flesch et al., 2005), odor (Galvin et al., 2006) and PM_{10} (McGinn et al., 2010) from beef cattle feedlots and GHGs from

dairy cattle facilities (Leytem et al., 2011). AERMOD also has been applied in feedlot studies on NH_3 (Faulkner et al., 2007) and PM_{10} (Bonifacio et al., 2012). Whereas the use of atmospheric dispersion models maybe acceptable, derived emission rates may differ from actual values by at least a factor of two (Flesch et al., 2004; National Research Council, 2003; Turner, 1994).

Micrometeorological techniques have long been used to quantify emission rates of various gases such as fumigants from agricultural croplands, which, like beef cattle feedlots, are open area sources. Although these techniques require complex and extensive instrumentations, they are the most direct, unobtrusive methods of measuring mass and energy transfer rates between the surface and the atmosphere (Ham and Baum, 2007). A commonly used micrometeorological method in determining emissions is the flux-gradient technique (Prueger and Kustas, 2005; Muller et al., 2009). The flux-gradient method has been used to estimate emissions for NH_3 (Myles et al., 2011), nitric acid (Myles et al., 2011), ozone (Muller et al., 2009), sulfur dioxide (Myles et al., 2011) and pesticides (Prueger et al., 2005) for agricultural lands. This method also has been applied to cattle feedlots to quantify emissions of amines (Hutchinson et al., 1982), NH_3 (Baek et al., 2006; Hutchinson et al., 1982), H_2S (Baek et al., 2006), and, on a small scale, has simulated a cattle pen to measure CH_4 (Harper et al., 1999). Limitations associated with the use of micrometeorological techniques on feedlots, however, were not directly addressed in these studies.

Micrometeorological techniques are based on certain key assumptions. One key assumption is horizontal homogeneity of the source and consequently emission rates. Feedlots are non-ideal locations and are made up of different types of surfaces such as unpaved roads, lagoons, and buildings, but the largest surface area comprises pen areas. A recent paper by Baum et al. (2008) examined the feasibility of and presented guidelines on the use of micrometeorological techniques at challenging locations such as cattle feedlots. In implementing micrometeorological techniques on estimating cattle feedlot emissions, recommendations included using at least 20-Hz sampling frequency in measurements to lower flux estimate uncertainty, applying 70 to 80% modeled source area criterion in fetch calculation to minimize the effects of non-feedlot surfaces while retaining more data, and relating computed emission fluxes to pens closer to the measurement location.

The present study was designed to quantify PM_{10} emission fluxes from an open-lot commercial beef cattle feedlot under a variety of meteorological and cattle pen moisture

conditions. It is the first use of the flux-gradient technique for PM from cattle feedlots. Vertical profiling of PM_{10} concentrations and high-resolution meteorological measurements were used to compute concentration gradients and particle eddy diffusivity, respectively, required in the flux-gradient technique. Results of this work provide critical information for producers, conservation specialists and regulators on the magnitude of PM_{10} emissions, derived using a micrometeorological technique, from a cattle feedlot typical of those in much of the Western U.S.

6.2 Materials and Methods

6.2.1 Feedlot Description

The commercial beef cattle feedlot studied is rectangular in shape, with lengths of 1.7 and 0.5 km in north-south and east-west directions, respectively. Based on a previous study (Baum et al., 2008), this feedlot is relatively flat, with surface roughness of 4.1 $\pm$ 2.2 cm. The feedlot has a capacity of 30,000 head in a total pen area of approximately 59 ha surrounded by agricultural crop lands. Field monitoring, which included PM_{10} concentrations and micrometeorological measurements, were conducted continuously from May 2010 through September 2011; however, measurement data, which were also used in another study (Bonifacio et al., 2013), were incomplete in some months due to several instrumentation- and/or weather-related problems.

In 2010, the average head capacity at the feedlot was 27,000; for the whole year, the estimated mean percentage of empty pens was only about 10%. Dust emission controls for that year included manure scraping frequency of two to three times per pen, and water application on unpaved roads and alleys. In 2011, the average head capacity at the feedlot was lower at 25,000, so many more pens were empty (approximately 18%). In addition, manure scraping and water application practices were changed in 2011. Pen surfaces were scraped more frequently ($\geq$ 3 times per pen) than the previous year. More importantly, water was applied on pens rather than on unpaved roads and alleys to alleviate heat stress on cattle. Mortality due to excessive heat was around 800 cattle in 2010 but was reduced significantly to just 20 in 2011.

6.2.2 Micrometeorological Measurements

A 5.3-m tower, equipped with micrometeorological and eddy covariance (EC) instrumentation, was installed to measure micrometeorological conditions at the feedlot. The tower was set up in a pen approximately 0.4 km and 1.3 km away from north and south edges of

the feedlot, respectively (Figure 6-1a). The EC instrumentation included a 3D sonic anemometer (Campbell Scientific, Inc., Logan, UT) for measuring the three orthogonal wind velocity components (u_x,u_y,u_z) and temperature and an infrared hygrometer (LICOR, Inc., Lincoln, NE) for measuring water vapor density. A data logger (Campbell Scientific, Inc., Logan, UT) was used to measure and record variances and covariances of u_x,u_y and u_z and temperature as 15-min averages. Friction velocity (u_*), Monin-Obukhov length (L) and surface roughness (z_o) were computed from these measurements using formulations presented by Flesch et al. (2004) and Baum et al. (2008). These three parameters were initially computed as 15-min values and then integrated to hourly values.

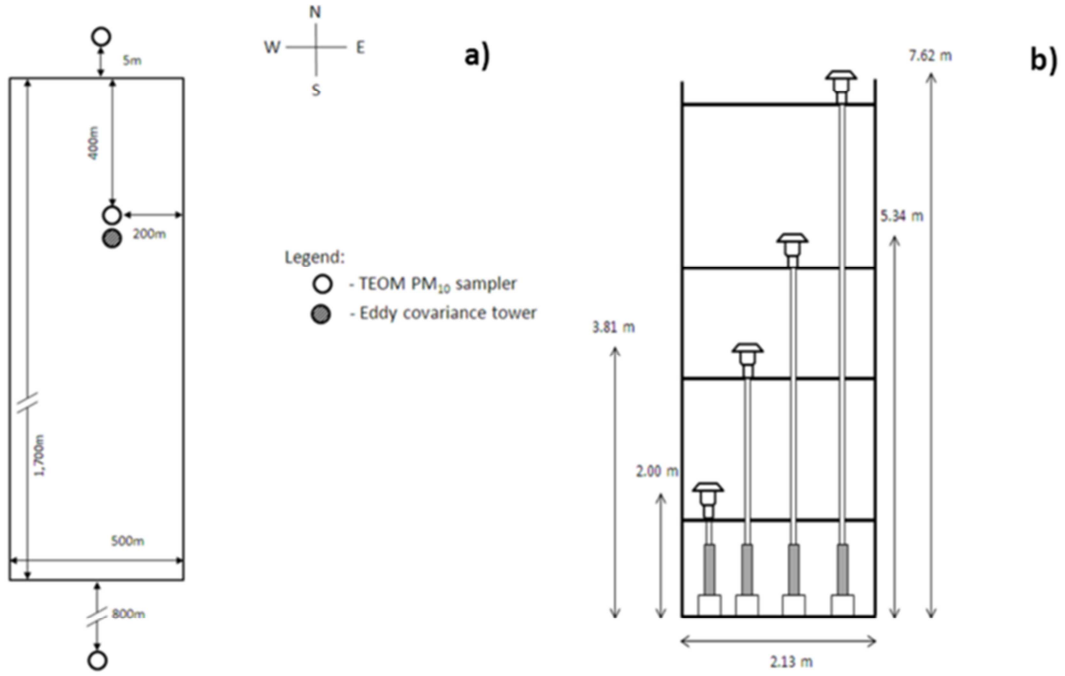

Figure 6-1. Location of the instrumentation: a) sampling site inside the feedlot; and b) sampling heights for TEOM PM_{10} samplers.

Starting in May 2011, the vertical profile of wind speed was also measured. Two wind anemometers (Model 05103-5, Campbell Scientific, Inc., Logan, UT) were installed, with one positioned at 3.81-m height and the other at 7.62-m height. A separate data logger (Campbell Scientific, Inc., Logan, UT) was used to record wind velocity measurements as 20-min and hourly averages.

6.2.3 PM_{10} Concentrations

Tapered element oscillating microbalance (TEOM) PM_{10} monitors (Series 1400a, Thermo Fisher Scientific, East Greenbush, NY; federal equivalent method designation No. EQPM-1090-079) were used to measure PM_{10} mass concentration at three sites simultaneously: (1) within the feedlot, approximately 5.5 m north of the EC tower; (2) 5 m away from the north edge of the feedlot; and (3) 800 m away from the feedlot south edge. Selection of these sites was based on feedlot layout, power availability and feedlot management approval. PM_{10} concentrations measured within the feedlot were used as downwind concentrations whereas PM_{10} concentrations at the north and south edges were used as upwind concentrations, depending on the wind direction (i.e., upwind at north site if wind was coming from the north, at south site if wind was from the south). Vertical profiling of PM_{10} concentrations was carried out at the sampling site within the feedlot by measuring PM_{10} concentrations at four heights (i.e., 2.0, 3.81, 5.34 and 7.62 m) (Figure 6-1b). A previous study indicated that the vertical concentration gradient upwind of a source was negligible (Ryden and McNeill, 1984) and because of equipment availability issue, PM_{10} concentration was measured only at one height (i.e., 2.0 m) for the other two sampling sites.

PM_{10} concentrations were measured at 20-min interval. In accordance with the TEOM manufacturer's recommendations, large negative 20-min PM_{10} concentrations ($< -10\ \mu g/m^3$) were not considered. Remaining 20-min downwind and upwind PM_{10} concentrations were then integrated into hourly averages. For each height, net concentrations (i.e., downwind concentration – upwind concentration) were computed for hours with both downwind and upwind concentrations. In addition, only positive net PM_{10} concentrations were considered because negative values could indicate either negligible particulate emissions from the feedlot or the presence of significant PM emissions from sources other than the feedlot.

6.2.4 Auxiliary Measurements

Precipitation data were obtained from a weather station located 2 km from the north edge of the feedlot. The weather station was equipped with a rain gauge (Model TE525, Campbell Scientific, Inc., Logan, UT) that measured and recorded precipitation.

Within the 17-month period, nine 4/5-day intensive sampling campaigns (n = 41 days) were performed to conduct pen surface water content measurements in addition to PM_{10} concentration and micrometeorological measurements. The manure/soil layer from the pen

surface was randomly sampled from the pen in which the tower was installed and two other adjacent pens. Sampling of the upper layer of the pen surface, approximately 2.5 to 5.0 cm, was done twice each day, one in the morning and another in the afternoon. Manure/soil samples were placed in separate sealed plastic bags. Wet-based water content of the sample was determined using the ASTM D2216-98 oven drying method (American Society for Testing Materials, 2002).

6.2.5 Data Screening

Prior PM_{10} emission flux calculation, hourly data points, each composed of PM_{10} concentration and micrometeorological measurements, were screened based on: (1) corresponding fetches of sampling heights with computed net PM_{10} concentrations; (2) number of sampling heights with net PM_{10} concentrations; and (3) vertical profile of net PM_{10} concentrations. The first screening was based on the fetch of each sampling height. For the measured PM_{10} concentration to be representative of PM emitted by pens, its corresponding fetch should fall within the feedlot boundary. The fetch for each sampling height was computed using:

$$x = \frac{-|L|}{k^2 \ln\left(F/S_o\right)} D\left(z_u/|L|\right)^P \tag{6-1}$$

where x is fetch (m), $|L|$ is absolute value of Monin-Obukhov length (m), F/S_o is assumed/desired normalized flux (dimensionless), z_u is new length scale (m), k is von Karman constant (0.4), and D and P are similarity constants (Hsieh et al., 2000). New length scale, z_u, was derived using the equation (Hsieh et al., 2000):

$$z_u = z_m \left(\ln\left(z_m/z_o\right) - 1 + z_o/z_m\right) \tag{6-2}$$

where z_m is sampler measurement height. Both L and z_o were derived from sonic anemometer measurements. Values for similarity constants D and P, which are both based on the atmospheric stability, are summarized by Hsieh et al. (2000). Normalized flux, F/S_o, was set at 0.7 to retain more data points without losing data quality (Baum et al., 2008).

The second screening was based on the number of measurement heights with measured net PM_{10} concentrations. As the PM_{10} emission flux determination using the flux-gradient technique involved vertical concentration gradients, hourly data points with at least two sampling heights with net concentration data were considered in the analyses (National Research Council, 2003). After the first two screenings, numbers of data points based on the number of sampling

heights with concentration data were 1,676 for data points with four net concentrations, 741 with three net concentrations, and 562 with two net concentrations; the total number of data points after the first two screenings was 2,979.

Lastly, data points were screened according to the net PM_{10} concentration vertical profile. The concentration should be approximately linear with the logarithm of height and decreasing with increasing height (Ryden and McNeill, 1984). Linearity between the net PM_{10} concentration and the logarithm of height was verified using Pearson correlation. As practiced in biostatistics (Colton, 1974; Gherman and Mironiuc, 2012; Lehman et al., 2009) and other research areas (U.S. Department of Agriculture, 2012), a Pearson correlation criterion of 0.75 was applied to indicate strong and robust linearity. Thus, hourly data points with Pearson correlation coefficients greater than or equal to 0.75 were used in emission flux computation.

6.2.6 Flux-Gradient Technique

Using the flux-gradient technique, PM_{10} emission flux from pens, Q_p, ($\mu g/m^2$-sec) was estimated with the expression:

$$Q_p = -K_c \frac{dc}{dz} \tag{6-3}$$

where K_c is eddy diffusivity for PM_{10} (m^2/sec) and dc/dz is vertical net PM_{10} concentration gradient ($\mu g/m^3$-m) (Meyers and Baldocchi, 2005; Myles et al, 2010; Prueger and Kustas, 2005; Prueger et al., 2005). Vertical concentration gradient, dc/dz, for each data point was estimated from net PM_{10} concentration data and their corresponding sampling heights. Eddy diffusivity for PM_{10}, K_c, was derived from eddy diffusivity for momentum, K_m, and Schmidt number, S_c, using the equation (Flesch et al., 2002; Prueger et al., 2005):

$$S_c = \frac{K_m}{K_c} \tag{6-4}$$

Eddy diffusivity for momentum, K_m (m^2/sec) was computed using the expression:

$$K_m = \frac{k\, u_* z_m}{\phi_m} \tag{6-5}$$

where k is von Karman constant (0.4), u_* is friction velocity (m/sec), z_m is mean geometric height

(m), and ϕ_m is nondimensional correction parameter. Friction velocity was obtained from micrometeorological measurements. The mean geometric height for each hour was computed using sampling heights with acceptable fetches and net PM_{10} concentrations. ϕ_m was calculated following the procedure by Flesch et al. (2002) and Prueger et al. (2005), as presented by Hogstrom (1996):

$$\phi_m = \left(1 - 19\frac{z_m}{L}\right)^{-0.25} \tag{6-6}$$

for unstable atmospheric conditions ($L < 0$) and:

$$\phi_m = \left(1 + 5.3\frac{z_m}{L}\right) \tag{6-7}$$

for stable atmospheric conditions ($L > 0$).

To calculate PM_{10} eddy diffusivity, K_c, S_c to be used for the feedlot's PM_{10} was estimated in accordance with the experiment done by Flesch et al. (2002). Combining eq. 6-3 and eq. 6-4, S_c is given by:

$$S_c = -\frac{K_m}{Q_p}\frac{dc}{dz} \tag{6-8}$$

PM_{10} emission flux, Q_p, used in eq. 8 was determined using the integrated horizontal flux technique and was also reduced by 20% to compensate for the inherent error (Flesch et al., 2002). Measurements used in deriving Q_p by the integrated horizontal flux technique were anemometer-based wind speed and PM_{10} concentration measurements for 3.81 and 7.62-m heights from May through September 2011, and their corresponding fetches. Hourly medians and lower and upper standard deviations for S_c for this 5-month period (n = 291 hourly data points) are shown in Figure 6-2. Overall median S_c was 0.63; this value was comparable to $S_c = 0.70$ applied in previous particle transport studies (Guo and Maghirang, 2012; Zhang et al., 2008) and $S_c = 0.64$ implemented in an area source dispersion model (Flesch et al., 2004). Therefore, in calculating PM_{10} emission fluxes using the flux-gradient technique (eq 6-3), $S_c = 0.63$ was applied for the whole measurement period.

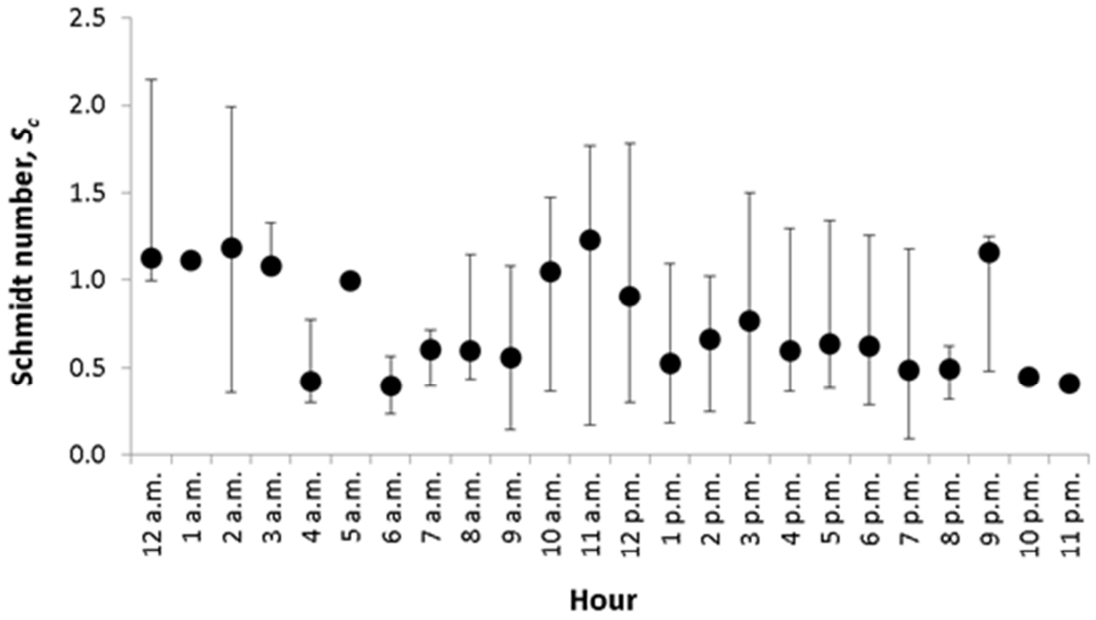

Figure 6-2. Hourly median PM_{10} Schmidt number, S_c, determined for May through September 2011 (n = 291). Error bars represent upper and lower standard deviations.

6.2.7 Data Analysis

Data were analyzed using SAS (2004; SAS Inst. Inc., Cary, NC). Mean values were presented for parameters that follow normal distribution (e.g., temperature, u_*); on the other hand, median values were reported for those that did not follow the normal distribution (e.g., PM_{10} concentrations, PM_{10} emission fluxes, S_c, K_c). Outlier analysis and standard deviation calculation were based on the procedure by Schwertman et al. (2004) for non-normal datasets. In determining the influence of micrometeorological parameters on dc/dz, K_c and PM_{10} emission flux, backward elimination was applied with a 5% significance level.

6.3 Results and Discussion

6.3.1 Micrometeorological Conditions

WindRose plots (WRPLOT View, Lakes Environmental) are provided to show wind speed and wind direction trends at 6-month intervals (Figure 6-3). For the first 6 months of the measurement period, most of the hourly data points (85%) had wind coming from the south (135° to 225°); for the second 6 months, 45% and 32% of the data points had wind from the north (0° to 45°, 315° to 360°) and the south, respectively; and for the last months, 19% and 59% from the north and the south, respectively. Overall, wind came from the south 55% of the time and from the north 25% of the time; wind coming from the east and west had occurrence percentages of only 14% and 6%, respectively.

Fetches for the four sampling heights were within the feedlot boundary 98%, 87%, 76% and 62% of the time for 2.0, 3.81, 5.34 and 7.62 m heights, respectively. Median fetch values for the acceptable hourly data points (n = 1,626) for the four measurement heights were 84, 163, 189 and 209 m, respectively (Table 6-1); note that the fetch of the instrumentation tower from the feedlot boundary ranged from 210 to 1,308 m.

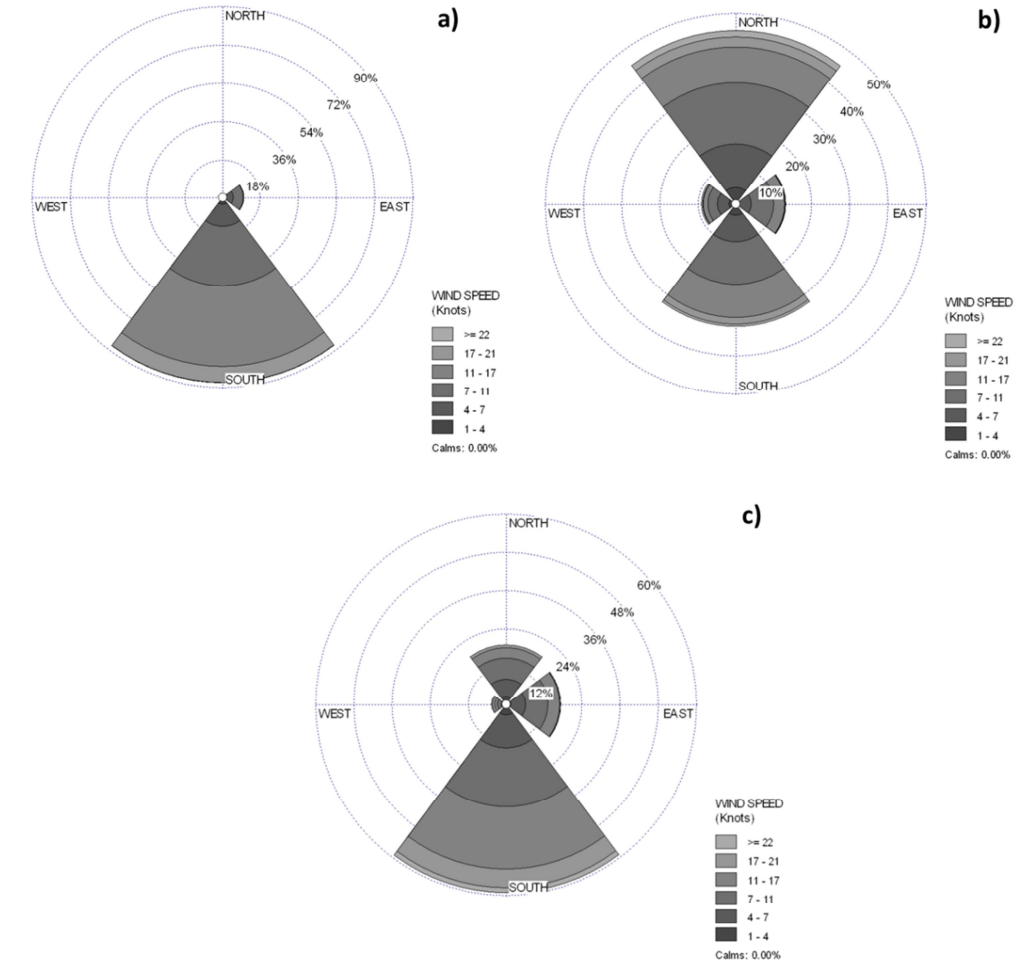

Figure 6-3. Wind speed and wind direction distribution at the studied feedlot: a) May through October 2010 (n = 811 hourly data points); b) November 2010 through April 2011 (n = 832 hourly data points); and c) May through September 2011 (n = 1,296 hourly data points).

Table 6-1. Fetch values (n = 1,626) for the four measurement heights as calculated using the procedure by Hsieh et al. (2000)

	Fetches (m)				
	Feedlot [a]	2.0 m	3.81 m	5.34 m	7.62 m
Count	1,626	1,626	1,626	1,397	1,104
Median	420	84	163	189	209
Minimum	210	7	12	16	21
Maximum	1,308	401	1,214	1,281	1,246
Standard deviation [b]					
Lower range	-	33	85	87	86
Upper range	-	29	104	176	141

[a] Feedlot fetch based on feedlot dimensions
[b] Two values for standard deviations, for lower and upper ranges, because of non-normality of distribution.

Overall values for micrometeorological parameters at the feedlot were as follows: temperature of 14 °C; wind speed of 5.0 m/sec; u_* of 0.40 m/sec; and z_o of 4.0 cm (Table 6-2). Sensible heat fluxes were 66 and -10 W/m^2 for surface-to-atmosphere and atmosphere-to-surface heat flux directions, respectively (Table 6-2). During the 17-month measurement period, August was the hottest month in both 2010 (32 $\pm$ 5 °C) and 2011 (27 $\pm$ 5 °C); December was the coldest month in 2010 (-3 $\pm$ 6 °C) and January was the coldest in 2011 (-5 $\pm$ 7 °C). Highest wind speeds were observed in July (5.5 $\pm$ 1.8 m/sec) and August (5.2 $\pm$ 1.6 m/sec) in 2010, and May (5.6 $\pm$ 2.7 m/sec) and June (5.6 $\pm$ 2.3 m/sec) in 2011; consequently, these months also had the highest friction velocities (0.43 $\pm$ 0.17 m/sec). Lowest wind speeds were measured in October 2010 (2.5 $\pm$ 0.5 m/sec), which also had the lowest friction velocities (0.22 $\pm$ 0.04 m/sec). Overall median z_o was 4.0 cm, which was comparable to the median value (3.6 cm) reported by Baum et al. (2008) for the same feedlot.

Table 6-2. Micrometeorological parameters at the feedlot for May 2010 through September 2011

	Temperature (°C)	Wind speed (m/sec)	u_* (m/sec)	z_o (cm)	Sensible heat (W/m^2)	
					I [a]	II [b]
Mean	14	5.0	0.40	4.0 [c]	66 [c]	-10 [c]
Minimum	-24	0.5	0.06	1.2×10^{-3}	0.03	-0.05
Maximum	39	28.9	3.00	100	772	-1,425
Standard deviation	14	2.3	0.18	1.9 / 7.1 [d]	71 / 158 [d]	16 / 8 [d]

[a] Heat flux direction from surface to atmosphere
[b] Heat flux direction from atmosphere to surface
[c] Value based on median due to non-normal distribution for z_o
[d] Two values for standard deviations, for lower and upper ranges, due to non-normal distribution for z_o.

6.3.2 PM_{10} Concentration and Vertical Concentration Gradient

PM_{10} concentrations measured at all four measurement heights exhibited diurnal trends, with highest concentrations measured during the early evening period (7:00 p.m. to 9:00 p.m.) and lowest during early morning period (2:00 a.m. to 5:00 a.m.) (Figure 6-4). Overall hourly net PM_{10} concentrations (SD = lower, upper) for the four heights were 96 (SD = 101, 197), 62 (SD = 67, 126), 55 (SD = 58, 115) and 57 (SD = 59, 103) $\mu g/m^3$ for 2.0-m (n = 1,965), 3.8-m (n = 1,915), 5.3-m (n = 1,538) and 7.6-m (n = 1,148) heights, respectively. Although not significantly different (P = 0.44), PM_{10} concentration was slightly higher at the 7.6-m height than at the 5.34-m height due to the difference in numbers of data points. Considering only points with concentrations for both heights (n = 1,088), median concentrations were 73 (SD = 68, 123) and 61 (SD = 59, 104) $\mu g/m^3$ for the 5.3-m and 7.6-m heights, respectively. For this set, statistical analyses showed that PM_{10} concentration was significantly higher ($P < 0.05$) at the 5.34-m height. Using overall concentration values, regression analysis between the logarithm of measurement height and PM_{10} concentration indicated a strong linear relationship ($R^2 = 0.82$) as expected (Ryden and McNeill, 1984).

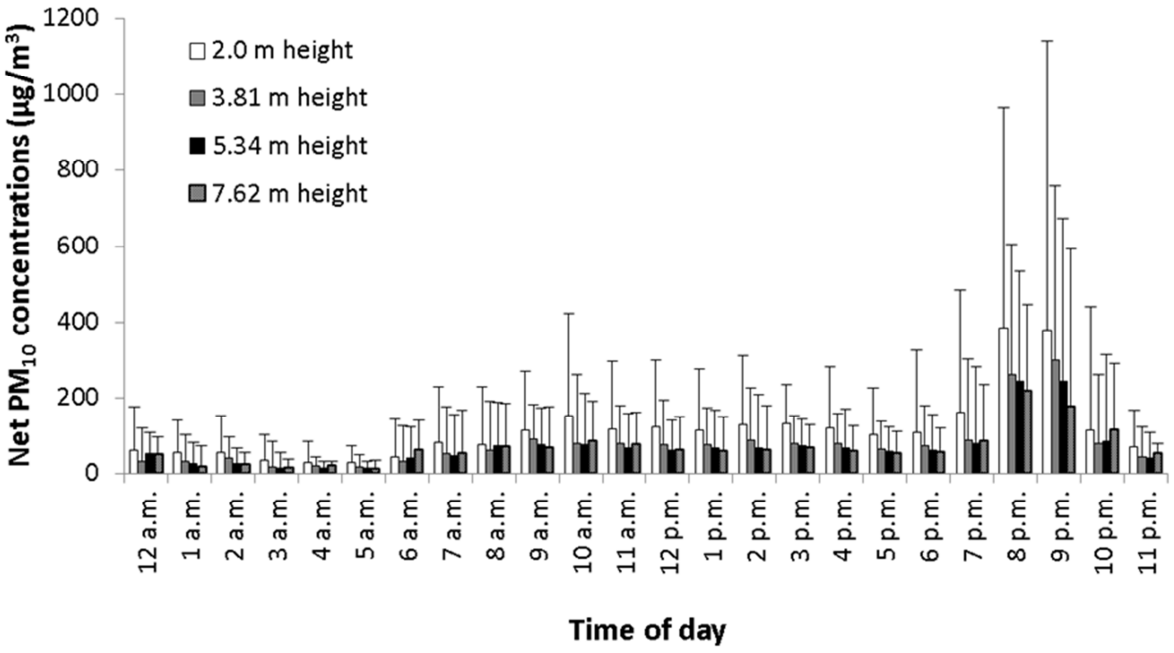

Figure 6-4. Hourly median net PM_{10} concentrations as measured from the four measurement heights for May through September 2011. Error bars represent upper standard deviation estimates.

Calculation of hourly vertical concentration gradient, *dc/dz*, showed that PM_{10} concentration decreased by approximately 10 µg/m^3 for every meter increase in height (n = 1,626). Within the day, the 7:00 p.m. to 9:00 p.m. period had the largest PM_{10} concentration gradient, 20 (SD = 49, 22) µg/m^3-m, and the 2:00 a.m. to 5:00 a.m. period had the lowest gradient, 4 (SD = 7, 3) µg/m^3-m. Also, the vertical concentration gradient for the mid-morning to late afternoon period (9:00 a.m. to 6:00 p.m.) was 12 (SD = 13, 10) µg/m^3-m.

Based on statistical analyses of daily values (n = 238), temperature had a significant influence ($P < 0.05$) on vertical PM_{10} concentration gradient whereas both u_* ($P = 0.96$) had none. Analysis indicated that temperature and vertical PM_{10} concentration gradient were inversely correlated. For z_o, analysis suggested that it also might have some effect ($P = 0.11$) on the resulting vertical concentration gradient.

6.3.3 PM_{10} Eddy Diffusivity

With S_c = 0.63, overall mean hourly eddy diffusivity for PM_{10}, K_c, was 1.10 $\pm$ 0.60 m^2/sec for the 17-month period (n = 1,626 hourly values). Within the day, K_c was highest from 12:00 p.m. to 3:00 p.m., and lowest and relatively steady from 8:00 p.m. to 8:00 a.m. (Figure 6-5). The hourly variation of the different micrometeorological parameters might explain the observed trend for K_c. Figure 6-6 shows hourly trends of sensible heat, u_*, temperature and z_o for the entire measurement period. The first three parameters had the same trend as K_c: the parameter was highest in the mid-afternoon and was lowest and steady from evening to mid-morning. Statistical analyses also showed that sensible heat, u_* and temperature significantly affected K_c ($P < 0.05$). Atmospheric conditions within the day could help explain this trend. The presence of solar radiation in the afternoon results in higher heat flux and temperature that make atmospheric conditions unstable (i.e., strong vertical dispersion) whereas the absence of solar radiation keeps the atmosphere stable (i.e., minimum vertical dispersion) (Turner, 1994). Unstable atmospheric conditions could explain the high K_c values estimated for the afternoon period, and stable conditions could explain the low and stable K_c values at night. Compared with K_c and other micrometeorological parameters, z_o was essentially stable the whole day, ranging from 2.7 to 5.8 cm (Figure 6-6); in addition, statistical analyses suggested that z_o did not influence ($P = 0.56$) on K_c.

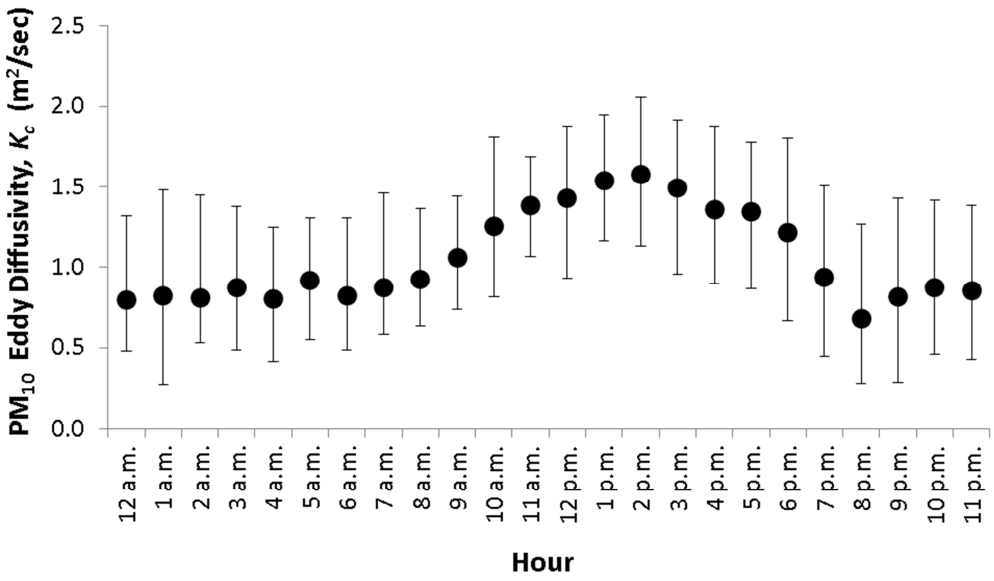

Figure 6-5. Hourly median PM_{10} eddy diffusivity, K_c, calculated for May 2010 through September 2011 (n = 1,626 hourly data points). Error bars represent upper and lower standard deviations.

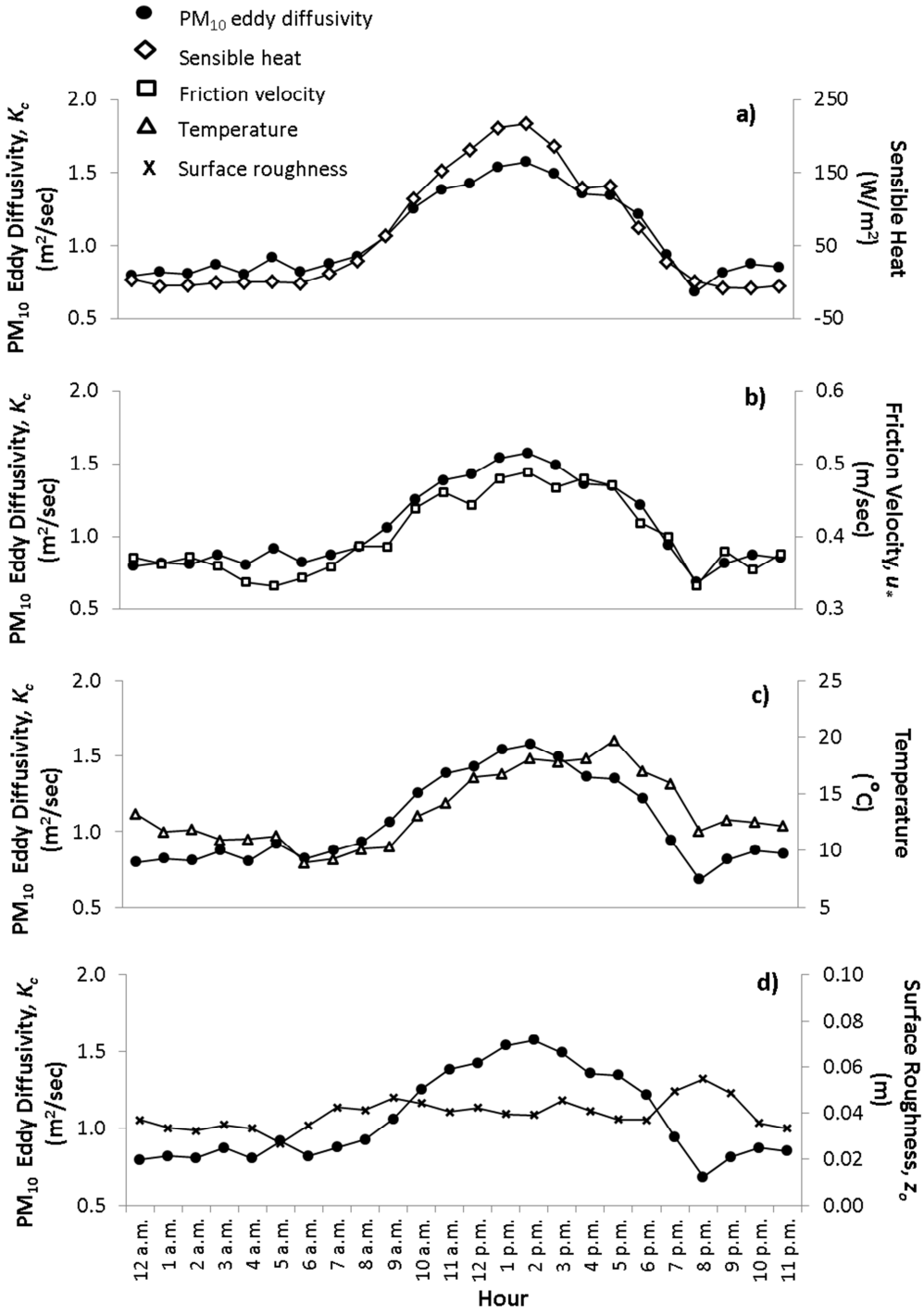

Figure 6-6. Hourly trends of a) sensible heat; b) friction velocity, u_*; c) temperature; and d) surface roughness, z_o, plotted with PM_{10} eddy diffusivity, K_c, for the entire measurement period.

6.3.4 PM_{10} Emission Flux

During the 17-month measurement period (n = 1,626 hourly data points), hourly PM_{10} emission flux ranged from ~0 to 272 mg/m^2-hr, with an overall median value of 36 mg/m^2-hr. Based on days with at least 12 hourly emission fluxes (n = 44), the overall median daily PM_{10} emission flux was 1.81 g/m^2-day, which was slightly higher but within range of those recently published for beef cattle feedlots (McGinn et al., 2010; Bonifacio et al., 2012). McGinn et al. (2010) reported values of 1.45 and 1.61 g/m^2-day for Australian feedlots based on reverse dispersion modeling with WindTrax. Bonifacio et al. (2012) reported median PM_{10} emission fluxes of 1.10 and 1.60 g/m^2-day for Kansas feedlots based on reverse dispersion modeling with AERMOD. Differences in approaches and feedlot conditions/characteristics could help explain the difference among these PM_{10} emission fluxes. Reverse dispersion modeling was applied to determine PM_{10} emission fluxes in the two previous studies whereas the flux-gradient technique was used in this study. Water application on pens was done using a solid-set sprinkler system at one feedlot evaluated by Bonifacio et al. (2012); but at the feedlot evaluated, water was occasionally applied on either unpaved roads/alleys (2010) or pens (2011) using water trucks. Although the feedlot studied was comparable to Kansas feedlots examined by Bonifacio et al. (2012) in terms of temperature, wind speed and wind direction, it received far less precipitation (420 mm in 2010, 152 mm in 2011) than other feedlots (average of 622 mm). As noted in a previous study (Bonifacio et al., 2011), rainfall effects on lowering PM emission generally lasted from 3 to 7 days. In calculation of overall PM_{10} emission flux (1.81 g/m^2-day), 78% of the days used (n = 44) was preceded by at least 7 days with no rainfall.

PM_{10} emission fluxes for these 44 days (with at least 12 hourly values) were plotted as 24-hr averages in time series with wind u_*, temperature, and measured z_o (Fig. 6-7). Based on both the plot (Fig. 6-7b) and statistical analysis, temperature significantly influenced ($P < 0.05$) the daily PM_{10} emission flux. Relatively high temperatures might have contributed to large PM_{10} emissions at the feedlot from June through July 2010 (temperature of 28 to 33 °C, median PM_{10} emission of 85 mg/m^2-hr) and May 2011 (temperature of 5 to 23 °C, median PM_{10} emission of 100 mg/m^2-hr) as seen in Fig. 6-7b. Days with low temperatures, however, also could have high PM_{10} emission rates. For example, November 1 and 4, 2010, despite having 24-hr average temperatures of 4 and 2 °C, respectively, had daily PM_{10} emission fluxes of 87 and 129 mg/m^2-hr, respectively. Another example was January 31, 2011 that had below freezing temperatures (-

12 °C, 24-hr average) but high PM_{10} emission fluxes (66 mg/m^2-hr, 24-hr average). The high PM emissions determined for periods with low temperatures could be attributed to the absence of precipitation (e.g., rainfall, snow, water application) for extended periods of time. The high emissions in November 2010 could be largely due to negligible precipitation (2.0 mm) in October 2011. Statistical analysis showed that the number of days without rain significantly affected ($P = 0.02$) the resulting PM_{10} emissions. Although not evident from the plot (Fig. 6-7a), the other micrometeorological parameter that affected the daily PM_{10} emission flux was u_* ($P < 0.05$).

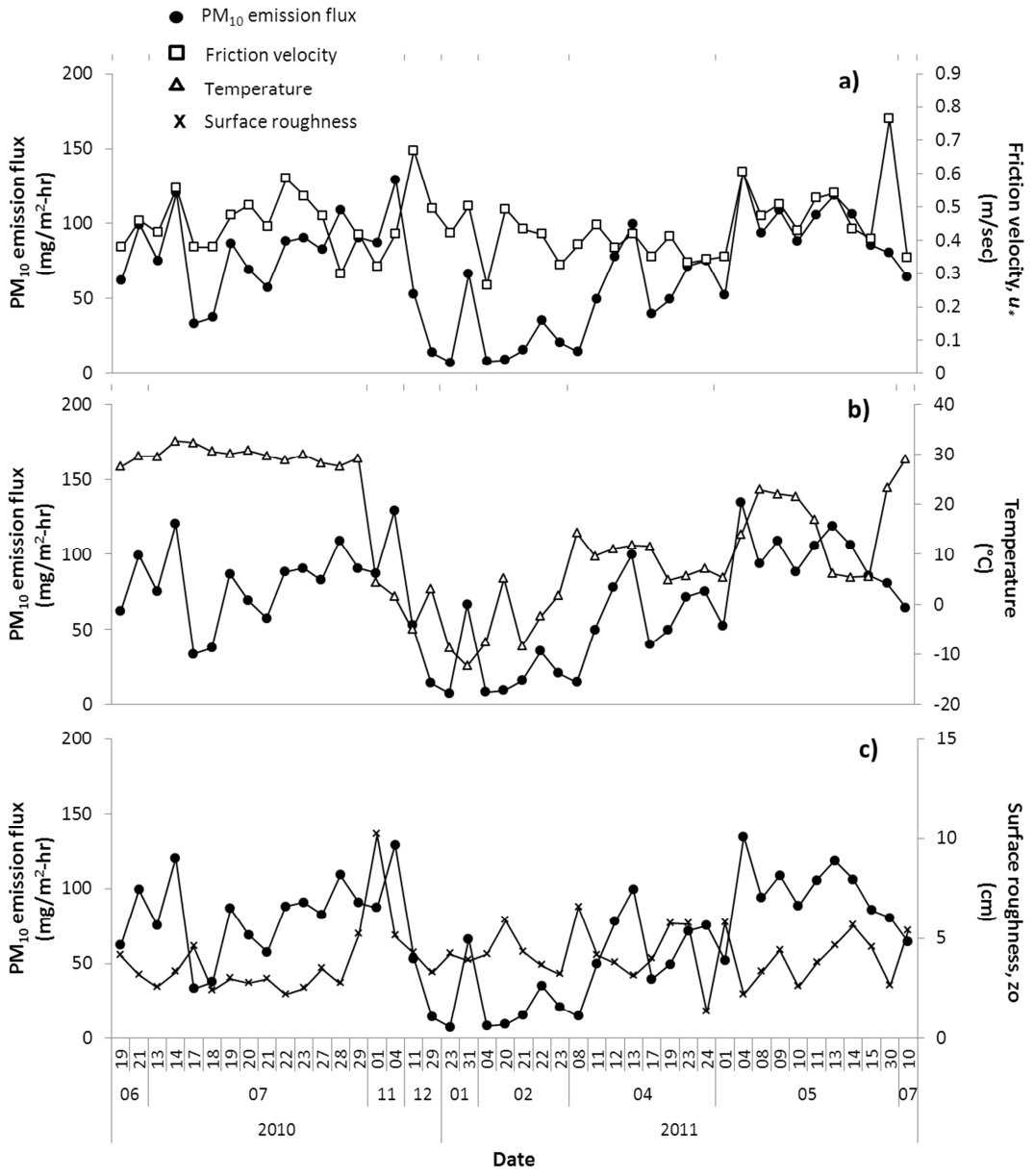

Figure 6-7. Daily PM_{10} emission fluxes plotted with a) friction velocity u_*; b) temperature; and c) surface roughness, z_o. Days considered were those with at least 12 hourly data points (n = 44).

Statistics of the hourly PM_{10} emission fluxes at the feedlot are summarized in Table 6-3. Within a day, PM_{10} emission flux at the feedlot remained relatively high and steady from 9:00 a.m. to 9:00 p.m. This trend was different from other cattle feedlot studies: the highest PM_{10} emissions within a day were observed in the afternoon (10:00 a.m. to 5:00 p.m.) at two Kansas cattle feedlots (Bonifacio et al., 2012) and in the early evening at two Australian feedlots

(McGinn et al., 2010). Still, similar to these previous studies, increase in PM_{10} emissions was observed during the early evening period (8:00 p.m. to 9:00 p.m.). Reasons for these different PM_{10} emission trends could include differences in feedlots characteristics (e.g., animal spacing), dust control methods (e.g., pen scraping frequency, water application), emission estimation technique, and measurement design (e.g., location of samplers, measurement period). In addition, note that PM_{10} emission estimates presented by all these studies for the evening period might be suspect because of measurement and meteorological limitations associated with atmospheric stable conditions (Massman and Lee, 2002). Based on statistical analyses, u_*, temperature, sensible heat and z_o all influenced ($P < 0.05$) hourly PM_{10} emissions. High u_*, temperature and sensible heat, and small effective z_o were conditions favorable to high PM emissions at the feedlot.

Differences were observed in hourly PM_{10} emissions between warm (21 ± 10 °C) and cold (-2 ± 8 °C) conditions (Fig. 6-8). Using median values, warm conditions had significantly higher PM_{10} emission fluxes, ranging from 9 to 146 mg/m^2-hr, than cold conditions, which had only 3 to 27 mg/m^2-hr PM_{10} emissions. For the trend within the day, peak in PM_{10} emissions for warm conditions occurred during the early evening period, from 8:00 p.m. to 9:00 p.m. (116 and 146 mg/m^2-hr, respectively). For cold conditions, on the other hand, the highest estimated PM_{10} emissions (14 to 27 mg/m^2-hr) were from the afternoon, from 11:00 a.m. to 3:00 p.m.; surprisingly, no increase in PM_{10} emissions was measured in the evening (< 7 mg/m^2-hr starting at 8:00 p.m.). Similar to the previous analyses, PM_{10} emissions during warm conditions were largely influenced ($P < 0.05$) by u_*, temperature, sensible heat and z_o; however, during cold conditions, PM_{10} emissions were no longer influenced ($P = 0.97$) by z_o.

Table 6-3. Hourly medians and standard deviations for PM_{10} emission flux (n = 1,626) as quantified by flux-gradient technique

Hour	Count	Median (mg/m^2-hr)	Standard deviation [a] (mg/m^2-hr)	
			Lower standard deviation	Upper standard deviation
12 a.m.	74	23	20	51
1 a.m.	75	21	21	32
2 a.m.	60	19	17	27
3 a.m.	61	14	15	25
4 a.m.	58	10	7	24
5 a.m.	53	8	6	22
6 a.m.	57	14	14	31
7 a.m.	58	26	19	47
8 a.m.	69	35	33	38
9 a.m.	76	56	64	90
10 a.m.	66	59	66	117
11 a.m.	63	68	49	67
12 p.m.	67	62	55	105
1 p.m.	66	72	71	65
2 p.m.	78	72	60	86
3 p.m.	73	59	58	54
4 p.m.	69	53	48	96
5 p.m.	81	59	52	64
6 p.m.	86	59	64	72
7 p.m.	79	47	40	90
8 p.m.	71	63	81	135
9 p.m.	53	55	66	143
10 p.m.	70	36	42	115
11 p.m.	63	22	22	35
Overall	1,626	36	38	85

[a] Two values for standard deviations, for lower and upper ranges, because of non-normality of distribution.

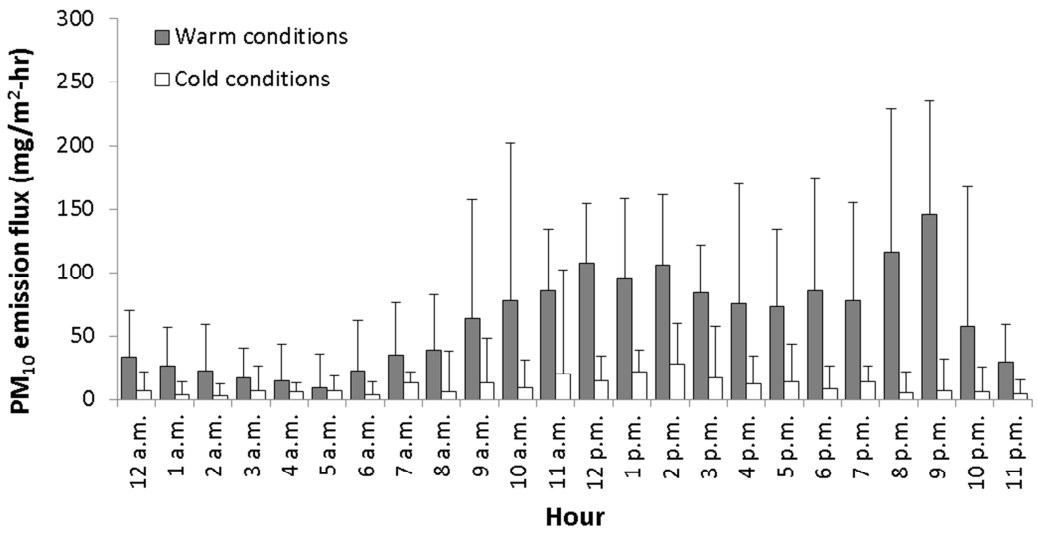

Figure 6-8. Hourly median PM_{10} emission fluxes for warm and cold conditions.

Aside from micrometeorological conditions, another important parameter affecting PM emission is the water content of the pen surface. Out of 41 days with pen surface water content measurement, 26 days had PM_{10} emission flux data. To keep at least 75% of 26 days with both water content and PM_{10} emission measurements, days with at least 7 hourly emission fluxes were considered in the analyses. A plot of pen surface water content and corresponding PM_{10} emission flux is illustrated in Fig. 6-9. As expected, statistical analyses revealed that pen surface water content had a significant influence ($P < 0.05$) on PM_{10} emission flux. Periods with water content greater than 20% had relatively smaller PM_{10} emission fluxes (Fig. 6-9). For the studied feedlot, pen surface conditions with water content greater than 20% (23 to 50%, n = 5) had PM_{10} emission fluxes ranging from 3 to 14 mg/m^2-hr, with a median of 11 mg/m^2-hr, whereas conditions with water content of 20% or less (8 to 20%, n = 16) had higher PM_{10} emission fluxes that ranged from 7 to 40 mg/m^2-hr and had a median of 15 mg/m^2-hr; this implies reduction in PM_{10} emissions of up to 60% for pens with surface water content of greater than 20%.

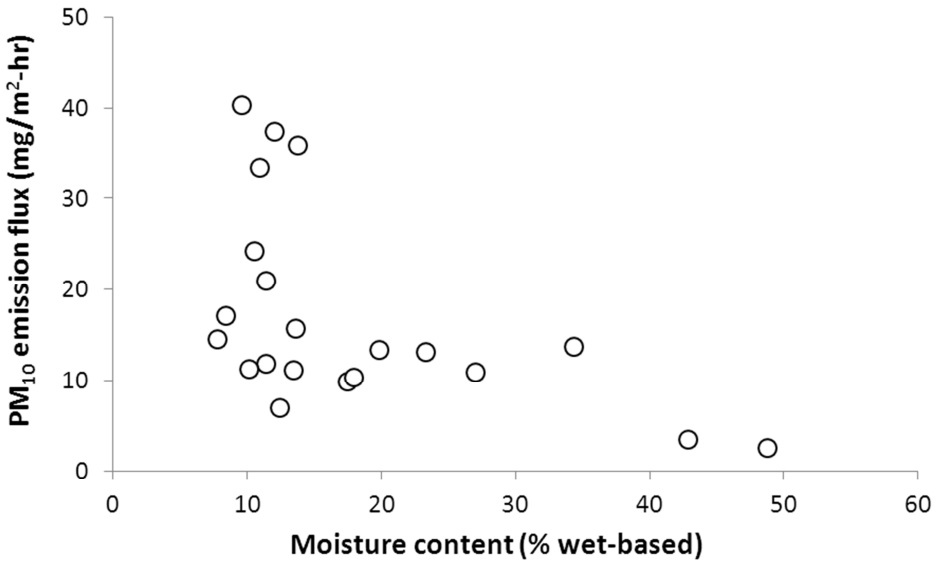

Figure 6-9. Effect of pen moisture content (wet-based) on PM_{10} emission flux (n = 21 days).

6.4 Conclusions

The flux-gradient technique was implemented to quantify PM_{10} emission fluxes from open-lot beef cattle feedlots. PM_{10} concentrations at a Kansas commercial beef cattle feedlot were vertical-profiled using TEOM PM_{10} samplers, and micrometeorological conditions were measured using eddy covariance instrumentation. PM_{10} emission fluxes at the feedlot varied diurnally and seasonally, with hourly emission fluxes ranging from ~0 to 272 mg/m^2-hr (overall median of 36 mg/m^2-hr). During warm conditions, PM_{10} emissions at the feedlot peaked at 8:00 p.m. to 9:00 p.m., whereas during cold conditions, which obviously had significantly lower PM emissions, the highest PM_{10} emissions occurred in the 11:00 a.m. to 3:00 p.m. period. Friction velocity, temperature, sensible heat flux, and surface roughness were all found to influence PM_{10} emission. Conditions favorable to high PM emission fluxes had high friction velocity, temperature, and sensible heat flux but low surface roughness. In addition, PM_{10} emission flux was highly affected by the pen surface water content; pen surface water content of at least 20% (wet basis) would significantly reduce PM emission at feedlots.

The flux-gradient technique was applied successfully to estimate PM emission fluxes at the cattle feedlot; however, more research is needed to improve its implementation and flux estimates for feedlots. Individual contributions of different PM sources, such as pens, unpaved roads, and feed mills, to the overall feedlot PM emission flux still need to be assessed. Because

pens may differ in soil type, soil/manure depth, and number of cattle, effects of pen characteristics on PM emission flux also must be studied. In addition, uncertainties associated with stable conditions must be addressed to have more reliable emission estimates.

6.5 References

American Society for Testing Materials. 2002. D2216-98: Standard test method for laboratory determination of water (moisture) content of soil and rock by mass. In *Annual Book of American Society for Testing Materials Standards.* Philadelphia, PA: American Society for Testing Materials.

Baek, B-H., R. Todd, N.A. Cole, and J.A. Koziel. 2006. Ammonia and hydrogen sulphide flux and dry deposition velocity estimates using vertical gradient method at a commercial beef cattle feedlot. *Int. J. Global Environmental Issues* 6:189-203.

Baum, K.A., J.M. Ham, N.A. Brunsell, and P.I. Coyne. 2008. Surface boundary layer of cattle feedlots: implications for air emissions measurement. *Agric. For. Meteorol.* 148:1882-1893. doi:10.1016/j.agrformet.2008.06.017.

Bonifacio, H.F., R.G. Maghirang, B.W. Auvermann, E.B. Razote, J.P. Murphy, and J.P. Harner III. 2012. Particulate matter emission rates from beef cattle feedlots in Kansas – reverse dispersion modeling. *J. Air & Waste Manage. Assoc*. 62:350-361. doi:10.1080/10473289.2011.651557.

Bonifacio, H.F., R.G. Maghirang, E.B. Razote, B.W. Auvermann, J.P. Harner III, J.P. Murphy, L. Guo, J.M. Sweeten, and W.L. Hargrove. 2011. Particulate control efficiency of a water sprinkler system at a beef cattle feedlot in Kansas. Trans. ASABE 54:295-304.

Bonifacio, H.F., R.G. Maghirang, E.B. Razote, S.L. Trabue, and J.H. Prueger. 2013. Comparison of AERMOD and WindTrax dispersion models in determining PM_{10} emission rates from a beef cattle feedlot. *J. Air & Waste Manage. Assoc*. doi:10.1080/10962247.2013.768311.

Colton, T. 1974. *Statistics in Medicine*. New York, NY: Little Brown and Company.

CFR. 2005. Code of Federal Regulations, 40 CFR, Part 51: Revision to the guideline of air quality models: Adoption of a preferred general purpose (flat and complex terrain) dispersion model and other revisions.

CFR. 2011. Code of Federal Regulations, 40 CFR, Part 60: Call for Information: Information related to the development of emission-estimating methodologies for animal feeding operations.

Faulkner, W. B., J.J. Powell, J.M. Lange, B.W. Shaw, R.E. Lacey, and C.B. Parnell. 2007. Comparison of dispersion models for ammonia emissions from a ground-level area source. *Trans. ASABE* 50:2189-2197.

Flesch, T.K., J.H. Prueger, and J.L. Hatfield. 2002. Turbulent Schmidt number from a tracer experiment. *Agric. For. Meteorol.* 11:299-307.

Flesch, T.K., and J.D. Wilson. 2005. Estimating tracer emission with a backward Lagrangian Stochastic technique. *Micrometeorology in Agricultural Systems, Agronomy Monograph no. 47*. Wisconsin: American Society of Agronomy, Inc., Crop Science Society of America, Inc., Soil Science Society of America, Inc.

Flesch. T. K., J.D. Wilson, L.A. Harper, and B.P. Crenna. 2005. Estimating gas emissions from a farm with an inverse-dispersion technique. *Atmos. Envrion.* 39:4863-4874. doi:10.1016/j.atmosenv.2005.04.032.

Flesch. T. K., J.D. Wilson, L.A. Harper, B.P. Crenna, and R.R. Sharpe. 2004. Deducing ground-to-air emissions from observed trace gas concentrations: a field trial. *J. Appl. Meteorol.* 43:487-502.

Galvin, G., C. Henry, D. Parker, R. Ormerod, P. D'Abreton, and M. Rhoades. 2006. Efficacy of Lagrangian and a Gaussian model for back calculating emission rates from feedyard area sources. Paper presented at the Workshop on Agricultural Air Quality, Potomac, Maryland, June 5-8, 2006.

Gherman, C.D., and A.I. Mironiuc. 2012. Evaluation of serum adipokines in peripheral arterial occlusive disease. *Mediators of Inflammation* Volume 2012, Article ID 257808. doi:10.1155/2012/257808.

Guo, L., and R.G. Maghirang. 2012. Numerical simulation of airflow and particle collection by vegetative barriers. *Engineering Applications of Computational Fluid Mechanics* 6:110-122.

Ham, J.M., and K.A. Baum. 2007. Measuring ammonia fluxes from cattle feedlots using averaged relaxed eddy accumulation. Paper presented at International Symposium on Air Quality and Waste Management for Agriculture, Broomfield, Colorado, September 16-19, 2007. ASABE Publication No. 701P0907cd.

Harper, L.A., O.T. Denmead, J.R. Freney, and F.M. Byers. 1999. Direct measurements of methane emissions from grazing and feedlot cattle. *J. Anim. Sci.* 77:1392-1401.

Hogstrom, U. 1996. Review of some basic characteristics of the atmospheric surface layer. *Boundary-Layer Meteorol.* 78:215-246.

Hutchinson, G.L., A.R. Mosier, and C.E. Andre. 1982. Ammonia and ammine emissions from a large cattle feedlot. *J. Environ. Qual.* 11:288-293.

Hsieh, C.I., G. Katul, and T. Chi. 2000. An approximate analytical model for footprint estimation of scalar fluxes in thermally stratified atmospheric flows. *Advances in Water Resources* 23:765-772.

Lehman, S. J., C.L Schlett, F. Bamberg, H. Lee, P. Donnelly, L. Shturman, M.F. Kriegel, T.J. Brady, and U. Hoffman. 2009. Assessment of coronary plaque progression in coronary computed tomography angiography using a semiquantitative score. *JACC: Cardiovascular Imaging* 2:1262-1270. doi:10.1016/j.jcmg.2009.07.007.

Leytem, A.B., R.S. Dungan, D.L. Bjorneberg, and A.C. Koehn. 2011. Emission of ammonia, methane, carbon dioxide, and nitrous oxide from dairy cattle housing and manure management systems. *J. Environ. Qual.* 40:1383-1394. doi:10.2134/jeq2009.0515.

Massman, W.J., and X. Lee. 2002. Eddy covariance flux corrections and uncertainties in long-term studies of carbon and energy exchanges. Agric. Forest Meteorol. 113:121-144.

McGinn, S. M., T.K. Flesch, D. Chen, B. Crenna, O.T. Denmead, T. Naylor, and D. Rowell. 2010. Coarse particulate matter emissions from cattle feedlots in Australia. *J. Environ. Qual.* 39:791-798. doi:10.2134/jeq2009.0240.

Meyers, T.P., and D.D. Baldocchi. 2005. Current micrometeorological flux methodologies with applications in agriculture. *Micrometeorology in Agricultural Systems, Agronomy Monograph no. 47.* WI: American Society of Agronomy, Inc., Crop Science Society of America, Inc., Soil Science Society of America, Inc.

Myles, L., J. Kochendorfer, M.W. Heuer, and T.P. Meyers. 2011. Measurement of trace gas fluxes over an unfertilized agricultural field using the flux-gradient technique. *J. Environ. Qual.* 40:1359-1365. doi:10.2134/jeq2009.0386.

National Research Council. 2003. *Air Emissions from Animal Feeding Operations: Current Knowledge, Future Needs.* Washington, D.C.: National Academy of Sciences.

Prueger, J.H., T.J. Gish, L.L. McConnell, L.G. McKee, J.L. Hatfield, and W.P. Kustas. 2005. Solar radiation, relative humidity, and soil water effects on Metolachlor volatilization. *Environ. Sci. Technol.* 39:5219-5226.

Prueger, J.H., and W.P. Kustas. 2005. Aerodynamic methods for estimating turbulent fluxes. *Micrometeorology in Agricultural Systems, Agronomy Monograph no. 47.* WI: American Society of Agronomy, Inc., Crop Science Society of America, Inc., Soil Science Society of America, Inc.

Purdue Applied Meteorology Laboratory. 2009. *Quality Assurance Project Plan for the National Air Emissions Monitoring Study*, Revision No. 3. West Lafayette, IN: Purdue University.

Ryden, J.C., and J.E. McNeill. 1984. Application of the micrometeorological mass balance method to the determination of ammonia loss from a grazed sward. *J. Sci. Food Agric.* 35:1297-1310.

SAS Institute, Inc. 2004. *SAS system for Windows*, release 9.1.3. North Carolina: SAS Institute, Inc.

Schwertman, N.C., M.A. Owens, and R. Adnan. 2004. A simple more general Boxplot method for identifying outliers. *Comput. Statist. Data Anal.* 47:165-174. doi:10.1016/j.csda.2003.10.012.

Turner, D. B. 1994. *Workbook of Atmospheric Dispersion Estimates – An Introduction to Dispersion Modeling*.2nd ed. Florida: Lewis Publishers.

U.S. Department of Agriculture. 2012. *Farm Service Agency, Conservation Reserve Program – Soil Rental Rates.* Washington, D.C.: Office of Inspector General, U.S. Department of Agriculture.

Zhang, N., Z.C. Zheng, and R.G. Maghirang. 2008. Numerical simulation of smoke clearing with nanoparticles aggregates. *International Journal for Numerical Methods in Engineering* 74:601-618. doi:10.1002/nme.2186.

CHAPTER 7 - **Numerical Simulation of Transport of Particles Emitted from a Ground-level Area Source**

7.1 Introduction

Air emissions from animal feeding operations (AFOs), including commercial beef cattle feedlots, have been studied because of their potential impact on both health and environment. These studies are generally designed to establish accurate emission rates, and develop or evaluate emission estimation methodologies that can be applied when assessing the potential impact of these pollutants on the surrounding locality (CFR, 2011). The accuracy of these emission estimates depends greatly not only on the quality of concentration measurements but also on the reliability of methodologies.

Various techniques are available for simulating dispersion of particles in the atmosphere. They include box, Gaussian, Lagrangian, statistical, and computational fluid dynamics (CFD) models (Holmes and Morawska, 2006; Turner and Schulze, 2007). Currently, the preferred regulatory dispersion model in the U.S. is the American Meteorological Society/Environmental Protection Agency Regulatory Model or AERMOD (CFR, 2005). For AFOs, AERMOD has been used in assessing dispersion of odor (Koppolu et al., 2002; Sarr et al., 2010) and gaseous (Sarr et al., 2010) emissions downwind of swine facilities; and by reverse dispersion modeling technique, AERMOD has been applied in determining particulate emission rates from cattle feedlots (Bonifacio et al., 2012). Due to limitations of AERMOD inherent to all Gaussian models, the accuracy of its dispersion simulation, particularly for emissions from area sources like AFOs, is still for further investigation.

CFD models have been used in solving fluid flow problems in engineering applications. These models simulate fluid flow by solving Navier-Stokes equations. For turbulent flows, CFD models are categorized as direct numerical simulation (DNS), large eddy simulation (LES), Reynolds-averaged Navier-Stokes (RANS), and Reynolds stress models (Ferziger and Peric, 2002). With the increasing performance of latest computers, the potential of using CFD models in emission studies on AFOs and other open area sources is already being explored. Coupled with a partial differential equation for mass transport, CFD models, such as LES model and the RANS-based k-ε model, have been applied to simulate dispersion of odor from a livestock facility (Hong et al., 2011) and of particulates at an exposed land area (Seo et al., 2010). Even

with limited research data on the dispersion performance of CFD models, these models have been used in evaluation studies as alternatives to experimental research, which can be costly and measurement-intensive. For AFOs, several research evaluating emissions within and outside these facilities employed CFD models exactly for this reason. CFD models like k-ε and k-ω models, which are both RANS-based, have been used in determining efficiencies of vegetative barriers in reducing odor (Lin et al., 2007) and particulates (Guo and Maghirang, 2012) downwind of AFOs facilities. One study compared LES model and CALPUFF, a Gaussian dispersion model, in simulating odor dispersion at an AFO facility and found that higher concentrations were predicted by the CFD model (Li and Guo, 2006). The k-ε model had been used to assess the performance of a micrometeorological method in estimating CO_2 emission rates in an agricultural study (Magliulo et al., 2004).

In this study, two techniques were used to simulate dispersion of particles from a ground-level area source. The first technique was atmospheric dispersion modeling using AERMOD (ver. 09292, U.S. EPA; www.epa.gov). The second was numerical approach using CFD based on the k-ε turbulence model for velocity simulation and on the scalar convection-diffusion transport equation for particle transport simulation. CFD simulation was performed using OpenFOAM (ver. 2.1.1, ESI-OpenCFD; openfoam.com), an open-source CFD software package. In comparing AERMOD and CFD, a feedlot pen in a three-dimensional domain was used to evaluate dispersion downwind, crosswind, and vertical directions of a ground-level area source.

7.2 Materials and Methods

7.2.1 Computational Domain

A three-dimensional (3-D) computational domain (Figure 7-1) was created to simulate transport of particles emitted from the feedlot pen in downwind (x), crosswind (y), and vertical (z) directions. The feedlot pen was 1,000 m long and 200 m wide. The computational domain had dimensions of 2,000 m along downwind direction and 600 m along crosswind direction. The domain height was based on the boundary layer height (h_{abl}) computed at a wind speed of 1 m/sec (low wind). Numbers of cells were 120, 60, and 60 in x, y, and z directions, respectively, and the total cell number for simulation was 432,000. The cell size was constant in the x and y directions. For the z-direction, an expansion ratio, defined as the ratio of the last cell (i.e., top) to the first cell (i.e., bottom), was set at 20 to have finer grid near the ground.

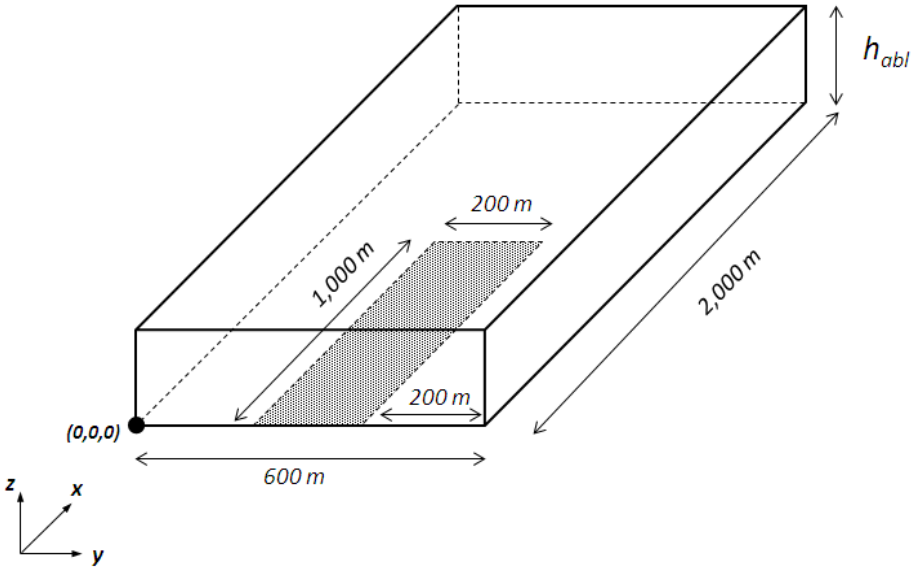

Figure 7-1. The computational domain for simulating particle dispersion for a ground-level area source (i.e., simulated feedlot pen).

7.2.2 AERMOD Dispersion

7.2.2.1 Dispersion Modeling

AERMOD is based on the general concentration equation for Gaussian models given by:

$$u_x \frac{\partial C}{\partial x} = D_y \frac{\partial^2 C}{\partial y^2} + D_z \frac{\partial^2 C}{\partial z^2} \qquad (7\text{-}1)$$

where C is concentration, u_x is wind speed in downwind (x-) direction, and D_y and D_z are diffusion coefficients in crosswind (y-) and vertical (z-) directions, respectively. The overall mass transport for Gaussian models is defined by the convective mass transport in downwind direction with constant u_x, and the diffusion mass transports in crosswind and vertical directions with constant D_y and D_z (Heinsohn and Kabel, 1999). The general analytical solution to eq 7-1 is commonly referred to as the Gaussian plume model (Heinsohn and Kabel, 1999). AERMOD is different from other Gaussian models in the way it simulates dispersion as it uses a well-characterized planetary boundary layer structure. Also, for unstable conditions, AERMOD

applies bi-Gaussian distribution to represent vertical concentration distribution rather than a Gaussian distribution (Cimorelli et al., 2004; Perry et al., 2005).

In AERMOD modeling, an emission flux of 20.0 µg/m^2-sec was assumed for the simulated feedlot pen based on the study described in Chapter 3. Concentrations were calculated for cells of the designed computational domain. The following conditions were specified:

1. The feedlot pen had a flat terrain with a constant emission flux for the 1-hr averaging period.
2. Effects of precipitation were not considered. Only the dry depletion of particles was included as the main removal mechanism. Particle depletion due to gravitational effects was considered by assuming a 13-µm aerodynamic particle size, based on the mean geometric diameter derived for a commercial cattle feedlot (Gonzales et al., 2011)

7.2.2.2 Meteorological Parameters

Previous CFD studies on ground-level area sources investigated the effects of atmospheric stability and wind speed on dispersion (Li and Guo, 2006; Hong et al., 2011). These meteorological parameters served as basis of comparison in this study. Using the classification presented by Seinfeld and Pandis (2006), five atmospheric stability classes were considered. These stability classes were as follows, with their respective Monin-Obukhov length (L) settings parenthesized: very stable (L = 50 m), stable (L = 500 m), neutral (L = 500,000 m), unstable (L = -500 m), and very unstable (L = -50 m) conditions. While neutral conditions could have high negative L values ($L \leq$ -500, 000 m), these were not allowed in AERMOD, and therefore, not considered. Downwind wind speeds of 1 and 5 m/sec at the height of 2.5 m were applied to represent low and high wind conditions, respectively. In total, 10 conditions were evaluated by each transport simulation.

Other meteorological parameters were needed to run AERMOD. Temperature, surface roughness (z_o), and wind direction were fixed to remove their influence on the simulation: temperature was set at 15 ^{o}C, the average temperature measured at a Kansas cattle feedlot (Chapters 4 and 6); z_o was set at 5 cm, the typical roughness value for cattle feedlots (Chapter 6); and wind direction was constant along downwind direction (x-axis), starting from the edge with the origin. Other meteorological parameters, such as friction velocity (u_*), sensible heat, and mixing heights, were derived using formulations presented by Cimorelli et al. (2004).

7.2.3 CFD Simulation

CFD simulation involved three major steps: (1) mesh generation based on the designed computational domain (Figure 7-1); (2) velocity simulation with the standard k-ε model; and (3) particle transport simulation using a scalar transport equation.

7.2.3.1 Velocity Simulation

7.2.3.1.1 Governing Equations for Velocity Transport

Air flow was assumed to be incompressible (i.e., constant air density), isothermal, and steady state. Incorporating turbulence into Navier-Stokes equation by Reynolds decomposition leads to RANS (i.e., Reynolds-average Navier-Stokes) equation given by:

$$\rho \frac{\partial}{\partial x_i}\left(\overline{u_i}\ \overline{u_j}\right) = -\frac{\partial \overline{P}}{\partial x_j} + \frac{\partial}{\partial x_i}\left(\overline{\tau_{ij}} - \rho\ \overline{u_i' u_j'}\right) \tag{7-2}$$

where i is subscript for all three directions (x, y, and z), j is subscript for the direction evaluated (x, y, or z), ρ is air density, u is velocity component in either i- or j- direction, P is pressure force in j-direction, τ_{ij} is viscous stress component, g_j is gravitational force in j-direction, apostrophe means fluctuations, and overbar means time-averaged (Glasgow, 2010). The viscous stress component, τ_{ij}, is given by:

$$\overline{\tau_{ij}} = \mu\left(\frac{\partial \overline{u_j}}{\partial x_i} + \frac{\partial \overline{u_i}}{\partial x_j}\right) \tag{7-3}$$

where μ is fluid viscosity (Feistauer et al. 2003; Ferziger and Peric, 2002). With ρ constant, the corresponding continuity equation for RANS equation is:

$$\frac{\partial \overline{u_i}}{\partial x_i} = 0 \tag{7-4}$$

RANS equations are solved using turbulence models. At steady state, the transport equations for the turbulent kinetic energy (k) and turbulent dissipation rate (ε) are given by:

$$\frac{\partial}{\partial x_i}\left(\overline{u_i}\ \ k\ \right) = \frac{1}{\rho}\frac{\partial}{\partial x_i}\left[\left(\mu\ + \frac{\mu_t}{\sigma_k}\right)\frac{\partial k}{\partial x_i}\right] + \frac{\mu_t}{\rho}\left(\frac{\partial \overline{u}_j}{\partial x_i} + \frac{\partial \overline{u}_i}{\partial x_j}\right)\frac{\partial \overline{u}_i}{\partial x_j} - \varepsilon \tag{7-5}$$

$$\frac{\partial}{\partial x_i}\left(\overline{u_i}\ \varepsilon\right)=\frac{1}{\rho}\frac{\partial}{\partial x_i}\left[\left(\mu+\frac{\mu_t}{\sigma_\varepsilon}\right)\frac{\partial \varepsilon}{\partial x_i}\right]+\frac{C_1\mu_t}{\rho}\frac{\varepsilon}{k}\left(\frac{\partial \overline{u}_j}{\partial x_i}+\frac{\partial \overline{u}_i}{\partial x_j}\right)\frac{\partial \overline{u}_i}{\partial x_j}-\frac{C_2\varepsilon^2}{k} \quad (7\text{-}6)$$

where μ_t is turbulent viscosity, σ_k and σ_ε are turbulent Prandtl numbers for k and ε, respectively, and C_1 and C_2 are turbulent model constants with values of 1.44 and 1.92, respectively (Launder and Spalding, 1974). Turbulent viscosity is computed from k and ε using the expression:

$$\mu_t=\frac{\rho\ C_\mu k^2}{\varepsilon} \quad (7\text{-}7)$$

where C_μ has a value of 0.09.

The turbulence model applied in this study was the standard k-ε model, and this was implemented using OpenFOAM standard solver '*simpleFoam.*' Similar to other OpenFOAM steady-state solvers, the semi-implicit method for pressure-linked equations (SIMPLE) algorithm is applied in '*simpleFoam*' in solving velocity and pressure iteratively (OpenFOAM, 2011). For convergence, an iterative solution was considered sufficiently accurate when: (a) residuals were less than 0.00001; and/or (b) ratios of latest to previous residuals were below 0.1.

7.2.3.1.2 Boundary Conditions

Settings for u, k, and ε must be specified in the k-ε turbulence model. Effects of atmospheric stability were introduced into CFD simulation through these three parameters as they are all functions of L. For the computational domain (Figure 7-1), conditions were set at six boundaries, namely inlet (where the origin is located) and outlet along x-direction, upper and lower walls along z-direction, and the two side walls along y-direction. Within the domain, values of these parameters were initially set to zero. The inlet profile for u was composed of the downwind component (u_x) only; the crosswind (u_y) and vertical (u_z) components were assumed zero. Based on AERMOD formulations, the inlet profile for u_x was computed using:

$$u_x=\frac{u_*}{k_v}\left[\ln\left(\frac{z}{z_o}\right)-\psi_m\left\{\frac{z}{L}\right\}+\psi_m\left\{\frac{z_o}{L}\right\}\right] \quad (7\text{-}8)$$

where k_v is von Karman constant (0.4), z is measurement height at which u_x is computed, and ψ's are stability terms (Cimorelli et al., 2004). Values for ψ's were also computed using formulations

in AERMOD. For 1 and 5 m/sec wind speed settings, u_*'s derived and used in vertical profiling of u_x are summarized in Table 7-1.

Table 7-1. Friction velocities (u_*) and atmospheric boundary layer heights (h_{abl}) computed using AERMOD formulations

Atmospheric stability classification	1 m/sec		5 m/sec	
	u_* (m/sec)	h_{abl} (m)	u_* (m/sec)	h_{abl} (m)
Very stable	0.096	67	0.482	770
Stable	0.102	73	0.508	833
Neutral	0.102	73	0.511	841
Unstable	0.103	74	0.514	847
Very unstable	0.107	78	0.533	895

With u_*, the inlet vertical profile for k was set with one of these expressions:

$$k = 5.97\ u_*^2 T_{wn}^{1.5} \tag{7-9a}$$

$$k = 5.97\ u_*^2 T_{wn}^2 + w_*^2 \left(0.3 + 0.2 T_{wc}^2\right) \tag{7-9b}$$

$$k = 5.97\ u_*^2 T_{wn}^2 \tag{7-9c}$$

and T_{wn} and T_{wc} were:

$$T_{wn} = 1 - a_s \frac{z - z_o}{h_{abl} - z_o} \tag{7-10a}$$

$$T_{wc} = 2.1 \left(\frac{z - z_o}{h_{abl} - z_o} \right)^{1/3} T_{wn} \tag{7-10b}$$

where a_s is a constant whose value depends on stability condition and/or measurement height z, w_* is mixing layer velocity scale, and h_{abl} is atmospheric boundary layer height (Lin et al., 2007). Equations 7-9a, 7-9b, and 7-9c are equations for stable, unstable, and neutral conditions, respectively. Values for w_* were calculated using formulations presented in Lin et al. (2007), whereas values for h_{abl} were the AERMOD-derived mixing heights (Table 7-1).

Inlet vertical profile for ε was derived from k (Hong et al., 2011):

$$\varepsilon = \frac{C_\mu^{0.75} k^{1.5}}{100\left(\frac{z}{30}\right)^{0.5}} \tag{7-11}$$

Conditions for u, k, and ε at the other five boundaries were the following: fully-developed flow at the outlet (i.e., zero velocity gradient); no-slip condition at the lower wall; and symmetry condition at upper and side walls. OpenFOAM boundary condition near-wall functions, declared by '*kqRWallFunction*' and '*epsilonWallFunction*' for k and ε, respectively, were applied in the simulation.

Change in pressure, $\partial P/\partial x_j$, was needed in solving velocity transport (eq 7-2), and therefore, boundary conditions and initial settings for pressure, P, were specified. Inlet and outlet boundary settings for P were dependent on settings for u: as inlet boundary for u was fixed, for P it was zero gradient; and in contrast, P was fixed (i.e., at 0 atm as eq 7-2 is more concerned with $\partial P/\partial x_j$ than the absolute value for P) at the outlet as u had an zero gradient outlet setting. A symmetry condition was applied at the upper and side walls, whereas a zero gradient condition was implemented at the lower wall. P setting inside the domain was initially given a uniform value similar to the outlet boundary setting (i.e., at 0 atm).

7.2.3.2 Concentration Simulation

7.2.3.2.1 Governing Equation for Particle Transport

The transport of particles was modeled with Eulerian-Eulerian approach. Treating the particle concentration as passive scalar, the particle flow was solved using the convection-diffusion equation. The scalar transport solver in OpenFOAM was modified to apply steady-state assumption and include turbulence effects on diffusion. The resulting particle transport equation used in solving concentration, C, is given by:

$$\frac{\partial}{\partial x_i}\left(u_i C\right) - \frac{\partial^2}{\partial x_i^2}\left(\Gamma_D C\right) = 0 \tag{7-12}$$

where Γ_D is diffusion coefficient of particles. The diffusion coefficient Γ_D combined both laminar (Γ_L) and turbulent (Γ_T) diffusion components. Following the procedure by Guo and Maghirang (2012), the corresponding Γ_L for the 13 µm-aerodynamic size particle was 2.48×10^{-12} m^2/sec, whereas Γ_T was computed as the quotient of μ_t and turbulent Schmidt number (S_c). S_c in the modeling was set at 0.63. Values for μ_t (eq 7-7) were generated by the OpenFOAM solver '*simpleFoam*'. Gravitational effects were also incorporated by adjusting the turbulence model-derived u_z by 5.23×10^{-3} m/sec, the particle settling velocity for the assumed particle size (13 µm).

With only one equation to be solved for particle transport, stricter convergence criteria was applied without significantly increasing computation time. The criteria were as follows: (a) residuals should be less than 0.000001; and (b) ratio of latest to previous residuals should be below 0.01.

7.2.3.2.2 Boundary Conditions

Previous CFD studies on ground-level area sources used constant concentration at the source boundary (Seo et al., 2010; Wong and Liu, 2011). In this study, the concentration boundary settings for the feedlot pen were based on AERMOD predictions. With an emission flux of 20.0 µg/m^2-sec, AERMOD was run to calculate ground-level particle concentrations within the feedlot pen boundary. The ground-level height was arbitrarily set at 10 cm to have a value higher than z_o (5 cm). Ground-level concentration ranges for different atmospheric stability classes are summarized in Table 7-2, with the minimum value at the upwind edge of the feedlot pen (i.e., origin) and the maximum value at the downwind edge. Expectedly, higher ground-level concentrations were calculated for conditions with wind speed of 1 m/sec. Additionally, for a given wind speed, stable conditions ($L > 0$) resulted in higher concentrations, whereas very unstable conditions ($L < 0$) resulted in lower concentrations.

Table 7-2. Ranges of ground-level particle concentrations ($\mu g/m^3$) based on AERMOD simulation (emission flux = 20.0 $\mu g/m^2$-sec)

Atmospheric stability classification	1 m/sec	5 m/sec
Very stable	371 - 1,573	74 - 280
Stable	352 - 1,227	71 - 224
Neutral	352 - 1,172	70 - 214
Unstable	299 - 885	60 - 172
Very unstable	269 - 780	54 - 147

Other boundary conditions for concentration simulation were as follows: zero concentration at the inlet (i.e., zero background concentration); zero concentration gradient at the non-source (non-feedlot pen) ground areas and outlet (i.e., fully-developed flow); and symmetry condition at upper and side walls.

All input values applied in CFD simulation are summarized in Table 7-3. Convergence was achieved with 3,000 to 7,500 iteration steps for velocity using the standard k-ε model, and with 99 to 113 iterations for the concentration (eq 7-12).

Table 7-3. Summary of input values for CFD simulation

Parameter	Symbol	Value
Air density (kg/m^3)	ρ	1.225
Air dynamic viscosity (kg/m-sec)	μ	1.79×10^{-5}
Kinematic viscosity (m^2/sec)	υ	1.46×10^{-5}
Turbulent Prandtl number of k	σ_k	1
Turbulent Prandtl number of ε	σ_ε	1.3
Turbulent model constant	C_1	1.44
Turbulent model constant	C_2	1.92
Turbulent model constant	C_μ	0.09
Settling velocity for particles with aerodynamic diameter of 13 µm (m/sec)		5.23×10^{-3}
Laminar diffusion coefficient for particles with aerodynamic diameter of 13 µm (m^2/sec)	Γ_L	2.48×10^{-12}
Schmidt number	S_c	0.63

7.2.4 Data Analysis

Simulation results for velocity and particle concentration were presented. Vertical profiles of u_x were plotted, and for CFD, values of u_y and u_z were summarized. Effects of atmospheric stability and wind speed on particle dispersion were examined for both AERMOD and CFD. For vertical dispersion, vertical gradients of plume centerline particle concentrations (i.e., concentrations at the 300-m crosswind distance from the origin, at the center of the feedlot pen) within the 20-m height were calculated for two locations: at the feedlot pen downwind edge; and at the 100-m downwind distance (i.e., recommended minimum modeling length for Gaussian-based models) from the pen. Also, vertical contour plots of plume centerline particle concentrations within the 20-m height were obtained. At the 100-m downwind distance, plume centerline concentrations at the 2.5-m height were checked to assess downwind particle dispersion. And with the same downwind distance, 2.5 m height-particle concentrations 100-m crosswind of the plume centerline were used as measures for crosswind particle dispersion.

Plotting of vertical gradients and vertical contours involved use of Excel (Microsoft Corporation, Redmond, WA) and Scilab (ver. 5.3, Scilab Enterprises; www.scilab.org), respectively.

In addition, the fractional bias method was employed to compare calculated concentrations from AERMOD and CFD (Li and Guo, 2006; U.S. EPA, 1992). The fractional bias (*FB*) was defined in this study as:

$$FB = 2\left(\frac{C_{CFD} - C_A}{C_{CFD} + C_A}\right) \tag{7-13}$$

where C_{CFD} is concentration calculated using CFD and C_A is concentration calculated using AERMOD. As described (U.S. EPA, 1992), *FB* values are bounded between 2 and -2, and values close to zero imply negligible bias between the two techniques. *FB* values falling within (-0.67, 0.67) range were considered to indicate reasonably good agreement between AERMOD and CFD. With CFD as the reference model, an $FB \geq +0.67$ indicates underprediction by AERMOD by a factor of 2 or more, whereas an $FB \leq -0.67$ indicates overprediction by the same factor value.

7.3 Results and Discussion

7.3.1 AERMOD

7.3.1.1 Velocity

In AERMOD, wind velocity has a logarithmic vertical profile that is assumed to be constant in both downwind and crosswind directions. Also, AERMOD only considers the downwind component of wind velocity (eq 7-1). With u_x normalized by dividing by u_*, vertical profiles for u_x for 1 and 5 m/sec wind speeds (i.e., 2.5 m height) were similar (Figure 7-2). Atmospheric stability classes in the order of highest to lowest wind speeds were: very stable, stable, neutral, unstable, and very unstable. Based on typical conditions, neutral atmospheric stability has high wind velocities whereas stable/very stable and unstable/very unstable conditions have low wind velocities (Turner, 1994).

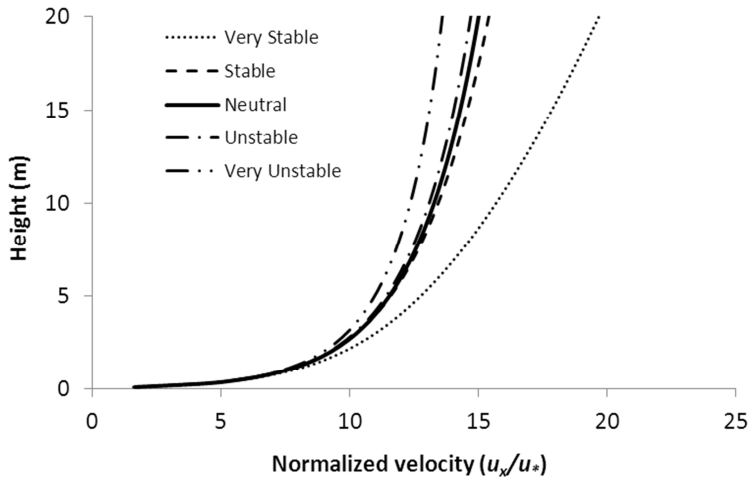

Figure 7-2. Vertical profiles of normalized u_x (i.e., u_x/u_*) within the 20-m height for both 1 and 5 m/sec wind speeds as derived using AERMOD formulations.

7.3.1.2 Concentration

Concentration profiles from AERMOD were generally the same for the five atmospheric stability conditions. To illustrate, shown in Figure 7-3 are contour plots of particle concentrations at the crosswind distance of 300 m from the origin, herein referred to as the plume centerline, for neutral condition at both 1 and 5 m/sec wind speeds. Particle concentrations directly above the feedlot pen (i.e., distances of 0 to 1,000 m) decreased with height. The vertical concentration gradient (i.e., change in particle concentration with height) was computed to demonstrate influence of atmospheric stability on vertical dispersion/mixing. At the downwind edge of the feedlot pen (i.e., distance of 992 m from the origin, downwindmost cell within the feedlot pen domain), vertical concentration gradients for all atmospheric stability-wind speed combinations are summarized in Table 7-4. Lower concentration gradients for unstable and very unstable conditions indicate stronger vertical dispersion of particles (i.e., more particles dispersed to higher heights, thus smaller concentration difference between heights), whereas relatively higher concentration gradients for the other three atmospheric stability conditions indicated the opposite. Comparing 1 and 5 m/sec wind speed settings, smaller vertical concentration gradients were obtained for the higher wind speed.

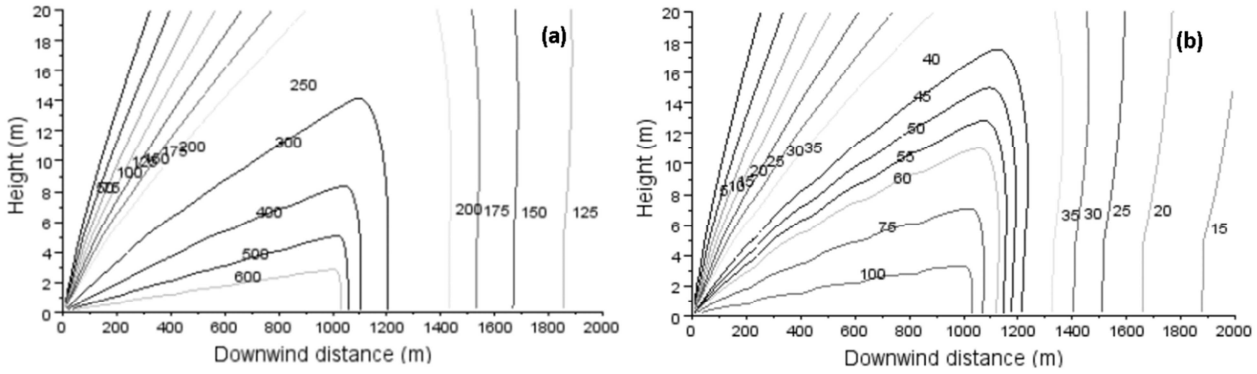

Figure 7-3. Vertical contour plots of AERMOD-based plume centerline particle concentrations (µg/m^3) within the 20-m height at a crosswind distance of 300 m for (a) 1 and (b) 5 m/sec wind speeds.

Table 7-4. Vertical concentration gradients (µg/m^3-m)[a] of AERMOD-based plume centerline particle concentrations at the feedlot pen downwind edge for (a) 1 and (b) 5 m/sec wind speeds

Atmospheric stability classification	1 m/sec	5 m/sec
Very Stable	55	11
Stable	35	8
Neutral	32	7
Unstable	23	6
Very Unstable	20	5

[a] Concentration gradient computed within the 20-m height from the ground.

Surprisingly, particle concentrations downwind of the feedlot pen (i.e., distances of 1,000 to 2,000 m) were simulated by AERMOD such that the vertical concentration gradient for the first few meters from the ground (z = 0 m) were almost negligible. As observed for both wind speeds, AERMOD-calculated concentrations at any given distance downwind of the source remained relatively constant from the ground up to a certain height (Figure 7-3). At the 100-m distance downwind of the feedlot pen, as an example, vertical concentration gradient up to a height of 5 m ranged only from 0.5 to 5.2 µg/m^3-m and 0.2 to 0.5 µg/m^3-m for 1 and 5 m/sec

wind speeds, respectively. In addition, the height at which the particle concentration remained relatively constant increased with downwind distance.

Effects of atmospheric stability on downwind particle dispersion were examined by comparing concentrations at a specific location downwind of the feedlot pen. With 2.5 m as the reference height and 100 m, the minimum modeling length recommended for Gaussian-based models, as the reference downwind distance, plume centerline particle concentrations for the 1 m/sec wind speed for very stable, stable, neutral, unstable, and very unstable conditions were 737, 468, 408, 283, and 247 $\mu g/m^3$, respectively. For the 5 m/sec wind speed, at which lower concentrations were expected due to faster horizontal dispersion, particle concentrations were 117, 76, 67, 52, and 39 $\mu g/m^3$, respectively. Based on these concentrations, the strongest downwind dispersions, and equivalently the longest fetches, were modeled for very stable, stable, and neutral conditions, whereas the weakest downwind dispersions (and the shortest fetches) were for very unstable and unstable conditions.

At 100-m downwind distance from the feedlot pen and 100-m crosswind of the plume centerline, 2.5 m height-particle concentrations were checked to verify effects of atmospheric stability on crosswind dispersion. Particle concentrations for the 1 m/sec wind speed for very stable, stable, neutral, unstable, and very unstable conditions were 369, 234, 204, 141, and 124 $\mu g/m^3$, respectively whereas for the 5 m/sec wind speed, concentrations were 61, 40, 35, 27, and 20 $\mu g/m^3$, respectively. Similar to downwind dispersion, crosswind dispersion was highest for very stable, stable, and neutral conditions. Comparison between 1 and 5 m/sec wind speed showed that increasing the wind speed narrowed the spread of the dispersion/plume.

7.3.2 CFD

7.3.2.1 Velocity

In CFD modeling, velocity conditions upwind of the feedlot pen (i.e., 0 m from the origin) were based on AERMOD formulations (eq 7-8, Figure 7-2), with crosswind and vertical components of the velocity both assumed to be zero. Simulation with the standard k-ε model resulted in changes in the velocity profile such that the downwind component (u_x) of the velocity now varied along the downwind distance. Figure 7-4 shows the vertical profiles for normalized u_x (i.e., u_x/u_*) for 1 and 5 m/sec wind speeds at the feedlot pen downwind edge (i.e., 1,000 m from the origin). Trends of u_x at upwind and downwind edges of the feedlot pen were similar

such that its vertical profile was logarithmic, the highest velocity was obtained for very stable condition, and the lowest velocity for very unstable condition. Calculated differences in u_x between upwind and downwind edges of the feedlot pen were observed to be largest at lowest heights (e.g., 193% at 0.18 m for very stable condition), possibly due to very small absolute wind speeds near the ground. Excluding the first 1 m from the ground, percentage differences in u_x between upwind and downwind feedlot pen edges are summarized in Table 7-5. In general, largest percentage differences were obtained for the lower wind speed. Very stable condition had the largest positive, or smallest negative, difference in u_x (35% and 1% for 1 and 5 m/sec wind speed, respectively), whereas very unstable condition had the smallest positive, or largest negative, difference (1% and -1% for 1 and 5 m/sec wind speed, respectively).

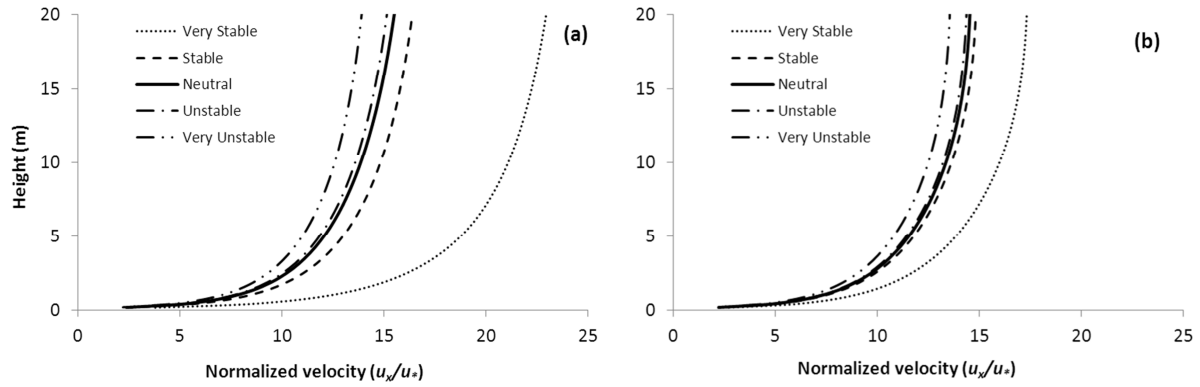

Figure 7-4. Vertical profiles of normalized u_x (i.e., u_x/u_*) within the 20-m height for (a) 1 and (b) 5 m/sec wind speed settings at the feedlot pen downwind edge as derived by CFD.

Table 7-5. Percentage differences in u_x between upwind and downwind edges of the feedlot pen as simulated by CFD[a]

Atmospheric stability classification	1 m/sec	5 m/sec
Very Stable	35% (30 to 51%)	1% (-1 to 10%)
Stable	10% (9.9 to 10%)	-0.2% (-1 to 0.1%)
Neutral	4% (2 to 5%)	-0.4% (-3 to 0.4%)
Unstable	3% (0.6 to 4%)	-0.5% (-4 to 0.6%)
Very Unstable	1% (-0.4 to 3%)	-1% (-9 to 2%)

[a] Values presented are medians for the first 20-m height; values in the parentheses are ranges.

Simulation with the standard k-ε model also led to crosswind (u_y) and vertical (u_z) components of velocity having non-zero values. Table 7-6 lists the ranges of u_y and u_z for both 1 and 5 m/sec wind speed settings at the downwind edge of the feedlot pen. Velocity values for each component were very small compared to u_x: u_y and u_z were lower by orders of magnitude of at least 8 and 3, respectively. Unlike u_x that had logarithmic vertical profile, no general trend was observed for both u_y and u_z as their respective profiles changed along the downwind distance.

Table 7-6. CFD-based u_y and u_z at the feedlot pen downwind edge[a]

Atmospheric stability classification	u_y		u_z	
	1 m/sec	5 m/sec	1 m/sec	5 m/sec
Very Stable	-1.1×10^{-8} to -1.9×10^{-9}	3.6×10^{-9} to 1.7×10^{-8}	1.0×10^{-5} to 8.8×10^{-4}	2.0×10^{-5} to 2.6×10^{-3}
Stable	-1.7×10^{-10} to 6×10^{-10}	9.2×10^{-10} to 5.9×10^{-8}	1.0×10^{-5} to 8.5×10^{-4}	2.0×10^{-5} to 2.4×10^{-3}
Neutral	-4×10^{-9} to 3.8×10^{-9}	1.8×10^{-9} to 4.4×10^{-8}	1.0×10^{-5} to 8.3×10^{-4}	2.0×10^{-5} to 2.4×10^{-3}
Unstable	-8.5×10^{-9} to -2.4×10^{-9}	-1.8×10^{-8} to 4.6×10^{-9}	1.0×10^{-5} to 9.3×10^{-4}	2.0×10^{-5} to 2.6×10^{-3}
Very Unstable	-1.9×10^{-9} to -5×10^{-10}	4.8×10^{-9} to 2×10^{-8}	1.0×10^{-5} to 1.1×10^{-3}	2.0×10^{-5} to 2.8×10^{-3}

[a] For u_z, minimum values for the second lowest cell were presented as values for the lowest cell (height of 0.18 m) were zero; ranges were based on the first 20-m height.

7.3.2.2 Concentration

Figure 7-5 shows the contour plots of plume centerline concentrations from CFD simulation for neutral condition and at the two wind speed settings. Similar to AERMOD results, particle concentrations above the feedlot pen varied with height. Vertical concentration gradients (i.e., at distance of 992 m from origin) were obtained and summarized in Table 7-7. Findings were similar to those for AERMOD: (1) very unstable and unstable conditions had smaller vertical concentration gradients compared to the other three atmospheric stability classes suggesting stronger vertical dispersion; and (2) the 5 m/sec wind speed setting, which was the highest setting evaluated in this study, had the smallest concentration gradients. Vertical concentration gradients obtained with CFD were lower than those calculated with AERMOD by 18 to 44% for the 1 m/sec wind speed and 29 to 40% for the 5 m/sec wind speed.

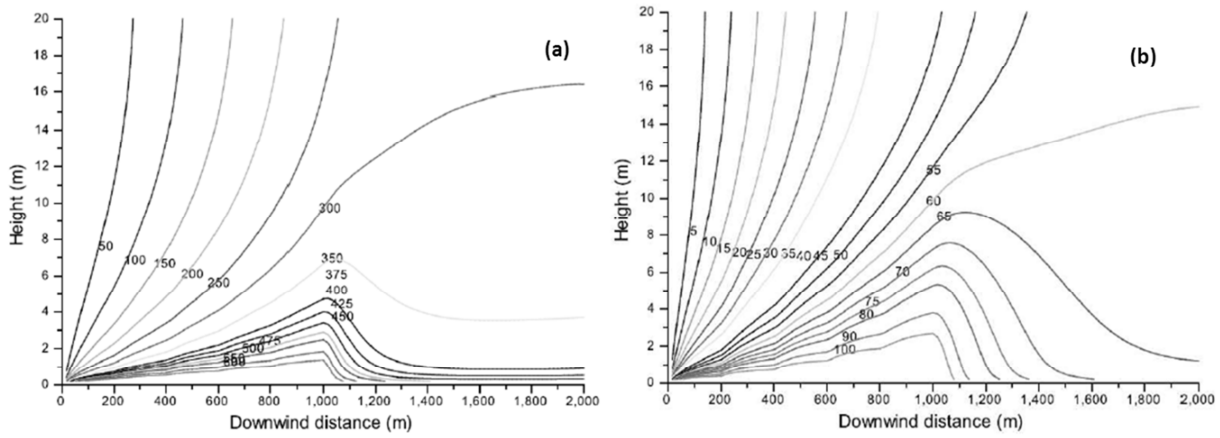

Figure 7-5. Vertical contour plots of CFD-based plume centerline particle concentrations ($\mu g/m^3$) within the 20-m height at a crosswind distance of 300 m for (a) 1 and (b) 5 m/sec wind speeds.

Table 7-7. Vertical concentration gradients ($\mu g/m^3$-m)[a] of CFD-based plume centerline particle concentrations at the feedlot pen downwind edge for (a) 1 and (b) 5 m/sec wind speeds

Atmospheric stability classification	1 m/sec	5 m/sec
Very Stable	31	7
Stable	25	5
Neutral	25	5
Unstable	19	4
Very Unstable	16	3

[a] Concentration gradient computed within the 20-m height from the ground.

Compared with AERMOD, CFD produced a different and more detailed vertical particle concentration profile downwind of the feedlot pen. CFD-derived downwind particle concentrations changed with height (Figure 7-5), unlike with AERMOD in which concentrations remained relatively constant for the first few meters from the ground (Figure 7-3). Notably, shapes of contour lines for downwind particle concentrations also differed between the two wind speed settings: for the 1 m/sec wind speed, concentration contour lines downwind of the source extended over distances considerably longer than those for the 5 m/sec wind speed. For both

wind speed settings, particle concentration downwind of the feedlot pen decreased with height. At the distance of 100 m from the feedlot pen, vertical concentration gradient for the first 5 m from the ground ranged from 25 to 36 µg/m^3-m and 2 to 5 µg/m^3-m for 1 and 5 m/sec wind speed settings, respectively, and were much larger than their AERMOD counterparts (0.5 to 5.2 µg/m^3-m and 0.2 to 0.5 µg/m^3-m, respectively). Similar to findings within the pen, very unstable and unstable conditions had the smaller vertical concentration gradients (i.e., stronger vertical dispersion), and the 5 m/sec wind speed had the smallest concentration gradients.

Using the 2.5-m height and 100-m downwind distance to examine influence of atmospheric stability on downwind dispersion in CFD, plume centerline particle concentrations for very stable, stable, neutral, unstable and very unstable conditions were 576, 448, 428, 325 and 295 µg/m^3, respectively, for the 1 m/sec wind speed and were 110, 90, 86, 69 and 61 µg/m^3, respectively, for the 5 m/sec wind speed. Like in AERMOD, the strongest downwind dispersion was modeled for very stable, stable and neutral conditions, and the weakest for very unstable and unstable conditions. Similar findings were also observed in previous studies that employed CFD modeling for simulating downwind dispersion (Hong et al., 2011; Li and Guo, 2006). The limited vertical mixing, particularly for very stable and stable conditions, leads to dispersion of air emissions further downwind of the source whereas the stronger vertical mixing during very unstable and unstable conditions results to dispersion of air emissions vertically rather than horizontally.

Effects of atmospheric stability on crosswind dispersion were also verified. The 2.5 m height-concentrations at the downwind distance of 100 m from the feedlot pen and crosswind distance of 100 m from the plume centerline at very stable, stable, neutral, unstable and very unstable conditions were as follows: for the 1 m/sec wind speed, 364, 293, 282, 218 and 195 µg/m^3, respectively; and for the 5 m/sec wind speed, 71, 59, 57, 45 and 39 µg/m^3, respectively. Similar in AERMOD, crosswind dispersion was much farther from the centerline for very stable, stable and neutral conditions, and at lower wind speed setting.

7.3.3 Fractional Bias (FB)

Applying the 100-m downwind distance as the reference location, *FB* was calculated for comparisons of downwind, crosswind and vertical dispersions between the two approaches. Using 2.5-m height plume centerline particle concentrations to compare downwind dispersion simulation performance, *FB* values between AERMOD and CFD ranged from -0.25 to 0.18 for

the 1 m/sec wind speed and -0.06 to 0.45 for the 5 m/sec wind speed for the five atmospheric stability classes evaluated. Based on *FB* values, AERMOD tended to underpredict downwind particle concentrations (*FB* > 0) as the atmospheric condition became more unstable. At the 1 m/sec wind speed, the bias between CFD and AERMOD was smallest for stable (*FB* = -0.04) and neutral (*FB* = 0.04) conditions and largest for very stable (*FB* = -0.25) and unstable (*FB* = 0.18) conditions; at the 5 m/sec wind speed, the smallest and largest biases were determined for very unstable (*FB* = -0.06) and very unstable (*FB* = 0.45) conditions, respectively. In addition, comparison of *FB* between 1 and 5 m/sec wind speeds indicated that the bias between CFD and AERMOD would be larger at higher wind speeds.

At a distance of 100 m crosswind of the plume centerline, assessment of crosswind dispersion was also performed using 2.5-m height concentrations. Likewise, AERMOD calculated much lower particle concentrations as the condition became more unstable. For the 1 m/sec wind speed, excluding very stable condition (*FB* = -0.02), *FB* ranged from 0.22 (stable) to 0.45 (very unstable) indicating that AERMOD underpredicted concentrations even for downwind locations away from the plume. For the 5 m/sec wind speed, *FB* was smallest for very stable condition (*FB* = 0.16) and highest for very unstable condition (*FB* = 0.65). Similarly, *FB* values for the 5 m/sec wind speed were larger than those for the 1 m/sec wind speed.

Up to 20-m height, vertical profiles of *FB* at the 100-m downwind distance from the pen were plotted using plume centerline particle concentrations (Figure 7-6). *FB* values for the 1 m/sec wind speed were within +/- 0.67 criterion lines and lie near the zero line (Figure 7-6a), indicating good agreement between AERMOD and CFD. *FB* values for the 5 m/sec wind speed also were within +/- 0.67 criterion lines (Figure 7-6b), except that the values were more on the positive side (i.e., underprediction by AERMOD). Further evaluation revealed that the bias tended to become more highly positive (i.e., higher CFD concentrations) at farther downwind distances.

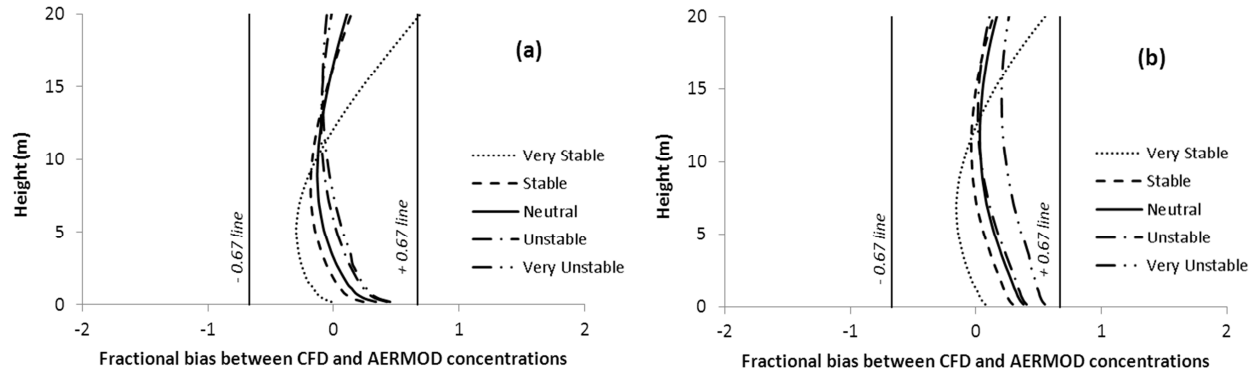

Figure 7-6. Fractional bias between AERMOD and CFD for (a) 1 and (b) 5 m/sec wind speeds using plume centerline particle concentrations at the 100-m downwind distance from the feedlot pen.

Although not verified in this study, differences in AERMOD and CFD results may be attributed to their respective approach in simulating dispersion. As a mass dispersion technique, AERMOD models mass transport based on a domain (i.e., boundary layer) characterized by meteorological parameter inputs (e.g., u_x, u_*, L), whereas CFD simulates mass transport based on a domain with simulated fluid flow parameters (e.g., in terms of u, k, ε). Mass transport for AERMOD is also simplified as it is steady-state and accounts only for one mass transport type (i.e., convection in x- direction, diffusion in y- and z-directions) in each direction but for CFD, such as the standard k-ε model, mass transport can consider convection and diffusion in all directions. AERMOD uses an algebraic equation to directly calculate mass concentration whereas CFD solves a partial differential equation/s for mass transport numerically before obtaining concentration values. In characterization of the simulation domain, partial differential equations for the three velocity components, turbulent kinetic energy and turbulent dissipation rate must be solved first numerically in CFD technique (i.e., k-ε model), and on the other hand, parameters required in AERMOD are just directly derived using algebraic formulations.

7.4 Conclusions

This study compared CFD and AERMOD in simulating dispersion of particles emitted downwind from a ground-level area source. CFD modeling involved velocity and particle dispersion simulations using the standard k-ε model and a convection-diffusion transport equation, respectively. Simulation conditions evaluated were based on five atmospheric stability

classes, classified according to Monin-Obukhov length, and two wind speeds. Predicated results indicated the following:

- AERMOD and CFD had similarities in simulating particle dispersion from the ground-level area source. As a function of atmospheric stability, vertical gradients of particle concentrations at the downwind edge of the source were smallest for very unstable and unstable conditions indicating stronger vertical dispersion. Very stable, stable and neutral conditions had stronger dispersion in both downwind and crosswind directions. As a function of wind speed, smallest vertical concentration gradients were obtained at the higher setting.
- AERMOD and CFD simulated the particle dispersion downwind of the source differently based on vertical particle concentration profiles. At any location downwind of the source, vertical gradients of AERMOD-based particle concentrations from the ground up to a certain height were negligible. In contrast, CFD was able to provide a more detailed profile for downwind concentrations such that the concentration decreased with height and that the simulated concentration gradients between adjacent heights, even those near the ground, were significant. In addition, the vertical profile of downwind particle concentrations changed with wind speed setting.

Although this study demonstrated the capability of CFD technique to provide more detailed vertical concentration gradients, further research on these two techniques is needed to determine the more accurate method for simulating particle dispersion from ground-level area sources. To accomplish this, extensive field measurements at ground-level area sources may be necessary. More important, the performance of AERMOD in modeling dispersion for ground-level area sources must be thoroughly investigated. As AERMOD's performance in modeling vertical profiles of downwind concentrations was found to be limited, this raises some concerns on its application as an emission estimation technique for area sources.

7.5 References

Bonifacio, H.F., R.G. Maghirang, B.W. Auvermann, E.B. Razote, J.P. Murphy, and J.P. Harner III. 2012. Particulate matter emission rates from beef cattle feedlots in Kansas – reverse dispersion modeling. *J. Air & Waste Manage. Assoc*. 62:350-361.

CFR. 2005. Code of Federal Regulations, 40 CFR, Part 51: Revision to the guideline of air quality models: Adoption of a preferred general purpose (flat and complex terrain) dispersion model and other revisions.

CFR. 2011. Code of Federal Regulations, 40 CFR, Part 60: Call for Information: Information related to the development of emission-estimating methodologies for animal feeding operations.

Cimorelli, A. J., S.G. Perry, A. Venkatram, J.C. Weil, R.J. Paine, R.B. Wilson, R.F. Lee, W.D. Peters, R.W. Brode, and J.O. Paumier. 2004. *AERMOD: Description of Model Formulation,* EPA-454/R-03-004. Research Triangle Park, NC: U.S. Environmental Protection Agency.

Feistauer, M., J. Felcman, and I. Straskraba. 2003. *Mathematical and Computational Methods for Compressible Flows.* Oxford, UK: Oxford University Press.

Ferziger, J.H. and M. Peric. 2002. *Computational Methods for Fluid Dynamics*. 3rd ed. Heidelberg. Germany: Springer-Verlag.

Glasgow, L.A. 2010. *Transport Phenomena.* Hoboken, NJ: John Wiley & Sons, Inc.

Gonzales, H.B., R.G. Maghirang, J.D. Wilson, E.B. Razote, and L. Guo. 2011. Measuring cattle feedlot dust using laser diffraction analysis. *Trans. ASABE* 54:2319-2327.

Guo, L., and R.G. Maghirang. 2012. Numerical simulation of airflow and particle collection by vegetative barriers. *Engineering Applications of Computational Fluid Mechanics*6:110-112.

Heinsohn, R. J., and R.L. Kabel. 1999. *Sources and Control of Air Pollution*. Upper Saddle River, NJ: Prentice-Hall, Inc.

Holmes, N.S., and L. Morawska. 2006. A review of dispersion modeling and its application to the dispersion of particles: An overview of different dispersion models available. *Atmos. Environ.* 40:5902-5928.

Hong, S., I. Lee, H. Hwang, I. Seo, J. Bitog, K. Kwon, J. Song, O. Moon, K. Kim, H. Ko, and S. Chung. 2011. CFD modeling of livestock odour dispersion over complex terrain, part II: Dispersion modeling. *Biosystems Engineering* 108:265-279.

Koppolu, L., D.D. Schulte, S. Lin, M.J. Rinkol, D.P. Billesbach, and S.B. Verma. 2002. Comparison of AERMOD and STINK for dispersion modeling of odorous compounds. In *2002 ASAE Annual International Meeting,* Chicago, IL, July 28-31, 2002.

Launder, B.E., and D.B. Spalding. 1974. The numerical computation of turbulent flows. *Computer Methods in Applied Mechanics and Engineering* 3:269-289.

Li, Y. and H. Guo. 2006. Comparison of odor dispersion predictions between CFD and CALPUFF models. *Trans. ASABE* 49:1915-1926.

Lin, X.J., S. Barrington, D. Choiniere, and S. Prasher. 2007. Simulation of the effect of windbreaks on odour dispersion. *Biosystems Engineering* 98:347-363.

Magliulo, V., G. Alterio, and A. Peressotti. 2004. Experimental and numerical test of the micrometeorological mass difference technique for the measurement of trace gas emissions from small plots. *Environ. Sci. Technol.* 38:2693-2700.

OpenFOAM. 2011. *OpenFOAM – The Open Source CFD Toolbox User Guide*, Version 2.1.0. Available at: openfoam.com. Accessed: May 04, 2012.

Perry, S.G., A.J. Cimorelli, R.J. Paine, R.W. Brode, J.C. Weil, A. Venkatram, R.B. Wilson, R.F. Lee, and W.D. Peters. 2005. AERMOD: a dispersion model for industrial source applications. Part II: model performance against 17 field study databases. *J. Appl. Meteorol.* 44:694-708.

Seinfeld, J.H., and S.N. Pandis. 2006. *Meteorology of the Local Scale. Atmospheric Chemistry and Physics - from Air Pollution to Climate Change.* 2nd ed. Hoboken, NJ: John Wiley & Sons.

Seo, I.H., I.B. Lee, M.H. Shin, G.Y. Lee, H.S. Hwang, S.W. Hong, J.P. Bitog, J.I. Yoo, K.S. Kwon, Y.H. Kim, and T. Bartzanas. 2010. Numerical prediction of fugitive dust dispersion on reclaimed land in Korea. *Trans. ASABE* 53:891-901.

Turner, D. B. 1994. *Workbook of Atmospheric Dispersion Estimates – An Introduction to Dispersion Modeling.*2nd ed. Boca Raton, FL: Lewis Publishers.

Turner, D.B., and R.H. Schulze. 2007. *Practical Guide to Atmospheric Dispersion Modeling.* Dallas, TX: Trinity Consultants, Inc. and Air & Waste Management Association.

U.S. Environmental Protection Agency. 1992. *Protocol for determining the best performing model*. EPA-454/R-92-025. Research Triangle Park, NC: U.S. Environmental Protection Agency.

Wong, C.C.C., and C.H. Liu. 2011. Pollutant dispersion over two-dimensional idealized street canyons: a large-eddy simulation approach. In *14th Conference on Harmonisation within*

Atmospheric Dispersion Modelling for Regulatory Purposes, Kos, Greece, October 2-6, 2011.

CHAPTER 8 - **Conclusions and Recommendations**

8.1 Summary and Conclusions

Field measurements of PM_{10} and meteorological conditions were conducted at several commercial beef cattle feedlots in Kansas and PM_{10} emission rates were determined using different techniques. The performance of AERMOD in modeling area sources such as cattle feedlots was also assessed by comparing it with other techniques. The following conclusions were drawn:

1. By reverse dispersion modeling with AERMOD, median PM_{10} emission rates for two Kansas cattle feedlots were 1.60 and 1.10 g/m^2-day for a 2-yr measurement period (241 and 186 days, respectively). These values, equivalent to PM_{10} emission factors of 27 and 30 kg/1,000 hd-day, respectively, were considerably smaller than the U.S. EPA published PM_{10} emission factor for cattle feedlots (82 kg/1,000 hd-day).
2. Comparison of AERMOD and WindTrax showed that AERMOD had higher back-calculated PM_{10} emission rates than WindTrax. Calculated values from the two methods were linearly correlated ($R^2 \geq 0.88$), suggesting the possibility of the conversion factor development between these two models. Furthermore, in each model, emission rates determined using two different meteorological data sets also had high linearity ($R^2 = 0.91$ for NOAA-derived and eddy covariance measurements in AERMOD, $R^2 = 0.98$ for empirically-derived and sonic anemometer measurements in WindTrax).
3. Examining the sensitivity of AERMOD and WindTrax to different modeling inputs indicated that both models responded similarly to changes in wind speed, surface roughness, atmospheric stability, and area source and receptor locations, with their profiles of concentrations as functions of these inputs highly similar. However, for a given emission rate, AERMOD calculated lower concentrations than WindTrax.
4. The flux-gradient technique, a micrometeorological method commonly used for estimating gaseous emissions, was successfully applied in quantifying PM_{10} emission rates at a cattle feedlot in Kansas. In addition, high values for friction velocity, temperature, and sensible heat, and low surface roughness were apparently favorable to high feedlot PM_{10} emissions. The water content of the pen surface highly affected

PM_{10} emissions and a water content of at least 20% (wet basis) is recommended to significantly reduce feedlot PM emissions.

5. AERMOD and CFD responded similarly to atmospheric stability and wind speed in general. However, unlike CFD, AERMOD was found to be limited in providing a more detailed vertical concentration profile as vertical concentration gradients for the first few meters from the ground were negligible. This may be a challenge for AERMOD when used in reverse dispersion modeling technique for area sources.

8.2 Recommendations for Further Study

Based on findings of this research, the following are recommendations for further study:

- Assess the performance of available emission estimation techniques, which include dispersion models and micrometeorological techniques, in determining gaseous and particulate emission rates from cattle feedlots using (extensive) field measurements.
- Assess performance of CFD turbulence models in simulating both gaseous and particulate dispersion for area sources like cattle feedlots. These models may include *k-e* and *k-w* models for simulating velocity transport, and both Eulerian and Lagrangian approaches for particle transport.
- Perform more detailed comparison of the flux-gradient technique and dispersion models (AERMOD, WindTrax) in estimating gaseous and particulate emission fluxes.
- Compare the flux-gradient technique and reverse dispersion modeling with the eddy covariance technique in determining gaseous emission rates for cattle feedlots and other ground-level area sources.

Appendix A - **Supporting Analysis for Chapter 6: Verification of PM_{10} Turbulent Fluctuations**

A.1 Verification of PM_{10} Turbulent Fluctuations

Use of the flux gradient technique requires that the air emission concerned follows turbulent behavior. Particles may not always follow turbulent fluctuations in cases, such as having large particle size and/or particle density, in which they can have high particle inertia (Lilly, 1973). Micrometeorological techniques might not be effective emission flux estimation tools in these situations as the particle transport is no longer governed by turbulent/eddy diffusion alone. As a supporting analysis to Chapter 6, PM_{10} turbulent fluctuations were verified, and thus the suitability of flux-gradient technique in quantifying particulate matter emission fluxes from the studied cattle feedlot. The measurement applied to do this was based on the concept presented by Lilly (1973) that involved particle relaxation time and Lagrangian time scale. Particle relaxation time, τ, is given by:

$$\tau = \frac{\rho_p d_p^2}{18\mu} \tag{A-1}$$

where ρ_p is particle density (i.e., 1,000 kg/m^3 for aerodynamic particle), d_p is particle diameter (m), and μ is air viscosity (kg/m-sec) (Lilly, 1973). Particle diameter was set at 13 µm (1.3 x 10^{-5} m), which was the geometric mean diameter reported for a Kansas cattle feedlot (Gonzales et al., 2011). Air viscosity was approximated using the Sutherland equation (White, 1991). The Lagrangian time scale, T_L, was calculated by:

$$T_L = \frac{K_m}{u'^2} \tag{A-2}$$

where K_m is eddy diffusivity for momentum (m^2/sec), and u' is root-mean-square of turbulent velocity fluctuations (m^2/sec^2) (Lilly, 1973). Eddy diffusivity for momentum, K_m, was estimated from micrometeorological measurements. The root-mean-square of turbulent velocity fluctuations was calculated using variances measured for u_x, u_y and u_z.

The ratio of τ and T_L was utilized to determine whether or not the particles followed turbulent fluctuations. The particle transport governed by turbulent/eddy diffusion had $\tau/T_L \leq$ 0.02 whereas the particle transport unaffected of turbulent fluctuations had $\tau/T_L > 10$ (Lilly, 1973). Analysis of the data (n = 1,653 hourly data points) indicated that the median τ/T_L was 0.0006, with only 5 points exceeding 0.02. Therefore, this confirmed the suitability of flux-gradient technique in particulate emission flux estimation given the particle characteristics and micrometeorological (i.e., turbulence) conditions in the feedlot considered.

A.2 References

Gonzales, H.B., R.G. Maghirang, J.D. Wilson, E.B. Razote, and L. Guo. 2011. Measuring cattle feedlot dust using laser diffraction analysis. *Trans. ASABE* 54:2319-2327.

Lilly, G.E. 1973. Effect of particle size on particle eddy diffusivity. *Ind. Eng. Chem. Fundam.* 12:268-275.

White, F.M. 1991. *Viscous Fluid Flow*. 3rd ed. New York, NY: McGraw-Hill, Inc.

Appendix B - **Comparison of AERMOD, WindTrax, and Flux-gradient Technique in Estimating PM_{10} Emission Rates**

PM_{10} emission rates estimated using the flux-gradient technique were compared to those determined using AERMOD and WindTrax dispersion models. AERMOD and WindTrax-derived PM_{10} emission rates in this analysis were from Chapter 4 (i.e., 3.81-m measurement height): PM_{10} emission rates derived using eddy covariance and sonic anemometer measurements were used for AERMOD and WindTrax, respectively. Based on 1,712 hourly data points, median PM_{10} emission rates for these three techniques were as follows: 47 mg/m^2-hr for the flux-gradient technique; 55 mg/m^2-hr for AERMOD; and 39 mg/m^2-hr for WindTrax (Table B-1). Paired t-test showed that the flux-gradient technique was not significantly different ($P = 0.65$) from AERMOD but was significantly different ($P < 0.05$) from WindTrax in terms of estimated PM_{10} emission rates. Similar to what was observed in Chapter 4, the two dispersion models were significantly different ($P < 0.05$) from each other.

Table B-1. Hourly median and standard deviations for PM_{10} emission rates (mg/m^2-hr) for flux-gradient, AERMOD and WindTrax techniques (n = 1,712)

	Flux-gradient [a]	AERMOD [b]	WindTrax [b]
Range [c]	~0 to 2,270	~0 to 1,660	~0 to 1,508
Median	47	55	39
Standard deviation [d]			
Lower	49	61	43
Upper	116	141	98

[a] PM_{10} vertical concentration gradients computed using measurement heights of 2.0, 3.81, 5.34 and 7.62 m
[b] PM_{10} emission rates back-calculated using 3.81 m height-measurements
[c] Outliers not removed
[d] Two values for standard deviations, for lower and upper ranges, because of non-normality of distribution.

PM_{10} emission rates calculated with these three emission estimation techniques are plotted as a scatter plot matrix (Figure B-1). As shown, the linearity in determined PM_{10}

emission rates could be observed between the flux-gradient technique and either of the two dispersion models (R^2 = 0.46 with AERMOD; R^2 = 0.52 with WindTrax). This linearity of the flux-gradient technique with AERMOD and WindTrax, however, was not as strong as the linearity (R^2 = 0.94) observed between the two dispersion models.

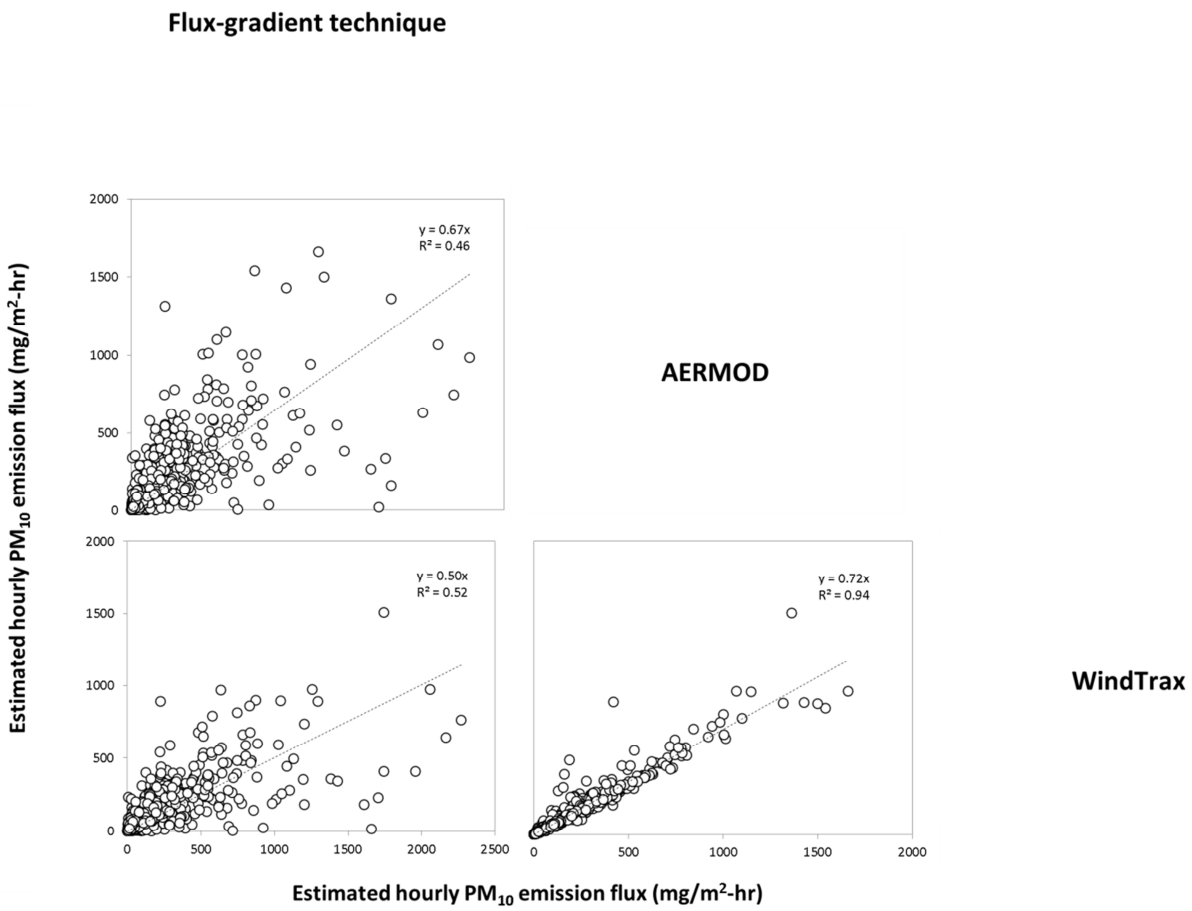

Figure B-1. Estimated hourly PM_{10} emission fluxes (mg/m^2-hr) for the three emission estimation techniques.

Note that for this analysis, PM_{10} emission rates for the flux-gradient technique were derived using one S_c value (0.63), which might cause some uncertainties in the emission rates calculated by flux-gradient technique.

Appendix C - **Additional Graphs from AERMOD and CFD Particle Dispersion Simulation**

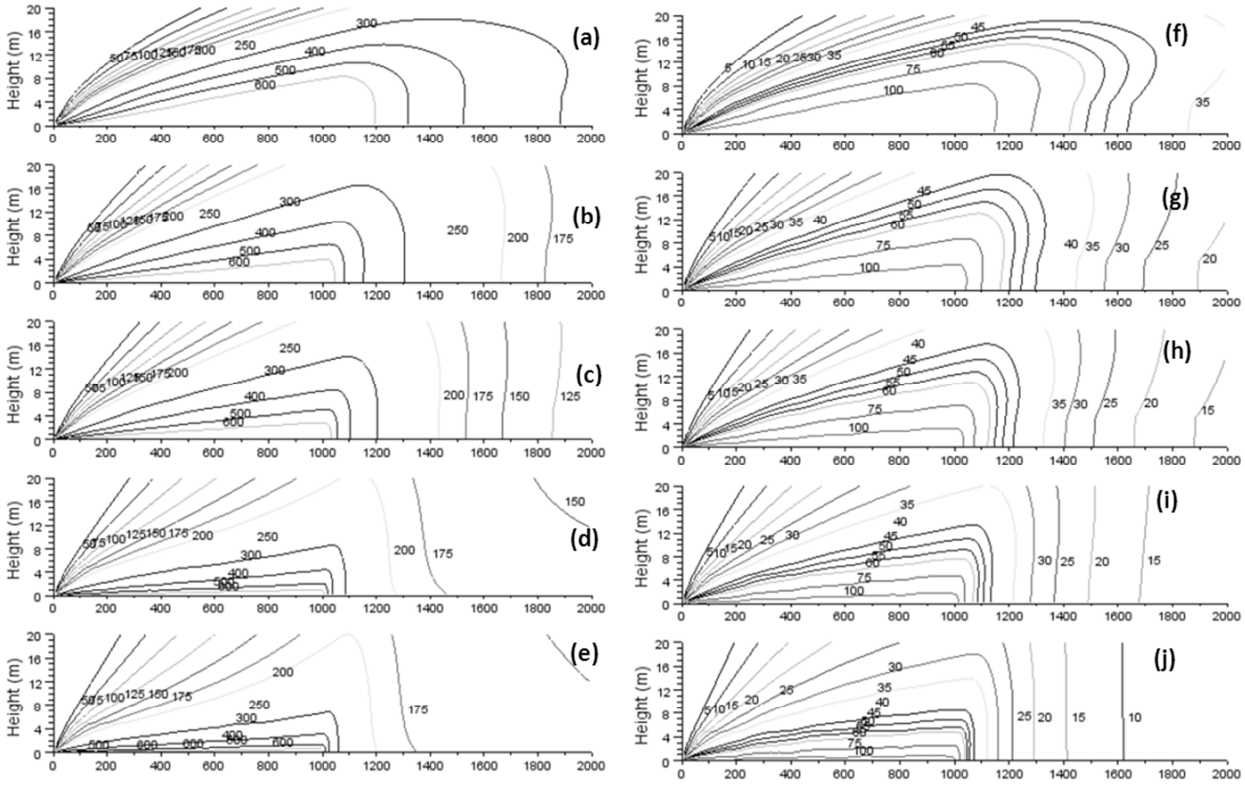

Figure C-1. Vertical contour plots of AERMOD-based plume centerline particle concentrations ($\mu g/m^3$): (a) to (e) for 1 m/sec wind speed; and (f) to (j) for 5 m/sec wind speed at very stable, stable, neutral, unstable, and very unstable conditions, respectively.

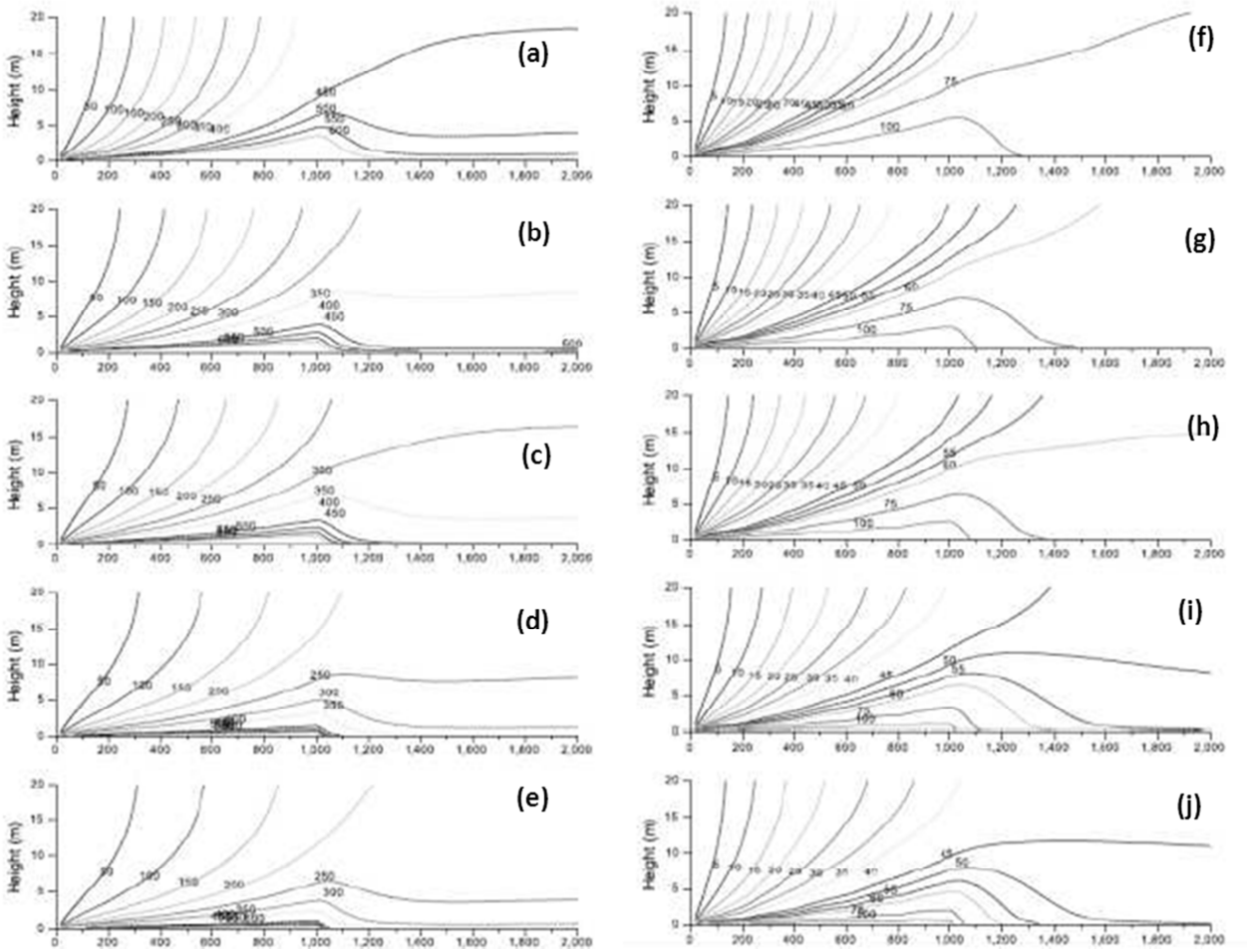

Figure C-2. Vertical contour plots of CFD-based plume centerline particle concentrations ($\mu g/m^3$): (a) to (e) for 1 m/sec wind speed; and (f) to (j) for 5 m/sec wind speed at very stable, stable, neutral, unstable, and very unstable conditions, respectively.

Appendix D - **Permissions to Use Published Manuscripts**

Taylor & Francis
Taylor & Francis Group

Permissions

T & F Reference Number: P010413-04

1/4/2013

Henry F. Bonifacio
Kansas State University
129 Seaton Hall
Manhattan, KS 66506-2906
hboni@k-state.edu

Dear Mr. Bonifacio:

We are in receipt of your request to reproduce your article

> "Particulate Matter Emission Rates from Beef Cattle Feedlots in Kansas-Reverse Dispersion Modeling", Harry F. Bonifacio, Ronaldo G. Maghirang, Brent W. Auvermann, Edna B. Razote, James P. Murphy, Joseph P. Harner III, 2012, *Journal of the Air & Waste Management Association, Volume* 62, Issue 3, pp.350-361.

to be included as part of your doctoral dissertation. This permission is for print and electronic use on a secure, password-protected web site.

We will be pleased to grant you permission free of charge on the condition that:

This permission is limited to non-exclusive English rights for this usage only.

This permission does not cover any third party copyrighted work which may appear in the material requested.

Full acknowledgement must be included showing article title, author, and full Journal title, reprinted by permission of Taylor & Francis (http://www.tandfonline.com).

Thank you very much for your interest in Taylor & Francis publications. Should you have any questions or require further assistance, please feel free to contact me directly.

Sincerely,

Mary Ann Muller

Permissions Coordinator

Telephone: 215.606.4334

E-mail: maryann.muller@taylorandfrancis.com

325 Chestnut Street, Suite 800, Philadelphia, PA 19106 • Phone: 215-625-8900 • Fax: 215-625-2940
Web: www.tandfonline.com

Taylor & Francis
Taylor & Francis Group

Permissions

T & F Reference Number: P022213-01

2/22/2013

Henry F. Bonifacio
Kansas State University
129 Seaton Hall
Manhattan, KS 66506-2906
hboni@k-state.edu

Dear Mr. Bonifacio:

We are in receipt of your request to reproduce your article

> "Comparison of AERMOD and WindTrax Dispersion Models in Determining PM10 emission rates from a beef cattle feedlot", *Journal of the Air & Waste Management Association*, Henry F. Bonifacio, Ronaldo Maghirang, Edna B. Razote, Steven L. Trabue & John H. Prueger, 2013.

for your doctoral thesis.

This permission is all for editions, both print and electronic.

We will be pleased to grant you permission free of charge on the condition that:

This permission is limited to non-exclusive English rights for this usage only.

This permission does not cover any third party copyrighted work which may appear in the material requested.

Full acknowledgement must be included showing article title, author, and full Journal title, reprinted by permission of Taylor & Francis (http://www.tandfonline.com).

Thank you very much for your interest in Taylor & Francis publications. Should you have any questions or require further assistance, please feel free to contact me directly.

Sincerely,

Mary Ann Muller

Permissions Coordinator

Telephone: 215.606.4334

E-mail: maryann.muller@taylorandfrancis.com